REMOVAL OF FLUORIDE FROM DRINKING WATER WITH CLAY-BASED DEFLUORIDATORS

PP Coetzee · J Haarhoff · C Chibi

WRC Report No. 1289/1/04

Water Research Commission

REMOVAL OF FLUORIDE FROM DRINKING WATER WITH CLAY-BASED DEFLUORIDATORS

Final Report

Prepared for the

WATER RESEARCH COMMISSION

by

PP Coetzee*, J Haarhoff and C Chibi****

*Department of Chemistry
**Department of Civil and Urban Engineering
Rand Afrikaans University

WRC Report No: 1289/1/04
ISBN No: 1-77005-024-8

June 2004

Disclaimer

This report emanates from a project financed by the Water Research Commission (WRC) and is approved for publication. Approval does not signify that the contents necessarily reflect the views and policies of the WRC or the members of the project steering committee, nor does mention of trade names or commercial products constitute endorsement or recommendation for use.

Printed by Sikowa Printers: 012 804 1164

EXECUTIVE SUMMARY

Background to the Project

This project is the culmination of a series of three projects, which progressed as follows:

- A first project during 1999 stressed the need for rural solutions to the commonly encountered problems of nitrate and fluoride, reviewed the sustainability of the commonly used technologies in rural context and came to the conclusion that new and more appropriate solutions need to be developed.
- A second project during 2000 took a closer look at a simple method reported from Sri Lanka where fluoride was successfully removed at domestic level with brick chips. A visit was made to Sri Lanka, the sketchy literature on this technology was systematically reviewed and some preliminary laboratory tests were conducted. The promising potential of this technology for South African conditions was confirmed.
- This third project, carried out over a period of 30 months, systematically continued the investigation of clay-based defluoridation in four main parts. Firstly, a broad sample of South African clays were sampled and tested. Secondly, the fundamental adsorption mechanisms of fluoride onto clay were studied. Thirdly, methods were developed to immobilise the clay into pellets which could be exposed to water without decomposition. Fourthly, adsorption studies were conducted in laboratory columns which approached the domestic units used in Sri Lanka.

The Sri Lankan Case Study

The Sri Lankan case study was studied in detail, by means of the available literature as well as a site visit. Its main features, relevant to possible local application, are:

- The project is deemed to be successful with 1400 households in 60 villages participating, with the support of the WHO. The extension of this project to further phases seems likely.
- The units are only installed in homes where infants less than three years old reside, possibly pointing to some resistance if the units have to be maintained indefinitely.
- The clay used is mainly kaolinitic and similar clays are available in South Africa.
- The clay is fired into bricks by low-temperature wood-fuelled fire, and the brick fragments from the kilns are used in the defluoridators.
- The removal is very good and units run for about two months or more before they have to be recharged with fresh brick chips.
- There is no attempt to regenerate the chips – they are simply discarded and replaced.
- Although good empirical research supports the findings, there is little fundamental work reported on the adsorption mechanisms.
- The literature search indicated research on fluoride adsorption onto clay by a number of other researchers from Africa and elsewhere.

- The only forum where these experiences are shared seems to be the International Society for Fluoride and Fluorosis (ISFF), which has had three international meeting up to now.
- An interest has been expressed by the ISFF organisers to have a future meeting hosted in South Africa.

Fundamental Considerations

A fundamental analysis of fluoride adsorption onto clay was undertaken first, with the following results:

- A theoretical model was derived based on chemical equilibrium and verified by successfully fitting experimental adsorption data, both obtained in this study and taken from the literature.
- Results obtained in this chapter support the exchange mechanism for F^- adsorption. The accurate determination of pH changes during adsorption and a thorough investigation of the acid-base properties of the substrate and its effect on the ion exchange properties, provided enough evidence to resolve uncertainties in the literature with regard to the nature of the F^- adsorption mechanism. This work confirms that a rise in pH should accompany the adsorption of F^- as predicted by the ion exchange model.
- Adsorption modelling based on thermo-dynamic considerations, i.e. the thermo-dynamic constants for the different equilibria in the adsorption process, proved to be successful in predicting adsorption curves for metal oxide substrates. Since metal oxides of Fe and Al are the predominant mineral structures found in clays showing F^- adsorption potential, the model provides a useful tool for the interpretation and prediction of adsorption behaviour of substrates under different pH conditions.

A Survey of South African Clays in terms of their Fluoride Adsorption Capacity

An extensive survey and testing programme of 23 South African clay samples was conducted next, as well as a bauxite sample from Australia and a Sri Lankan clay sample. The main findings were:

- Clay types can differ enormously in their adsorption capacities for F^-.
- Big differences also occur within a specific clay type, even if taken from the same deposit a small distance apart. This suggests that sampling for future work should possibly allow for multiple samples within the same deposit to obtain the optimal procust.
- A trend in adsorption capacity related to clay structure can, however, be observed. Adsorption capacity decreases as the concentration of exchangeable OH groups decreases.
- Clay types consisting of the metal oxides of Fe and Al were found to have the best potential as adsorbents for F^- from aqueous solutions.

The Manufacture of Pellets for Fluoride Adsorption

Water defluoridation by clay can only work if the clay can be effectively immobilised to keep the water clean and potable after treatment. A significant part of the total effort was thus devoted to a systematic investigation into the best and easiest way to achieve this. Although the emphasis of this project is to demonstrate the *technical feasibility* of water defluoridation by clay and not necessarily to develop the technology to a *practical, economical* and *sustainable* level, the results of this chapter nevertheless are also promising pointers towards full-scale implementation. The main findings of this work were:

- Of the three remaining candidate clays (after adsorption tests eliminated the fourth), practical methods could be developed to produce clay pellets that were stable.
- This could be achieved by using two of the clays directly in a sun-dried form, and by adding only water to the third.
- The compression could be done with a manual press requiring no other power source and a simple set of moulds.
- The baking required a sustained temperature of about 600°C for a period of 2 hours.
- The pellets produced had a fairly high internal porosity, which boded well for its eventual adsorption capacity.
- There was no serious turbidity increase of the water exposed to the pellets, and tests in larger, more quiescent reactors may have even smaller effects.

Measuring Fluoride Adsorption Efficiency with Laboratory Defluoridators

Three clays – KOP, RYE and MD2 were evaluated for performance in long term tests using cylindrical reactors for fluoride removal. The conclusions drawn were as follows:

- All three clays performed very well recording removal efficiencies of more than 70% for the smallest sized pellets.
- Predictably, the smallest sized pellet (12 mm dia) out-performed the other pellets of sizes 25 mm and 40 mm dia. The 25 mm pellet performed slightly better than the larger pellet.
- Structurally, the pellets proved to be sufficiently rugged and stable not to impart colour and turbidity to the product water. In the cases where the pellets collapsed, the failed clay particles invariably settled at the bottom of a column (this can be attributed, of course, to the relatively quiescent conditions prevailing in the columns due to the long contact times employed).
- No discernible or adverse odour was detected on the product water. In the product water, colour was consistently less than 5 Hazen units and nephelometric turbidity was consistently less than 1 NTU.
- Fluoride - spiked water to very high concentrations (30 mg/l and 50 mg/l) exhausted a full-scale column between 8 days and about 18 days.
- The initial fractional removal of fluoride, for the clay samples and pellet manufacturing conditions used, was about 70% which indicates good potential for further development and refinement.

Conclusions

- There is a need for a practical, simple defluoridation technology which will be sustainable for rural villages with limited monetary and manpower resources.
- The use of discarded brick fragments as piloted in Sri Lanka, is a promising technology with a proven track record at hundreds of households.
- The adsorption of fluoride onto clay was modelled successfully in this project and a rational basis for this technology therefore exists.
- Clay deposits in South Africa could be potentially be just as successful, but great variations exist even within the same deposits. Careful mining of the deposits is an important prerequisite.
- A practical, simple method of compression and baking was developed which will effectively immobilise the clay as pellets to ensure good water quality, while still attaining good defluoridation efficiency.
- The initial defluoridation efficiency of domestic units using these pellets was measured at about 70%.

Recommendations for Further Research

The groundwork had been done to expand this project to field-scale testing, with adequate demonstration of its potential to warrant further attention. This will require the following main elements:

- The location of the test sites, after which the most appropriate clay pits can be surveyed.
- A semi-automated method of pellet manufacture to produce adequate pellets for testing. During this project, pellets were produced manually which will not be practical for full-scale testing.
- A multi-disciplinary approach which should not only include the technical aspects covered in this project, but also sociologists and health professionals to explain the relevance of the technology to the community, and to evaluate its success and acceptance.

ACKNOWLEDGMENTS

The Project Team acknowledges the Project Steering Committee who guided the project in a supportive, constructive way:

Dr IM Msibi	Water Research Commission (Chairman)
Ms N Basson	Sedibeng Water
Mr CS Crawford	Department of Water Affairs & Forestry
Dr PR de Gasparis	Development Bank of South Africa
Ms C Galen	Development Bank of South Africa
Dr S Jooste	Department of Water Affairs & Forestry
Mr LL Maisela	Department of Water Affairs & Forestry
Mr MC Nel	Magalies Water
Dr FJ Smit	Department of Health
Mr GF Titus	Sedibeng Water

The technical support staff of the Departments of Geology, Chemistry and Civil Engineering at the Rand Afrikaans University continuously contributed to this project over a period of thirty months. Mrs. EP de Kock of the Faculty of Engineering at the Rand Afrikaans University took care of the financial management of the project.

TABLE OF CONTENTS

Chapter 5 Preparation of Clay Pellets

Chapter 6 Defluoridation Efficiency

Chapter 7 Conclusions and Recommendations

Chapter 8 Bibliography

CHAPTER ONE

INTRODUCTION

1.1 BACKGROUND

Fluoride is universally recognised as a necessary compound to grow strong, attractive teeth. At the same time, it is also recognised that an excess of fluoride leads to dental fluorosis and even to skeletal fluorosis at higher levels of exposure. In South Africa, there are regions where natural waters lack the required fluoride concentration required for healthy teeth, which is the drive behind the recent legislation for the enforcement of water fluoridation . Similarly, there are regions in South Africa where the natural fluoride concentration in water exceeds the concentrations generally recognised to be acceptable to the health of the general public.

The most serious cases of excessive fluoride concentration are found where communities rely on groundwater for drinking water. The worst affected communities are therefore those that are small and rural, beyond the reach of existing central water supply systems which could have provided an alternative source. These communities, for obvious reasons, are also those that are ill equipped to afford expensive technology, or to operate complicated systems.

1.2 INVESTIGATING THE OPTIONS FOR DEFLUORIDATION

The Water Research Commission funded a first project in 1997/8 which enabled Mr. Cecil Chibi (from the company Options to Solutions) to conduct a literature survey on the different methodologies for removing fluoride and nitrate from drinking water supplies. The proposal for this contract flowed from the difficulties experienced by small water systems when confronted with fluoride and nitrate problems, which were commonly encountered by Mr. Chibi during his previous tenure with Mvula Trust, which funded many of these projects. The contract was for one year only and the contract amount R30000. At the end of the contract, the findings were presented to a WRC-funded workshop held in Mafeking during March 1999.

Amongst the many alternatives considered, it turned out that very few of them were feasible and sustainable options for smaller, rural communities – those commonly plaqued by fluoride and nitrate problems. One of the most promising options was the defluoridation with clay, which was reported as a case study in the international literature.

1.3 ASSESSING THE FEASIBILITY OF DEFLUORIDATION BY CLAY

The recommendation from the previous project was that defluoridation with clay should be further investigated. After careful deliberation, it was deemed best to tackle the project in two steps. As a first step, the Sri Lankan case study would be studied in more depth, the literature on defluoridation by clay would be consulted, and some preliminary tests would be done. Should this option still remain promising, a proposal for a more comprehensive study would be submitted as the second step.

The Rand Afrikaans University, with Mr. Chibi as the principal investigator, therefore submitted a proposal in 1999 which led to a second WRC contract in 2000 which allowed the investigation to proceed for a further 12 months at a cost of R90000.

During this project, the literature was thoroughly examined and found to contain much anecdotal information and findings based on case studies, but very little work that reflected fundamental mechanisms and understanding. Mr. Chibi visited Sri Lanka for a few days, visited the clay pits, the brick manufacturing sites and a number of household installations, and retrieved some clay and brick samples to South Africa for local testing. A working relationship between the departments of Civil Engineering and Chemistry at RAU was forged and some preliminary tests were done.

The main conclusions and recommendations from this project were:

- The pilot project in Sri Lanka demonstrated the feasibility of the technology on a domestic scale.
- There is a lack of fundamental understanding of the adsorption mechanisms, reaction kinetics and adsorption capacity, without which no firm engineering design guidelines can be developed.
- The analyses of the Sri Lankan clay at the RAU showed these clays to be principally kaolinite and bentonite – clays which also are abundantly found in SA.
- There is a need to continue this work in South Africa, with local clays, to address the deficiencies noted above.

1.4 WRC CONTRACT K5/1289 – EFFICIENCY OF DEFLUORIDATION BY CLAY

The WRC was consequently requested to consider a third research proposal to address the needs previously identified. This proposal was accepted and registered as Contract K5/1289, which commenced in January 2001, ran for 30 months and was concluded at the end of June 2003. The RAU research partners for this project were the Department of Civil and Urban Engineering (with Prof. Haarhoff as project coordinator and Mr. Cecil Chibi as principal investigator), the Department of Chemistry (with Prof. Coetzee as principal investigator) and the Department of Geology (with Prof. Beukes as principal investigator).

This report is the culmination of this contract.

1.5 RESEARCH PRODUCTS

The anticipated research products of this contract were originally stated as:

- A physical explanation of how fluoride adsorption onto baked clay works
- A prototype of a domestic unit for the removal of fluoride from drinking water

It was further anticipated that a prototype would be field-tested in a rural village. During the second steering committee meeting (when about nine months of the budgeted project time was left), this intention was reconsidered. The laboratory efficiency of the unit was then only 50%

and it was deemed to be inadvisable to move a relatively inefficient unit to site. The team was requested to rather divert the resources for the final part of the project towards attaining higher efficiency.

1.6 STRUCTURE OF THE REPORT

The report follows the following structure:

- This Chapter One sketches the background and overall objectives of the project
- Chapter Two reviews the state of the art of defluoridation with clay, with particular emphasis on the Sri Lankan case study
- Chapter Three develops the necessary theoretical basis for understanding fluoride adsorption onto clay minerals
- Chapter Four reports the results of a comprehensive survey on the defluoridation efficiency of a wide range of South African clay samples
- Chapter Five describes how the raw clay was eventually immobilised into stable clay pellets
- Chapter Six reports on the defluoridation efficiency of the laboratory columns
- Chapter Seven summarises the main findings and suggests further avenues of research towards the further development of this technology
- Chapter Eight contains a bibliography of the sources collected and consulted during this project.

1.7 REFERENCES

Chibi, C., and Vinnicombe, D.A. (1999) Fluorides and Nitrates: Their Occurrence in Rural South Africa, Current Removal Technologies and Promising New Approaches. Unpublished Report to the Water Research Commission.

Chibi, C., and Haarhoff, J. (2000) Fluoride Removal with Unconventional Low-Cost Media. Unpublished Report to the Water Research Commission.

CHAPTER TWO

DEFLUORIDATION BY CLAY – CASE STUDIES

2.1 THE SRI LANKAN CASE STUDY

The largest pilot project to date, using clay for water defluoridation, is being conducted in Sri Lanka, a small south East Asian country just south of India, where high fluoride concentrations occur in a significant part of its groundwater supplies. A significant proportion of the country relies on groundwater for fresh supplies. Over 40% of wells in some parts of the country (the so-called "dry zone" in the north), however, contain fluorides in excess of WHO guideline limits. After encouraging laboratory results with clay as defluoridating agent, the WHO eventually funded a pilot project involving the installation of 1400 household sized defluoridators, covering a total of 60 villages in the Kekirawa region. Due to the scale and reported success of the technology, Mr. Chibi visited this pilot project in Sri Lanka between 20 and 27 September 1999, during the preceding WRC contract. The remainder of this section summarises his main findings and impressions.

The National Water Supply and Drainage Board (NWSDB) is mandated with the provision of water to all Sri Lanka – both urban and rural areas. The pilot project is therefore conducted under its wing, with Mr JP Padmasiri as project leader and researcher, who is a senior chemist at the water authority. He is stationed in a regional office in Peradeniya, a surburb of the 2nd largest city in Sri Lanka called Kandy. The NWSDB works through local NGOs who presumably have a better insight into the local demographics, dynamics and cultural influences. Due to difficult communication with Mr. Padmisiri in Kandy, all arrangements for the RAU visit was made through another NGO called COSI, represented by its director, Mr. Palitha Jayaweera.

About six villages in and around Kekirawa were visited, and in each about three household defluoridators were observed in use. Participating households are chosen on the basis of having an infant 3 years and younger. A few village kilns were also visited in order to establish the clay firing techniques used. Clay samples were obtained from the villages and retrieved to the RAU campus for analysis by the Chemistry and Geology Departments. These results will be reported on in subsequent chapters.

The design of the defluoridation units developed in Sri Lanka is illustrated in Figure 2.1. The filter system comprises of a reactor made of either a PVC pipe or a square brick column. The filters are packed with broken pieces of freshly burnt bricks of the size of 8 to 16 mm, to a height of 750 mm. At the centre of the reactor is a perforated pipe funnel. Initially the filter is filled with the high F^- concentration water for 12 hours. This is to obtain equilibrium, as well as hydration of the burnt media. During operation, the water if fed into the pipe funnel, allowing the water to flow through the brick media (in "plug flow" fashion) and then over-flow for usage.

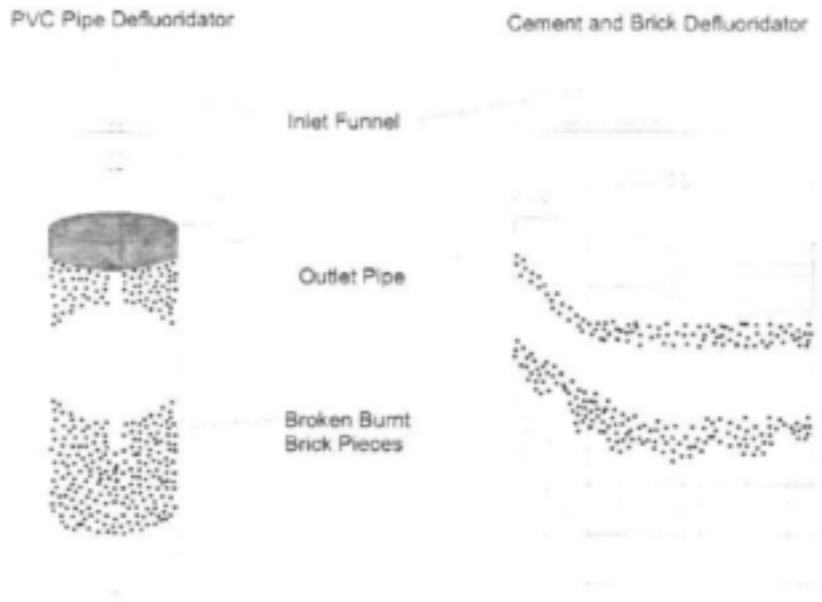

Figure 2.1 The Sri Lanka low cost defluoridator, illustrated for both the column and brick style. (Source: Padmasiri, 1997).

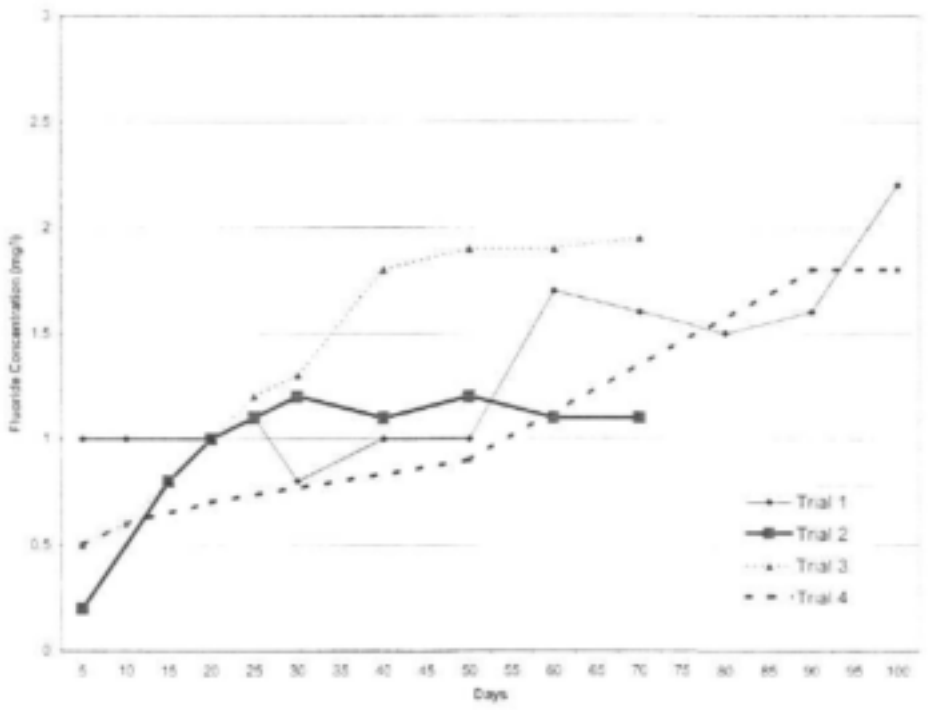

Figure 2.2 Removal capacity during 4 trials of one defluoridator (Source: Padmasiri, 1997).

The efficiency of these low cost defluoridators, based on the results from Sri Lanka, varies from 85% at the beginning of a filter run, to 25% at the end, depending on the length of time taken for each run. The removal of F^- by one such defluoridator is shown in Figure 2.2 for four runs of the same defluoridator over 70 to 100 day trials each. This unit achieved a product water averaging 1 mg/l F^- from an initial concentration of 5 mg/l.

As a general rule, influent fluoride concentrations of 2 to 5 mg/l were consistently reduced to concentrations of less than 1 mg/l for periods of 3 to 6 months using the same media. Thereafter, it was found more cost effective to simply discard the media as opposed to regenerating it again. The vast majority of the defluoridators installed in the Sri Lankan pilot programme are reported as still operational, showing the sustainability and acceptability of this technique on a domestic level. The WHO appeared to be pleased with the results from the current project and was considering funding a phase 2 of the programme.

During the same visit, a meeting was arranged with Mr. Kumari Jayasinghe, a geology lecturer at the University of Peradeniya. Although extensive empirical testing has verified the performance and reliability of the units, the work in Sri Lanka did not contribute much to the fundamental mechanisms at work in the fluoride adsorption process. All the parties in Sri Lanka expressed their interest in the outcomes and findings of the South African research project.

The final page of this chapter shows five pictures taken by Mr. Chibi during his visit to Sri Lanka, to provide some practical perspective on their implementation of the technology.

2.2 EXAMPLES FROM AFRICA

Work on the removal of fluorides using clays is not confined to Sri Lanka. Some work had been carried out in Africa, most notably that along the Great Rift Valley, including Ethiopia, Cameroon, Tanzania and Kenya. In the latter the use of clay shards from broken pots had been studied as a fluoride adsorption agent. These researchers (Dissanayake, 1991; Bjorvatn et al, 1997; Bjorvatn and Bardsen, 1995; Zevenbergern, 1996) have published encouraging findings based on preliminary work carried out on the technique. Most conclusions suggest further investigations so that the method can be further developed for application in poor developing areas.

2.3 EXAMPLES FROM ELSEWHERE

Following is a selected list of institutions, in no particular order, outside of Africa that have carried out and reported similar work on defluoridation of water with clays and soil materials, to illustrate the broad interest in the potential of this technology:

- Dept of Hydrogeology & Environmental Engineering, China University of Geosciences
- Dept of Earthsciences, University of Waterloo, Canada
- Dept of Chemistry, Dayalbagh Educational Institute, India
- Institute of Soil Science, Chinese Academy of Sciences, Peoples' Republic of China

- Institute of Earth Science, University of Utrecht, The Netherlands
- Chemistry Dept., Istanbul University, Turkey
- Intercountry Centre for Oral Health, Chiang Mang, Thailand
- Centre for International Health, University of Bergen, Norway
- The Environmental Development Cooperation Group, Denmark
- Institute of Agro-Industrial Technology, National University of La Rioja, LAPRIAAODA Y
- Department of Chemistry, Gandhigram Rural Intitute, India

2.4 INTERNATIONAL NETWORKING AND COOPERATION

The International Society for Fluoride Research, a society promoting interdisciplinary research in fluoride related issues, hosted three symposia devoted specifically to Defluoridation and Fluorosis. The first two symposia were held in Tanzania and Ethiopia in 1995 and 1997, respectively. The 3rd Conference was held in Chiang Mai, Thailand in 2000 with another one planned possibly to be held in China. The last one in Thailand was attended by Mr Chibi where he gauged the interest of the leading event organisers of holding a future event of this kind in South Africa. This idea was met with enthusiasm and support, and could be considered at the conclusion of this project.

The Conference of the International Society for Fluoride Research is a forum for the interdisciplinary discussion of fluoride research where contributions from the major medical and dental disciplines, as well as chemistry and biochemistry are presented on a biennial basis. The XXV ISFR Conference was held in Dunedin, New Zealand in January 2003. This conference was attended by Prof. P.P. Coetzee who presented some results of this project related to the adsorption chemistry of fluorides onto mineral sorbents. Interest in this work was expressed by researchers from India and China in particular. Chinese researchers presented results based on clay-based column defluoridation in conjunction with a regeneration procedure with aluminium sulphate. This paper created a heated discussion after it was pointed out that this procedure could introduce aluminium contamination into the water with even more serious consequences than fluoride!

2.5 REFERENCES

Chibi, C., and Vinnicombe, D.A. (1998) Fluorides and Nitrates: Their Occurrence in Rural South Africa, Current Removal Technologies and Promising New Approaches. Unpublished Report to the Water Research Commission.

Chibi, C., and Haarhoff, J. (2000) Fluoride Removal with Unconventional Low-Cost Media. Unpublished Report to the Water Research Commission.

Padmasiri, J.P. (1997) Low Cost Domestic Defluoridation, Peradeniya, Sri Lanka. Presented at the Second International Workshop on Fluorosis and Defluoridation of Water, Nazreth, Ethiopia.

Sri Lanka – clay is typically excavated from a shallow pit.

Sri Lanka – the size of a typical brick chunk used in the domestic units.

Sri Lanka – bricks are fired with wooden logs.

Sri Lanka – the bricks are fired in small local kilns.

Sri Lanka – a typical domestic unit as installed in a home.

CHAPTER THREE

ADSORPTION MECHANISMS AND ADSORPTION MODELLING FOR FLUORIDE ON TO MINERAL SUBSTRATES

3.1 INTRODUCTION

Adsorption of F^- onto different sorbents including clays and soils has been studied with regard to rate of adsorption (Wu et al, 1979), preheating of clays at high temperatures (Hauge et al, 1994), effect of pH (Choi and Chen, 1979), and the effect of concentration through the measurement of adsorption isotherms (Chaturvedi et al 1988, Chhabra et al, 1980). Very few studies, however, focused on gaining a proper understanding of the adsorption mechanisms involved in F^- adsorption onto different materials. Most mechanistic work was done on activated aluminium (Hao et al, 1986). The lack of a proper understanding and detailed description of the mechanism of F^- adsorption onto different sorbents of mineral origin prompted this systematic study of the theoretical aspects of F^- adsorption. Adsorption was studied in relation to the chemistry and structural properties of the sorbent and the aqueous solution chemistry of F^-. The results include experimental evidence based on adsorption isotherms, adsorption kinetics, adsorption curves, and changes in pH during sorbent equilibration and F^- adsorption. The evidence compiled in this way provided the basis for the development an adsorption modelling procedure. This model was used to predict optimum solution conditions and best structural properties of sorbents to achieve maximum adsorption capacity.

The specific objectives of the research project reported on in this chapter are listed below.

- To investigate the mechanisms of F^- adsorption in relation to the mineralogical structure and surface chemistry of selected clay types.
- To model the F^- adsorption process with the aim of predicting the optimal surface properties of the sorbent.

3.2 ADSORPTION MECHANISMS

An ion exchange mechanism (Hao et al, 1986) whereby F^- is exchanged with OH^- groups in the mineral structure, is generally assumed to be the rate determining step in the adsorption process. This ion exchange process can be presented by the following equilibria, here given for an aluminium oxide substrate. Similar equilibria can be written for other metal oxides such as Fe oxides. Underlined species denote the solid state:

$$\underline{AlOH_2^+} + F^- \leftrightarrow \underline{AlF} + H_2O \qquad 3.1$$

$$\underline{AlOH} + F^- \leftrightarrow \underline{AlF} + OH^- \qquad 3.2$$

Easily exchangeable OH^- groups are those found in metal hydroxides or hydrated metal oxides such as aluminium or iron oxides, although it is known that not all structural forms of metal oxides have exchangeable OH^- groups with F^-, notably magnetite (Fe_4O_6) and corundum (α-

Al_2O_3). Lattice OH^- groups such as found in aluminiumsilicates, for example kaolinite, have a low tendency to be replaced by F^-.

The pH of the system is a very important parameter and determines the degree of protonation of the OH^- exchange sites and the degree of protonation of F^-. The pH will therefore determine the specific charge of an exchange site and therefore ultimately also the adsorption tendency of the substrate. This is because the surfaces of clays generally contain pH dependable ionizable functional groups which constitute the active exchange sites. If the clay contains metal oxides, commonly Fe oxides and less frequently Al oxides, exchange sites consist of OH^- groups depending on the degree of hydration and the specific structural characteristics of the mineral. For a metal oxide such as gibbsite, the OH^- group can undergo proton transfer in the following way.

$$\underline{AlOH_2^+} \leftrightarrow \underline{AlOH} + H^+ \qquad 3.3$$

$$\underline{AlOH} \leftrightarrow \underline{AlO^-} + H^+ \qquad 3.4$$

The dissociation constants for these reactions are defined in the same way as acid dissociation constants for soluble acids:

$$K_{a1} = \frac{[\underline{AlOH}][H^+]}{[\underline{AlOH_2^+}]} \qquad 3.5$$

$$K_{a2} = \frac{[\underline{AlO^-}][H^+]}{[\underline{AlOH}]} \qquad 3.6$$

The process of protonation (by adding acid) changes the substrate surface from negative to positive charge and therefore also forms a neutral surface at a specific pH, the point of zero charge given by the symbol pH_{ZPC}. Either a positive surface when the $pH < pH_{ZPC}$ or a negative surface when the $pH > pH_{ZPC}$ can therefore exist for each substrate depending on the pH of the medium. This pH at the point of zero charge will differ from substrate to substrate depending on the acid dissociation constants (pK_a) of the functional groups. The pH at the point of zero charge for metal oxide surfaces is given by the equation:

$$pH_{ZPC} = \tfrac{1}{2}(pK_{a1}+pK_{a2}) \qquad 3.7$$

In Table 3.1 pK_a values for selected metal oxide surfaces are listed. The strong dependence of the numerical values of pK_a's on mineral structure even for minerals with the same chemical composition is evident.

Table 3.1 Surface acidity in terms acid dissociation constants for mineral oxides

Mineral	pK_{a1}	pK_{a2}	pH_{zpc}	Reference
Activated alumina Type F1	4.2	10.5	7.4	Hao et al 1986
Activated alumina Type F1	6.0	9.4	7.7	Gosh and Yang 1984
Y-Al_2O_3	7.7	9.3	8.5	Huang and Stumm, 1973
α-Al_2O_3	8.5	9.7	9.1	Yopps and Fuerstenau, 1964
α-FeOOH	7.0	8.4	7.7	Atkinson et al, 1967
α-Fe_2O_3	8.9	9.8	9.3	Atkinson et al, 1967

The distribution of the protonated and deprotonated surface species as a function of pH can be calculated using α fractions. Equations for α fractions can easily be derived from the dissociation constant expressions and are given below for MOH_2^+, MOH, and MO^- species, typical for metal oxide surfaces.

$$\alpha_{MOH_2^+} = \frac{[H^+]^2}{[H^+]^2 + [K_{a1}[H^+] + K_{a1}K_{a2}} \qquad 3.8$$

$$\alpha_{MOH} = \frac{[H^+]K_{a1}}{[H^+]^2 + [K_{a1}[H^+] + K_{a1}K_{a2}} \qquad 3.9$$

$$\alpha_{MO^-} = \frac{K_{a1}K_{a2}}{[H^+]^2 + [K_{a1}[H^+] + K_{a1}K_{a2}} \qquad 3.10$$

The distribution curves for the surface species as a function of pH for Al, Fe, and Si oxide surfaces are given in Figure 3.1. It is clear from these distribution diagrams that the number of protonated groups, and therefore the surface positive charge, will steadily increase as the pH falls below the point of zero charge. This means that the adsorption of F^- onto an aluminium oxide surface should steadily increase as the pH decreases from 8 to lower values. It is important to note that the region of positive charge shifts to lower pH values in the following sequence in metal oxides: Al>Fe>Si. In the case of Si a positive surface only occurs at low pH values, pH<2. Because silicate is a major component in most clays the occurrence of negatively charged clay particles is very common in the pH range (5 to 8) normally observed in natural waters. It is understandable that clays preferentially adsorb positively charged metal ions and are known to be good sinks for metal pollutants (Benjamin, 1981). F^- on the other hand is negatively charged in these pH ranges and will not be readily adsorbed onto negatively charged clay surfaces. For F^- to be adsorbed from solution it is therefore important to maximise the number of positive sites in the pH range 5 to 8. Figure 3.1 indicates that Al oxides give the highest concentration of positive

charge in the required pH range. The range in which iron oxides have a positive surface extend to slightly lower pH values and would therefore be more suitable to extract F^- from more acidic waters.

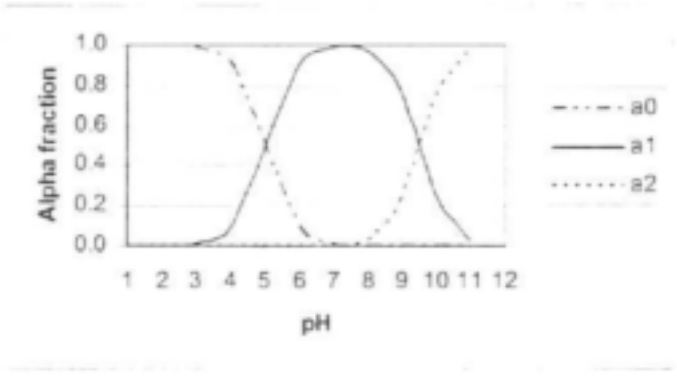

(a)

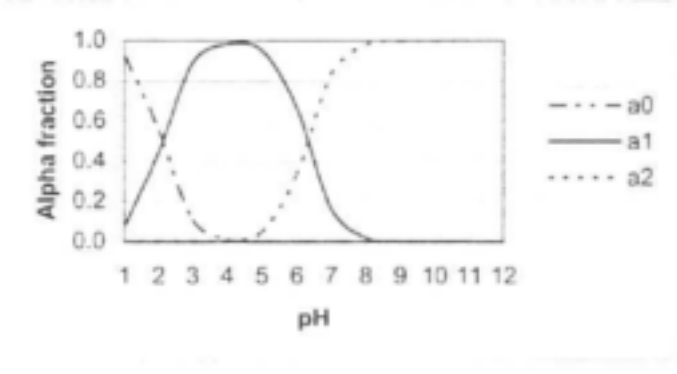

(b)

Figure 3.1 Distribution of surface species MOH_2^+, MOH, and MO^- as a function of pH for (a) Al and (b) Si oxide surfaces.

The pH of the solution also effects the degree of protonation of F^-.

$$HF \leftrightarrow H^+ + F^- \qquad K_a = 6.8 \times 10^{-4} \qquad 3.11$$

The distribution of F^- species as a function of pH is given in Figure 3.2. It is clear that F^- is completely protonated below pH 3. The neutral HF species existing in acidic media will not be adsorbed. At pH 4 about 50% of F is protonated and at pH > 5, F^- is completely deprotonated and will exist as free F^- ions in the absence of complexing agents. It is therefore expected that maximum F^- adsorption will occur at pH > 5.

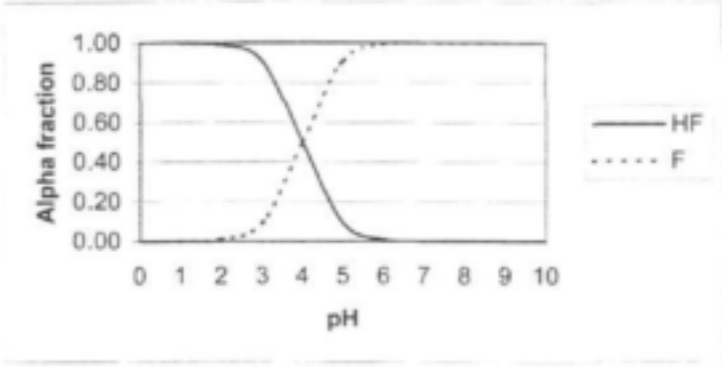

Figure 3.2 Distribution curves for F^- species as a function of pH

3.3 VERIFICATION OF FLUORIDE-HYDROXIDE EXCHANGE MECHANISM THROUGH ΔPH MEASUREMENT.

From inspection of the adsorption equilibria (E_2 3.1 and 3.2) for aluminium oxide given above one would expect that the adsorption of F^- would be accompanied by a concomitant rise in the pH of the solution as a result of the neutralisation of H^+ in the first equilibrium and the release of OH^- in the second. This was, however, not consistently observed in some experiments reported in the literature (Hao et al, 1986; Wang and Reardon, 2001) casting some doubt on the proposed mechanism. The fact that linear Langmuir isotherms (see Chapter 3 Section 4) were observed in many studies of F^- adsorption onto activated alumina is also not reconcilable with an ion exchange mechanism. In view of these uncertainties it was necessary in this work to investigate the mechanism of F^- adsorption and to provide reliable experimental evidence to enable the correct description of the adsorption process.

The chosen method was to study the change in pH after the addition of F^- to an adsorbent at different initial pH values. The procedure is described in Appendix B Section 8.

(a) *Equilibration of sorbent surfaces*

Experiments were done to ensure that proper equilibration of the activated alumina and other sorbents, which were used as substrate in these tests, at different pH values was achieved.

Results obtained for activated alumina in the acid form (ALU), given in Table 3.2 show the pH value 1 h after pH adjustment and again 14 to 18 h later. The pH remained constant after overnight equilibration, that is after a period of 16 to 20 h, indicating that equilibrium was established between solid surfaces and the solution. Since the pH of a suspension of ALU in 0.1 M $NaClO_4$ was about 4.6, acid ($HClO_4$) was added to prepare solutions with pH < 5 and NaOH added for solutions with pH > 5.

TABLE 3.2 pH at different equilibration times after pH adjustment of activated alumina

pH at indicated equilibration time					
Time (h) after pH adjustment					
1	**14**	**15**	**16**	**17**	**18**
3.26	4.21	4.18	4.23	4.23	4.23
4.04	4.82	4.80	4.81	4.81	4.81
5.25	5.27	5.22	5.24	5.25	5.25
6.20	5.5	5.45	5.47	5.50	5.5
7.23	5.88	5.74	5.74	5.78	5.78
8.11	7.16	7.05	7.00	6.98	6.98
9.13	8.46	8.33	8.29	8.28	8.28

The change in pH, ΔpH is calculated by subtracting the non equilibrium pH at 1 h from the equilibrium pH at 18 h. In Figure 3.3 ΔpH is plotted against the pH value after 1h for equilibration of activated alumina at different pH values.

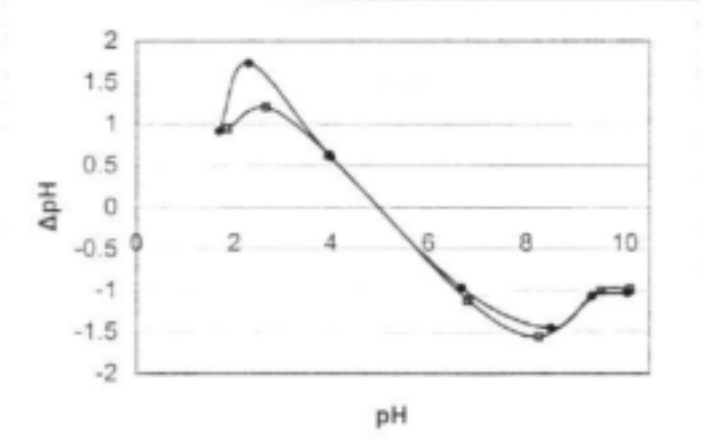

Figure 3.3 ΔpH vs pH_{1h} for the equilibration of activated aluminium (ALU) at different pH values. Results for two repeats.

A steady decrease in ΔpH is observed for pH values up to a pH of about 5. At this point ΔpH equals zero. At pH > 5 the ΔpH value becomes increasingly negative up to pH of about 7. Above pH 8 the curves turn upward indicating smaller ΔpH values. The values are still negative which means that the pH decreases during equilibration. This data give an important insight into the protonation and deprotonation behaviour of the aluminium oxide surface of activated alumina in the acid form. The results can be explained in terms of the rather slow equilibration rate and the

effect of pH on the distribution of protonated and deprotonated species as shown in Figure 3.1. The curve, however, is partly defined by the experimental procedure that was followed. After the addition of acid to adjust the pH to values less than 5 at equilibrium, the protonation reaction takes place in which $AlOH_2^+$ species are formed from sites still not protonated. The pH value therefore rises as protons are removed from solution until equilibrium is attained. The pH in solution of the activated alumina that was used for these studies was 4.6. The amount of acid added to the attain an equilibrium pH of 3, for example, would of course be more than that needed to attain pH 4. Because of the slow kinetics of the protonation reaction, the excess added will also be more and the difference between initial pH measured at 1h after addition of acid and equilibrium pH will be more in the case of the lower pH value. This explains the decreasing ΔpH for the pH range 3 to 5. In this range the reaction is governed by the reciprocal of the first dissociation constant, $1/K_{a1}$ for the protonation reaction:

$$AlOH + H^+ \leftrightarrow AlOH_2^+ \qquad 3.12$$

At pH above 5, OH^- had to be added to produce the desired equilibrium pH. In the pH range 5 to 7 ΔpH again increases for the same reasons as above but the sign is now reversed because the excess is OH^-. In this pH range the relevant reaction is governed by the constant K_{a1}/K_w:

$$AlOH_2^+ + OH^- \leftrightarrow AlOH + H_2O \qquad 3.13$$

Above pH 7 the curve suddenly reverses trend and the ΔpH values become smaller. This turning point coincides with the beginning of the formation of AlO^- species according to the deprotonation reaction governed by the constant K_{a2}/K_w:

$$AlOH + OH^- \leftrightarrow AlO^- + H_2O \qquad 3.14$$

It is important to note that the equilibration characteristics will differ substantially between surface types. In the case of RBM (an amorphous Al_2O_3), the surface is basic and equivalent to AlO^-. The pH of a RBM suspension in 0.1 M $NaClO_4$ was about 9.2. The ΔpH curves shown in Figure 3.3 therefore are quite different from that for ALU. In this case ΔpH decreased but never reversed its positive sign as the equilibrium pH progressed towards the substrate pH. Due to the high initial pH, acid was added to effect pH adjustments in all cases. These observations can be explained in terms of the protonation reactions

$$AlO^- + H+ \leftrightarrow AlOH \qquad 3.15$$

$$AlOH + H+ \leftrightarrow AlOH_2^+ \qquad 3.16$$

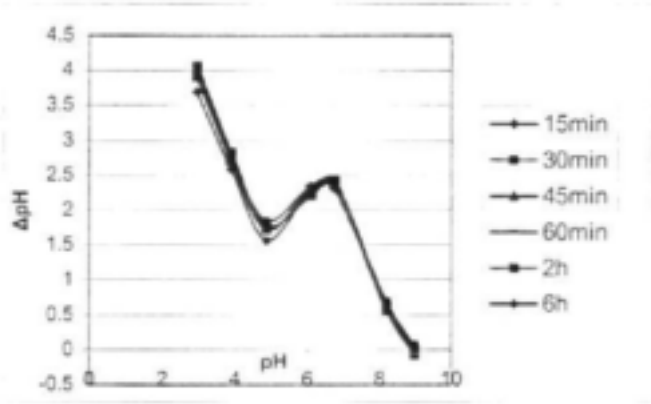

Figure 3.4 ΔpH vs $pH_{1\,h}$ for the equilibration of RBM at different pH values

To support this interpretation and to compare the kinetics of pH equilibration for ALU and RBM the pH change over time was measured after adjustment of the pH with acid or base. The results are shown in Figures 3.5 and 3.6 for ALU and RBM, respectively. The curves show that equilibrium is reached within 2 h after pH adjustment. As expected the change in pH decreases as the initial pH is closer to the substrate pH of about 5 for ALU and 9 for RBM. The curves for ALU show symmetrical but reversed behaviour above and below the substrate pH.

In the next section the observed changes in pH during adsorption onto these substrates will be explained in terms of the acid-base properties of the surfaces as discussed above.

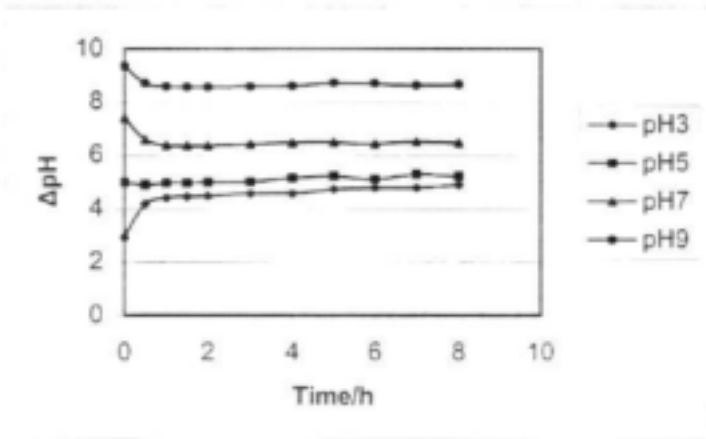

Figure 3.5 ΔpH vs time for the equilibration of ALU at different pH values.

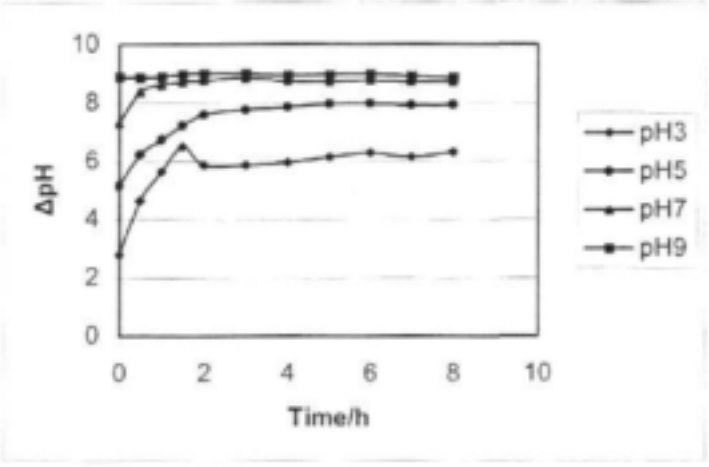

Figure 3.6 ΔpH vs time for the equilibration of RBM at different pH values

(b) *Change in pH during adsorption*

The change in pH during the adsorption process was studied after the addition of F^- solutions to properly equilibrated aluminium oxide suspensions. ΔpH was calculated by subtracting the pH at different times after addition of F^- from the initial pH (pH 16 is the pH after 16h equilibration of the substrate at a particular pH).

A plot of ΔpH vs the initial equilibrium pH value shown in Figure 3.7 reveals important characteristics of the adsorption process. In the pH range 2.5 to 6 a slight rise in ΔpH was observed after addition of F^- to the test sample of activated alumina in the acid form. The rise in pH is particularly strong at short time intervals, eg. 1.3 pH units after 15 min, after the addition of F^- for solutions with pH between 4 and 6. The pH in this pH range drops to an equilibrium value only slightly above the initial value after about 45 min. The decreasing ΔpH values over time indicated that OH^- released in the exchange reaction with F^- was removed from the solution by some process. This process is the neutralisation of remaining acid sites ($AlOH_2^+$) on the activated alumina. The rise in pH therefore suggests that the rate of the F^- exchange reaction is faster than the rate of the neutralisation reaction. Above pH 6 the ΔpH curve at equilibrium rapidly drops to 0 and then move into negative range, signifying a decrease in pH after addition of F^-. Note, that 15 min after addition of F^- all ΔpH values are positive as was expected in accordance with the ion exchange model.

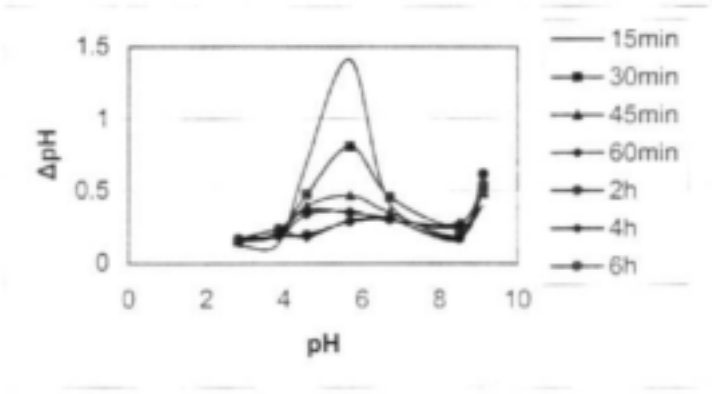

Figure 3.7 ΔpH vs the equilibrium pH for ALU at different times after the addition of 10 $mg.L^{-1}$ F^- solution

The pH changes vs initial pH during adsorption of F^- onto RBM given in Figure 3.8 show the same trend as that for ALU with a maximum ΔpH occurring at pH6. The direction of the change in pH with time allowed for equilibration is, however, reversed. The ΔpH increases with equilibration time, that is the pH rises with time. This phenomenon can be understood in terms of the fact that the RBM has a basic surface while the surface of the activated alumina is acidic. In the case of ALU the OH^- released on adsorption, is partially neutralised by the acidic surface whereas with RBM no such mechanism for the removal of OH^- is available. The pH thus increases with time as OH^- is released through F^- exchange. After 60 min a maximum is reached when the exchange process is complete. The study of the kinetics of exchange as discussed in Section 3.5 confirms that the adsorption process is practically completed in less than 60 min for most substrates.

Adsorption curves, % ads vs pH, for activated alumina (Type H-151, Hao et al. 1986) and RBM given in Figure 3.9 show adsorption maxima at pH 6. This is in agreement with the maximum positive ΔpH value also observed at pH 6. Recall that a positive ΔpH represent an increase in pH as a result of OH^- released in the exchange reaction with F^- during adsorption.

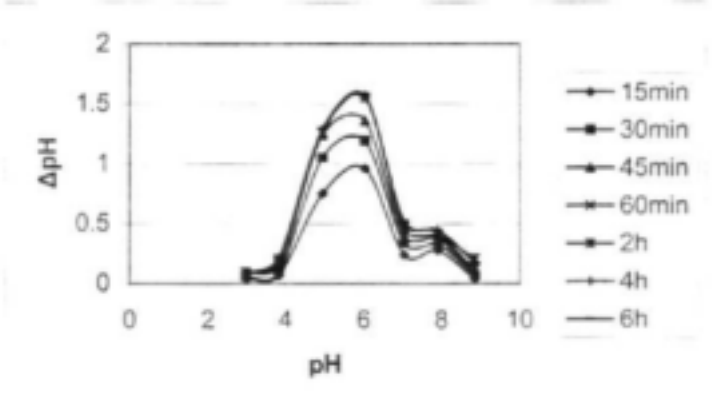

Figure 3.8 ΔpH vs the equilibrium pH for RBM at different times after the addition of 10 $mg.L^{-1}$ F^- solution

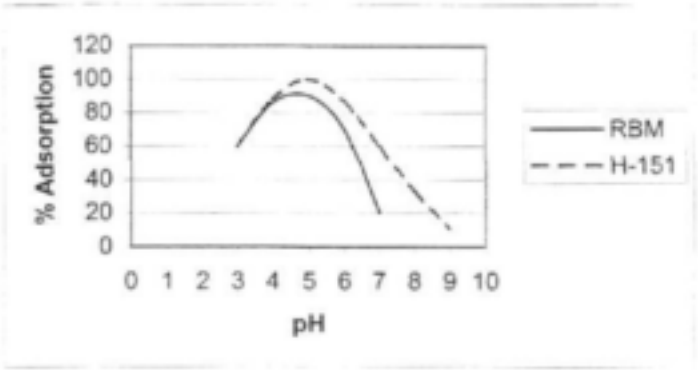

Figure 3.9 Adsorption curves for activated alumina (H-151) and RBM

3.4 ADSORPTION ISOTHERMS

Adsorption isotherms can be used to obtain information about the mechanism of adsorption. It can also be useful in determining adsorption capacities and Langmuir constants. Langmuir constants are useful in comparing adsorption characteristics of different substrates. In many studies (Chaturvedi et al, 1988) linear Langmuir adsorption curves or F^- adsorption onto metal oxide surfaces have been found. In this study adsorption isotherms for selection of clays and activated alumina were determined according to the procedure described in Appendix B Section 7. The results confirm the phenomenon of a linear Langmuir adsorption relationship (inverse of the amount of F^- adsorbed vs equilibrium F^- concentration) and are shown in Figure 3.10 for activated alumina (ALU) at pH 6. Similar curves were obtained for clay sorbents. At low equilibrium concentrations slight curvature is observed. Linear regression analysis of the linear portion of the graph gives the slope and intercept values which can be used to calculate the Langmuir constants Q, the adsorption capacity, and b (see Eq. 3.20). Table 3.3 compares the Langmuir constants obtained in this study with values reported in the literature.

Table 3.3 Langmuir constants for different sorbents

Sorbent	Q/mg.g^{-1}	b/L.mg^{-1}	Reference
Gibbsite	2.22	0.25	Bower 1967
activated alumina	2.2	0.12	This work

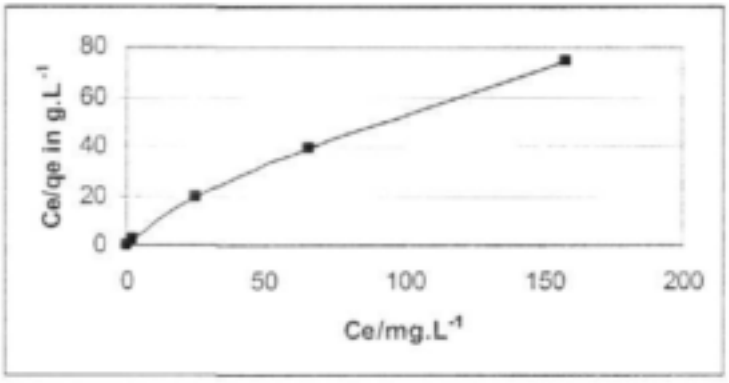

Figure 3.10 Langmuir isotherm for activated aluminium (ALU)

Langmuir adsorption assumes monolayer adsorption. At equilibrium the rate of adsorption, $k_1(1-\theta)[F]$ and the rate of desorption, $k_2\theta$ of a monolayer of F^- will be the same. θ is the fraction of the surface covered with adsorbed F^-. Therefore

$$k_1(1-\theta)[F] = k_2\theta \qquad 3.17$$

and

$$\theta = \frac{K[F]}{1+K[F]} \qquad 3.18$$

or written as a linear equation

$$\frac{F}{\theta} = \frac{1}{K} + [F] \qquad 3.19$$

If θ is written in terms of measured experimental quantities, where C_0 and C_e are the initial and equilibrium F^- concentrations respectively, w the mass of sorbent, then the Langmuir equation can be written in the form:

$$\frac{C_e}{q_e} = \frac{1}{bQ} + \frac{C_e}{Q} \qquad 3.20$$

where

$$q_e = \frac{C_0 - C_e}{w} \qquad 3.21$$

and θ is proportional to q_e: Q^{-1} is the slope and b the intercept.

The fact that F^- adsorption seems to comply with conditions for monolayer Langmuir adsorption resulting in linear isotherms is somewhat surprising if one considers the hydroxide exchange mechanism commonly assumed to be valid for F^- adsorption onto metal oxides such as activated alumina. Rearrangement of the equilibrium expression for the exchange mechanism reveals that a linear relationship between $[F^-]$ and adsorbed fraction can only occur if the $[OH^-]$ remains constant, which is not the case.

Consider the ion exchange reaction

$$\underline{AlOH} + F^- \leftrightarrow \underline{AlF} + OH^- \qquad 3.22$$

with equilibrium constant K_{ex} and let f be the fraction of OH^- exchanged with F^-, f is therefore the fraction of surface sites containing F^-. The equilibrium constant can then be written as:

$$K_{ex} = \frac{[AlF][OH]}{[AlOH][F]} \qquad 3.24$$

$$= \frac{f[OH]}{(1-f)[F]} \qquad 3.25$$

Rearrangement gives:

$$f = \frac{K_{ex}[F]}{[OH] + K_{ex}[F]} \qquad 3.26$$

or written in a form equivalent to the linear Langmuir equation:

$$\frac{1}{f} = 1 + \frac{[OH]}{K_{ex}[F]} \qquad 3.27$$

It is clear that I/f plotted against 1/[F] will only be a strait line if [OH] is constant. The fact that Langmuir isotherms are rectilinear either means that the exchange mechanism is wrong or that the [OH] remains constant during adsorption. In many reported (Chaturvedi et al 1988, Chhabra et al. 1980) measurements of pH changes during adsorption onto Fe and Al oxide surfaces no pH changes were observed. A detailed study of the pH changes during adsorption as discussed in Section 3.3 shows that pH changes do occur during adsorption if the proper account is taken of the buffer action of the substrate and provision is made for the equilibration of the substrate at a particular pH. It therefore seems that many researchers did not manage to control and take into account the buffer action of the substrate. The explanation for the anomalous linear isotherms lies in the fact that the [OH] is indeed kept relatively constant because of the buffer action of the substrate. This reaction is, however, slow and if insufficient time for equilibration is allowed substantial changes in [OH] may be measured.

3.5 KINETICS OF ADSORPTION AND PH EQUILIBRATION

The kinetics of adsorption was studied by measuring residual F^- concentration after addition of 10 $mg.L^{-1}$ F^- to 1g of sorbent at pH 6 over a time period of 8 h. It is clear from the residual F^- vs time curves given in Figure 3.11 that the adsorption is practically completed in under 60 min for all the tested substrates.

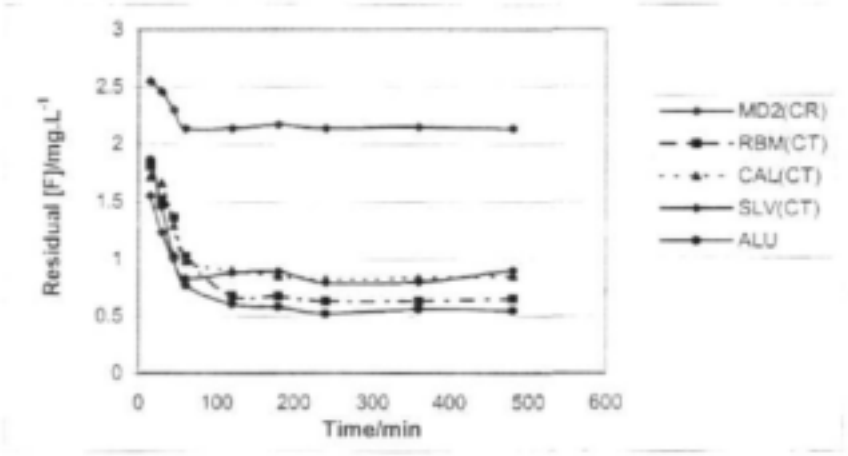

Figure 3.11 Residual F^- vs time curves for different substrates (1g) and 10 $mg.L^{-1}$ F^- solutions

3.6 DEVELOPMENT OF A MATHEMATICAL PROCEDURE FOR THE MODELLING OF F^- ADSORPTION ONTO MINERAL SUBSTRATES

In this section the derivation of a mathematical modelling procedure for the simulation of F^- adsorption onto mineral surfaces as a function of pH is presented. The model is based on the acid-base characteristics of the sorbent as determined by the dissociation constants, the protonation of F^-, and assuming a surface complexation mechanism for the adsorption of F^-. The assumption of a surface complexation mechanism is based on the fact that almost linear Langmuir adsorption isotherms were obtained for many sorbents containing metal oxide components. Numerous studies reported in the literature confirm that F^- adsorption in this context corresponds to a Langmuir isotherm. This is despite the fact that the mechanism proposed for F^- adsorption is ion exchange and not monolayer adsorption which is the primary condition for simple Langmuir adsorption. The significance of this assumption is that the data support a monolayer adsorption mechanism for which the Langmuir adsorption equation is valid. The Langmuir equation was therefore used to describe the adsorption process. This assumption, however, contradicts the ion exchange model. Equations 3.27 show that the ion exchange model should not lead to linear adsorption curves.

A simplified model for F^- adsorption based on:

- the known thermodynamic constants for protonation of metal oxide sorbents which occur in most clays,
- the protonation constant for F^- derived from the dissociation constant for HF, and
- the Langmuir equation for monolayer adsorption can be derived as shown below.

If it is assumed that the total number of active adsorption or exchange sites, N_t for a metal oxide surface is given by:

$$N_t = [MOH_2^+] + [MOH] \qquad 3.28$$

and θ is the fraction of active sites occupied by F^-, the number of sites substituted with F^- is given by

$$N_F = k\theta N_t \qquad 3.29$$

where k is a constant.

Derivation of an expression for θ

For monolayer chemisorption from solution with equilibrium F^- concentration [F], the Langmuir equation is given by

$$\theta = \frac{K[F]}{1 + K[F]} \qquad 3.30$$

where K is the Langmuir adsorption constant.

The free F^- concentration is pH dependent and is proportional to α_F,

$$[F] \sim \alpha_F = \frac{K_a}{K_a + [H^+]} \qquad 3.31$$

where K_a is the dissociation constant for HF and α_F is the fraction of total F, C_F in the F^- form.

$$\alpha_F = \frac{[F]}{C_F} \qquad 3.32$$

and

$$C_F = [F] + [HF] \qquad 3.33$$

Substitution of Eq. 3.31 into 3.30 gives θ in terms of the Langmuir constant, dissociation constant for HF, and $[H^+]$.

$$\theta = \frac{K\left(K_a / K_a + [H^+]\right)}{1 + K\left(K_a / K_a + [H^+]\right)} \qquad 3.34$$

Derivation of an expression for N_t

If the total concentration of active sites, N_t is assumed to be proportional to the sum of the α fractions for the two types of active site, then

$$N_t = k_1\left(\alpha_1 + \alpha_2\right) \qquad 3.35$$

where

$$\alpha_1 = \frac{[MOH_2^+]}{C_M} = \frac{[H^+]^2}{[H^+]^2 + K_{a1}[H^+] + K_{a1}K_{a2}} \qquad 3.36$$

$$\alpha_2 = \frac{[MOH]}{C_M} = \frac{K_{a1}[H^+]}{[H^+]^2 + K_{a1}[H^+] + K_{a1}K_{a2}} \qquad 3.37$$

$$C_M = [MOH_2^+] + [MOH] \qquad 3.38$$

By expressing the α fractions and surface species concentrations in terms of the acid dissociation constants, K_{a1} and K_{a2} and H^+ and equation for N_t can be derived.

$$N_t = k_1\left(\frac{[H^+]^2 + K_{a1}[H^+]}{[H^+]^2 + K_{a1}[H^+] + K_{a1}K_{a2}}\right) \qquad 3.39$$

Substitution of Eq 3.34 and 3.39 into Eq 3.29 gives the adsorption modelling equation for fraction of sites, N_F substituted with F^- in terms of the equilibrium $[H^+]$ concentration and equilibrium constants.

$$N_F = k\left(\frac{K}{1 + K + [H^+]\ K_a}\right)\left(\frac{[H^+]^2 + K_{a1}[H^+]}{[H^+]^2 + K_{a1}[H^+] + K_{a1}K_{a2}}\right) \qquad 3.40$$

The modelling equation can be used to calculate the form of the adsorption curve as a function of pH. The theoretical form of the adsorption curve is shown in Figure 3.12. The curve was calculated for an arbitrary selection of dissociation constants, $K_{a1} = 10^{-5}$ and $K_{a2} = 10^{-11}$, approximately similar to that of an Al oxide surface. The dotted lines indicate the effect of F^- protonation and the formation of HF which causes a sharp drop in adsorption at pH<4 and the effect of a rapidly decreasing number of exchange sites at pH>8 where a similar drop in adsorption is noted. In this pH region deprotonation of the metal hydroxide, leads to the formation of a negative surface according to the reaction:

$$MOH \leftrightarrow MO^- + H^+ \qquad 3.41$$

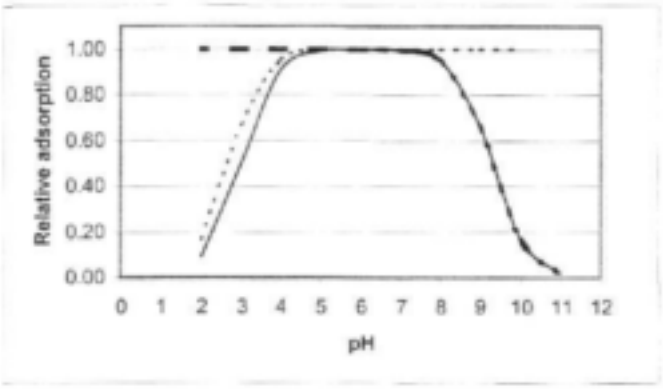

Figure 3.12 Theorectical form of adsorption vs pH curve. The dotted lines show the effect of protonation of F^- at pH < 3 and the deprotonation of MOH at pH > 8

3.7 EXPERIMENTAL VERIFICATION OF MODELLING EQUATION

The model was verified by fitting experimental adsorption data, both obtained in this study and taken from the literature to the predicted curve. Fig 3.11 shows the very good fit of normalised experimental data for F^- adsorption onto activated alumina to the theoretical curve predicted by the model. Absorption data were obtained by determining the % adsorption as a function of pH according to the procedure described in Appendix B, Section 6(b).

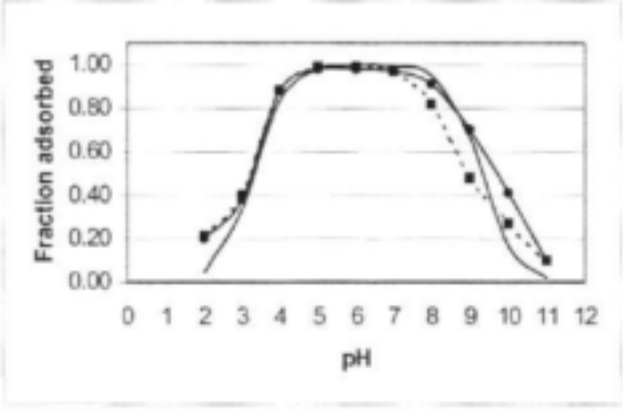

Figure 3.13 Fit of modelling equation to experimental data for activated alumina

3.8 DISCUSSION

Results obtained in this chapter support the exchange mechanism for F^- adsorption. The accurate determination of pH changes during adsorption and a thorough investigation of the acid-base properties of the substrate and its effect on the ion exchange properties, provided enough evidence to resolve uncertainties in the literature with regard to the nature of the F^- adsorption mechanism. This work confirms that a rise in pH should accompany the adsorption of F^- as predicted by the ion exchange model.

Adsorption modelling based on thermodynamic considerations, i.e. the thermo-dynamic constants for the different equilibria in the adsorption process, proved to be successful in prediction adsorption curves for metal oxide substrates. Since metal oxides of Fe and Al are the predominant mineral structures found in clays showing F^- adsorption potential, the model provide a useful tool for the interpretation and prediction of adsorption behaviour of substrates under different pH conditions

3.9 REFERENCES

ATKINSON RJ, POSNER AM and QUIRK JP (1967). Adsorption of potential-determining ions at the ferric oxide aqueous electrolyte interface. *J. Phy. Chem.* **71**, 550-558.

BENJAMIN M and LECKIE J (1981) Amorphous iron oxyhydroxide. J. Colloid Int. Sci. **79**, 209-221.

CHATURVEDI AK, PATHAK KC and SINGH VN (1988). Fluoride removal from water by adsorption on China clay. *Appl. Clay Sci.* **3**, 337-346.

CHHABRA R, SINGH A and ABROL IP (1980). Fluorine in sodic soils. *Soil Sci. Soc. AM. J.* **44**, 33-36.

CHOI W and CHEN Y (1979) The removal of fluoride from waters by adsorption. J. AWWA. Water Technology, 562-570.

GOSH MM and YANG YP (1984) Adsorption of trace arsenic and selenium on activated alumina. *Final Report. US Environmental Protection Agency*. No. R809425-01-0.

HAO OJ, ASCE AM, HUANG CP and ASCE M (1986). Adsorption characteristics of fluoride onto hydrous alumina. *J. of Environ. Eng.* **112**(6), 1054-1069.

HAUGE S, ÖSTERBERG R, BJORVATN K and SELVIG KA (1994). Defluoridation of drinking water with pottery: Effect of firing temperature. *Scand. J. Dent. Res.* **102**, 329-333.

HUANG CP and STUMM W (1973). Specific adsorption of cations on hydrous γ-Al_2O_3. *J. Colloid Interface Sci.* **43**, 409-414.

WANG Y and REARDON EJ (2001). Activation and regeneration of a soil sorbent for defluoridation of drinking water. *App. Geochem.* **16**, 531-539.

YEUN C WU, M ASCE and ANAN NITYA (1979). Water defluoridation with activated alumina. *J. Environ. Engineering Div., Proc. Amer. Soc. Civil Engineers* **105**, 358-367.

YOPPS JA and FUERSTENAU DW (1964). The zero point of charge of alpha-Al_2O_3. *J. Colloid Sci.* 19, 61-71.

CHAPTER FOUR

ADSORPTION CHARACTERISTICS OF SOUTH AFRICAN CLAYS

4.1 INTRODUCTION

A literature review reported elsewhere (Puka 2003), revealed that studies on F^- adsorption onto to clays and soils, and many other materials, have been conducted in almost all countries where high F^- natural waters present a health problem to the community – South Africa being a notable exception. No such study has been reported despite the fact that large parts of rural South Africa do not have access to good quality municipal water and are in many cases dependent on borehole waters containing dangerously high levels of F^-. The extent of the high F^- concentrations in groundwater problem in South Africa was brought to the attention by a comprehensive WRC report by McCaffrey and Willis (McCaffrey and Willis, 2001). In this report the geochemistry of F^- in the northern parts of South Africa is addressed and the fluorosis problem associated with prolonged consumption of water containing F^- concentrations > than 1.5 $mg.L^{-1}$ are discussed. A case is made for the development of cost-effective house-based methods for defluoridation.

Results of F^- adsorption studies on clays and soils indicate that large variations in adsorption capacities occur among the different types. Adsorption capacities are generally low and kinetics slow. These studies were generally conducted in a non-systematic way without taking into account the relation between the structural characteristics of the clay and its tendency to adsorb F^-. Nevertheless, useful defluoridation applications based on clays baked at low temperatures were developed by trial and error methods. The clay brick system used in Sri Lanka is a good example of a relative successful house-based approach to defluoridation and for that reason a clay sample of the clay type used for clay brick defluoridation in that country was included in this study.

In this chapter the characterisation of South African clays with regard to their F^- adsorption capacities is discussed. The selection of clay types with a high probability of being good sorbents for F^- was based on the predictions of the model discussed in Chapter 3. Clay bodies with these characteristics were sought in close proximity to the high F^- areas in the Northern Province, an area targeted for this study. Details of the sampling and mineralogical characterisation of the selected clays are presented in Appendix A. Adsorption capacities for the selected clays, 25 samples representing different mineral types, were determined at pH 6, a pH close to the pH range predicted for maximum adsorption. A sub sample of four clays showing potential to be used as sorbents for F^- was selected for further characterisation. Characterisation included the determination of adsorption curves (adsorption capacity vs pH) and the effect of physical (baking at different temperatures) and chemical pretreatment (wash with an acid and base) to determine whether enhancement in adsorption capacity can be induced by these methods.

Laboratory scale column defluoridators were developed to provide a quick and cheap way of assessing the performance of clays as sorbents for F^-. Breakthrough volumes were determined to assess the effect of different operational conditions on the defluoridation efficiency. This included column regeneration procedures. The performance of several clay types are compared.

The specific objectives of the research project reported on in this chapter, are listed below:

(a) To investigate the F^- adsorption characteristics of South African clay types and assess their potential as sorbents in a house-based F^- removal system.
(b) To develop chemical and physical pretreatment procedures to enhance adsorption properties of clays.
(c) To develop laboratory scale column defluoridators for rapid assessment adsorption and regeneration procedures.

4.2 F^- DISTRIBUTION IN SA GROUNDWATERS

The problem of high F^- concentrations in groundwaters and the risk of fluorosis associated with using such water for human consumption is a problem faced by many countries, notably India, Sri Lanka, China, the Rift Valley countries in East Africa, Turkey, and parts of South Africa. Fluorosis is a debilitating disease caused by drinking water with F^- concentrations higher than about 1 $mg.L^{-1}$ for extended periods. The disease is characterized by mottled teeth in dental fluorosis and brittle bones in severe skeletal fluorosis. Much research has been carried out during the last 20 years to find cost effective and practical solutions for the removal of excess F^- from groundwater. In a recent report McCaffrey and Willis (2001) discussed the F^- geochemistry of the North West Province, one of the areas in South Africa where fluorosis is a problem. They focused attention on a serious problem faced by many rural communities which depend on borehole water with a high F^- content for their drinking water requirements. The areas of high F^- groundwaters in South Africa include large parts of the Karoo, the Northern Cape, Limpopo, and North West provinces and are shown in Figure 4.1. It is evident from an analysis of about 3000 boreholes in the Pilanesberg and Western Bushveld area shown in Figure 4.2 that more than 30% of the boreholes have F^- concentrations > 1 $mg.L^{-1}$. In alkaline waters (pH > 9) F^- concentrations up to 30 $mg.L^{-1}$ were recorded. The seriousness of the problem is exacerbated by evidence for a much lower safe maximum F^- level in hot dry areas where the daily intake of water is much higher than normal. Brouwer et al (1988) estimated that the maximum safe F^- level in hot dry areas should be < 0.6 $mg.L^{-1}$. This value is confirmed by an empirical formula developed by Foss and Pittman (1986), which can be used to estimate safe limits for drinking water as a function of average temperature. At an average temperature of 28.5°C, typical for the North West Province, the equation estimates a threshold F^- concentration of 0.6 $mg.L^{-1}$, a value much lower than the 1.5 $mg.L^{-1}$ of the South African Drinking Water Standard.

Figure 4.1 F^- concentrations > 1.5 $mg.L^{-1}$ in South African groundwaters (McCaffrey and Willis, 2001)

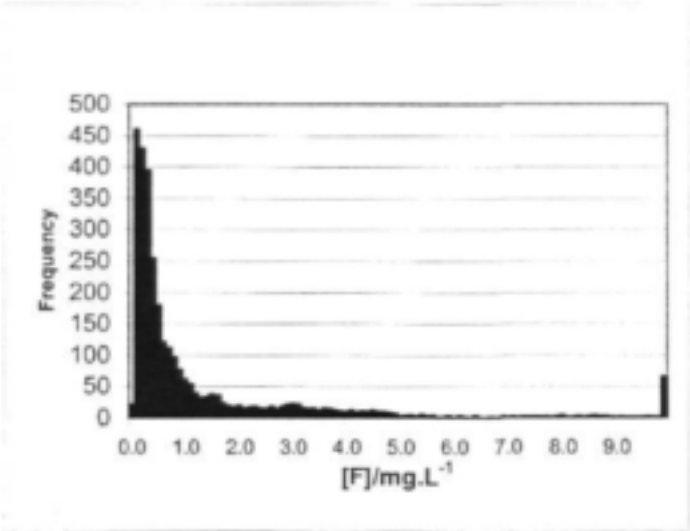

Figure 4.2 Distribution of F^- concentrations in ca 3000 boreholes in the North West Province

Figure 4.3 Major clay deposits (Horn and Strydom, 1998) and bauxite deposits (Barnardo, 1998) in the northern parts of South Africa

Excellent technologies for defluoridation are available based on using activated alumina or reverse osmosis, but these technologies are not always applicable in rural areas due to financial and technological constraints. Taking into consideration that the estimated capital cost for defluoridation amounts to ca. R5000 for a 50 L per day unit, based on either of these processes (Schoeman and Steyn, 2000), affordable alternatives, which would be easy to operate and which could be the basis for a house-based or do-it-yourself system, will have to be found. Various methods have been proposed ranging from adsorption on the inner walls of clay pots (Moges et al, 1996) in certain African countries to columns filled with clay brick chips in Sri Lanka (Padmasiri, 1991). F^- adsorption onto soils and clays have been studied extensively (Srimurali et al, 1998; Wang and Reardon, 2001) in practically all countries where the problem occurs. In general it was found that the adsorption capacity of soils and the clays was low and kinetics slow. Nevertheless, clay-based systems for defluoridation are used or are under investigation in many parts of the world.

4.3 SAMPLING AND SELECTION OF CLAY SAMPLES

(a) Clays as sorbents for F^-

The term clay is often used in a non-specific way and could refer to: (a) soil consisting of a range of small particle sizes (eg. particle size < 1/256 mm on the Udden-Wentworth scale), (b) very fine-grained earthy substances comprising of a combination of minerals, inorganic amorphous material and organic matter or (c) a specific clay mineral. The *clay minerals* are minerals in the phylosilicate mineral group and as the name implies (Greek: *pyllon*, leaf), most of these minerals have a platy habit.

In this study the term clay refers to natural occurring, very fine-grained earthy material composed primarily of clay minerals. Clays are potentially good adsorbers of anions since they contain crystalline minerals such as kaolinite, smectite and amorphous minerals such as allophane and other metal oxides and hydroxides which could adsorb anions such as F^-. The South African clay deposits shown in Figure 4.3, can be broadly classified according to the dominant clay mineral present into (1) Kaolin Fields (dominant clay mineral being kaolinite) (2) Bentonite Fields (dominant clay mineral being montmorillonite, which is part of the smectite group) and (3) Palygorskite Fields (dominant clay mineral being palygorskite). Bauxite, which is a rock type composed of one or more of the aluminium hydroxides gibbsite, boehmite or diaspore is potentially also a good adsorber of anions and therefore the Bauxite Fields of South Africa were also included in this study. Finally, the rock type laterite which represents a group of deposits consisting of residual insoluble ferric and aluminium oxides, clay minerals and quartz, formed by weathering of rocks, were also included in this study as potential adsorbers of anions.

The structure of the clay plays a very important role in determining the charge on the clay surface and type of exchange that can occur with ions in solution. In general the more negative the surface the better the sorption will be for positively charged metal ions. As discussed in detail in Chapter 3 the pH parameter plays a dominant role in determining the adsorption capacity as pH modifies the charges on edge positions in phyllosilicates and also those of variably charged minerals such as gibbsite, hematite and goethite. Charges are generally positive under acid conditions and negative in an alkaline environment. The specific pH range for positive and negative surface charge will of course be a function of the pK_a values of the metal hydroxides present. An acid pH will favour adsorption of negatively charge ions while alkaline conditions will enhance adsorption of positive ions.

Many studies report on the F^- adsorption capacities of clays and soils and their potential use as sorbents. The first comprehensive study of F^- adsorption onto minerals and soils was published in 1967 by Bower and Hatcher. The results showed that excess F^- in water could be removed to different degrees by adsorption on a variety of soil and mineral types, in particular aluminium hydroxides. It was found that the adsorption is concentration-dependent and can be described by a Langmuir isotherm. Adsorption is typically followed by the release of OH^- ions.

Since the above paper was published, F^- adsorption studies were conducted in many countries and on a variety of soil and clay types such as: Illinois soils in the USA (Omueti and Jones, 1977), sodic soils in India (Chhabra et al, 1980), activated alumina (Hao et al, 1986, Schoeman and MacLeod, 1987), clay pottery (Chaturvedi et al, 1988, Hauge et al, 1994), Ando soils in Kenya (Zevenbergen et al, 1996), fired clay chips in Ethiopia (Moges et al, 1996), fly ash (Chaturvedi et al, 1990), kaolinite (Kau et al, 1996), and illite-goethite soils in China (Wang and Reardon, 2001).

(b) South African clay deposits and the selection of clays

In the selection of clay types for this study, two criteria were considered:

- The clay structure most likely to have good F^- adsorption properties, i.e. exchangeable hydroxide-containing minerals and clays high in aluminium and iron oxides or hydroxides such as gibbsite and goethite/hematite minerals .

- The best possible clay deposits with potential F^- adsorption properties in the areas where high F^- groundwaters are used for drinking water and where fluorosis was demonstrated to be endemic. Although large parts of South Africa are under risk, this study focused on the western Bushveld area because it was extensively studied (McCaffrey and Willis, 2001) with regard to the F^- geochemistry and the distribution of F^- in groundwater. Clay deposits situated within 500 km from the endemic area were identified and sampled for this study.

Known major clay deposits in South Africa were identified from geological maps and are shown in Figure 4.3. Table 4.1 lists the areas and the types of clay deposit sampled for this study. Samples were collected using a manual auger to a maximum depth of 2.5 m. In many cases existing open pits allowed sampling at greater depths. In addition to samples collected in South Africa, clay samples obtained from Sri Lanka and Australia were included in the study for comparison.

TABLE 4.1 Descriptions and localities of samples examined during this study

KAOLIN CLAYS			
No	**Name**	**Description**	**Location**
1	ZEB1	Pure white clay from open pit.	Zebediela Kaolin Field (Fig. 1a) *Farm:* Rooiboschbaak 107KS
2	ZEB2	White clay with greenish tint, from open pit	
3	ZEB6	Blood red clay, from open pit	
4	RNF	Finely laminated orange and white clay in pan, 1 m to 2.5 m deep. Derived from weathering of Timeball Hill Shale	Koster Area *Farm:* Renosterfontein 494JP
PALYGORSKITE CLAYS			
5	LW1	Light brown colour, under 800mm of black topsoil, 800 mm – 950 mm deep	Modimolle Area, Springbok Flats *Farm:* Leeuwaarden 633KR
6	CAL	Light brown clay from open pit. Below calcrete bed, ±12 m deep. Weathering product of basalt	Immerpan Palygorskite Field (Fig. a) *Farm:* Calais 563KS
7	DB	Blue-white clay sampled at base of open pit approximately 5m deep	Dwaalboom Palygorskite Field (Fig. 1a) Artherstone Nature Reserve, obtained from G&W Base and Industrial Minerals
8	DB2	White clay bed, 1.2 m thick, below approximately 500mm black topsoil	

BENTONITE CLAYS			
9	BEN	Bentonite sample - dry and finely milled product, greenish colour.	Koppies Bentonite Field (Fig. 1(a)) Obtained from G&W Base and Industrial Minerals.
10	BBK2	Black clay, 50 mm to 300 mm deep, in shallow depression or pan	Pienaarsrivier Area, Springbok Flats *Farm:* Blaawboschkuil 20JR Bela-Bela
11	CF3	Main white clay bed, approximately 2 m thick. From open pit	Naboomspruit Area, Springbok Flats *Farm:* Cyferfonteine
12	CF4	Main red clay bed, approximately 2 m thick. From open pit	
13	NHM	Black clay, 2.00 m - 2.5 m deep	Northam Area
LATERITES AND BAUXITES			
14	LAT	Laterite, orange red in colour, below 600 mm brown topsoil	Pilanesberg Area
15	PTA-LAT	Laterite. Orange-red colour	Pretoria Area
16	BAUX1	Orange colour and surface texture that resembles a human brain "Brainstone"	Howic Area *Farm:* Lyndhurst
17	BAUX2	Orange colour, with dolerite core-stone	Kwazulu-Natal
18	BAUX3	Orange colour	Australian bauxite
19	MD1	Orange colour, weathering profile, below 50cm black soil.	Mooirivier Area *Farm:* Middeldraai
20	MD2	Orange colour, with dolerite core-stone	
21	MD3	Orange colour, with dolerite core-stone	
22	RYE1	Dark red nodular laterite	Ventersdorp Area Ryedale ferromanganese open pit mine.
OTHER SAMPLES			
23	SLV	Ochre to pale-brown nodules, dark-red to purple on fresh fractures	Sri Lanka clay used in clay brick defluoridation systems
24	RBM	Processed bauxite, 100% amorphous Al_2O_3	Australian bauxite Obtained from Richards Bay Minerals
25	ALU	Activated aluminium	Fluka, Type 504 C

4.4 F⁻ ADSORPTION CHARACTERISTICS OF SELECTED CLAY TYPES

(a) Methods

Detailed descriptions of the methods, procedures and analytical techniques used in this study are given in Appendix B.

(b) Adsorption capacities at pH 6

Adsorption capacities for the different samples were determined by shaking 1 g of washed and dried (2 h at 105°C) clay with 50 mL of 10 mgF.L^{-1} NaF solution for 2 h in polyethylene bottles at 22°C. The initial pH was adjusted to 6 using NaOH or HCl depending on whether acidic or basic clays were tested. After equilibration the solutions were centrifuged, the pH measured to ensure that the pH was within ±0.2 pH unit from the target pH, and the residual F⁻ concentration determined using ion chromatography or a F⁻ ion selective electrode.

The mineral composition and percentage F⁻ adsorbed from 10 mgF.L^{-1} solutions at pH 6 are given in Table 4.2 for 25 clay samples selected from more than 50 collected from the northern parts of South Africa. The samples are grouped according to the major clay types: bauxite, laterite, palygorskite, bentonite and kaolinite. Adsorption capacities ranged from almost zero for certain kaolinites to up to 80% for a bauxitic clay of Australian origin and 99% for a processed bauxite obtained from Richard Bay Minerals and consisting of armorphous Al_2O_3. Anion chromatography and a F⁻ ion selective electrode were used to determine residual F⁻ after completion of the adsorption process. Reproducibility was determined by three repeat measurements. The standard deviation ranged from less than 10% for the bauxite samples to about 15% for the other sample types with lower adsorption capacities than the bauxites. For the processed bauxite (RBM) and activated alumina (ALU) where adsorption was close to 100% the reproducibility was better than 1%. The results show that high adsorption can be correlated with bauxitic and lateritic samples where the gibbsite and goethite/hematite contents are high. The lowest adsorption was found for kaolin samples.

TABLE 4.2 Mineralogical composition of clay samples and % F⁻ adsorption at pH 6 from 10 mgF.L^{-1} solutions. xxxx: dominant(>50%); xxx: major (20-50%); xx: minor (5-20%); x: trace (<5%)

Sample	% F ads	quartz	dolomite	kaolinite	palygorskite	mixed-layer clay	smectite	illite	talk	Gibbsite	Goethite/hematite
BAUXITE (gibbsite / goethite)											
ALU	100									xxxx	
RBM	99									xxxx	
BAUX3	80	xxx								xxxx	x
BAUX1	65	xx								xxxx	xx
BAUX2	50	xx								xxxx	xx

Sample	% F ads	quartz	dolomite	kaolinite	palygorskite	mixed-layer clay	smectite	illite	talk	Gibbsite	Goethite/hematite
MD1	68	xxx		xxx		x		xx		xx	xx
MD2	71	xxx				x				xxxx	xx
MD3	73	xxx				x				xxxx	xx
LATERITE (goethite / hematite / kaolinite)											
SLV	72	xx		xxxx							xxx
RYE1	50	xxx		Xx			x				xxx
PTA/LAT	40	xxx		xxx							xxx
LAT	23	xxx		Xx		xxx		xx			
PALYGORSKITE (dolomite / palygorskite)											
CAL	58	x	xxx		xxx		xxx				
DB1	43	xxx	xx		xxxx						
DB2	21	xx	xxxx		xxx						
LW1[1]	23	xxxx			xxx	xx	xx				
BENTONITE (smectite)											
NHM	45	xx		Xx			xxxx				
BBK2	30	xxx					xxx				
BEN	20	xx					xxxx				
CF3	15	xxx					xxxx				
CF4	0	xx		X		xxx	xxx				
KAOLINITE											
RNF	25	xxx		Xxx			xxx	x	xx		x
ZEB1	5	xx		xxxx				x			
ZEB2	4	xx		xxxx					xx		
ZEB6	6	xx		xxxx		xx	xx	x			

Table 4.3 gives the idealised chemical composition of the major mineral types found in the clays investigated in the order in which they were found to adsorb F^- from aqueous solutions. Adsorption capacities were estimated from adsorption data at pH 6 and initial F^- concentrations of 10 $mgF.L^{-1}$.

TABLE 4.3 Major clay types and the ability to adsorb F^- from aqueous solution at pH 6 from a solution containing 10 $mgF.L^{-1}$

Clay type	Idealised chemical Composition	F^- adsorption capacity $mg.g^{-1}$	F^-adsorption
Gibbsite	$Al(OH)_3$	0.25 - 0.4	high
Goethite	FeO.OH	0.2 – 0.3	high
Palygorskite	$(Mg,Al)Si_8O_{20}(OH)_2.8H_2O$	0.1 – 0.3	intermediate
Smectite	$Ca(Mg,Fe)(Si,Al)_4O_{10}(OH)_2.nH_2O$	0.1 – 0.2	low intermediate
Kaolinite	$Al_2Si_2O_5(OH)_4$	< 0.05	low

In Table 4.4, published adsorption capacity data for different soil and clay types are compared with the values obtained in this study. Data estimated for an initial F^- concentration of about 10 $mg.L^{-1}$ and pH between 5 and 7 are included. The comparison gives an approximate indication of F^- adsorption trends for a wide variety of soils and clays from all over the world although the numerical adsorption values are not exactly comparable because experimental conditions differed. These results support the conclusion that hydrated alumimium oxide and iron oxide surfaces occurring in bauxites and goethites/hematites are useful substrates for F^- adsorption.

TABLE 4.4 Comparison of F^- adsorption capacity data in $mg.g^{-1}$ for different soils and clays. Conditions: $[F^-]_{initial}$ = 10 $mg.L^{-1}$, 1 g clay, pH = 5 – 7, equilibration time > 2h

Sorbent type	*Sample name and description*	*Capacity* $mg.g^{-1}$	*Reference*
	BAUXITE		
activated alumina	Type 504C, Fluka	0.5	This work
gibbsite	BAUX3 Australia	0.4	This work
	BAUX1, BAUX2 South Africa	0.25 - 0.4	This work
	GOETHITE		
goethite / kaolinite	PTA-LAT South Africa	0.2	This work
goethite / illite	Tertiary soil Shanxi China	0.23	Wang and Reardon, 2001
goethite / kaolinite	SLV Sri Lanka	0.35	This work
	PALYGORSKITE		
palygorskite / dolomite	DB1, CAL South Africa	0.21– 0.29	This work
	BENTONITE		
smectite	BEN South Africa	0.1	This work
	Bentonite Wyoming, USA	trace	Bower and Hatcher, 1967
	Alkaline soils USA	0.04–0.08	Bower and Hatcher, 1967
	KAOLINITE		
kaolinite	ZEB6 South Africa	0.03	This work
	Acid soils USA	0.17–0.25	Bower and Hatcher, 1967
	Acid soils Illinois, USA	0.13	Omueti and Jones, 1977
	Potter's clay, 30% Al_2O_3 1106 White St Thomas	0.12	Bårdsen and Bjorvatn, 1995
	Clay pots Ethiopia	0.07	Moges et al., 1996

(c) Adsorption capacities vs pH

The pH dependence of the adsorption process is illustrated in Figure 4.4 for a few mineral types. Data for H-151 and GOETH were taken from the literature (Hao et al. (1986). H-151 is a commercial activated alumina type and GOETH is a goethite sample. Typically the adsorption is low at pH values < 3 and > 8. Maximum adsorption is achieved at pH 5 for aluminium oxide type sorbents and pH 3.5 for iron oxide types such as goethite.

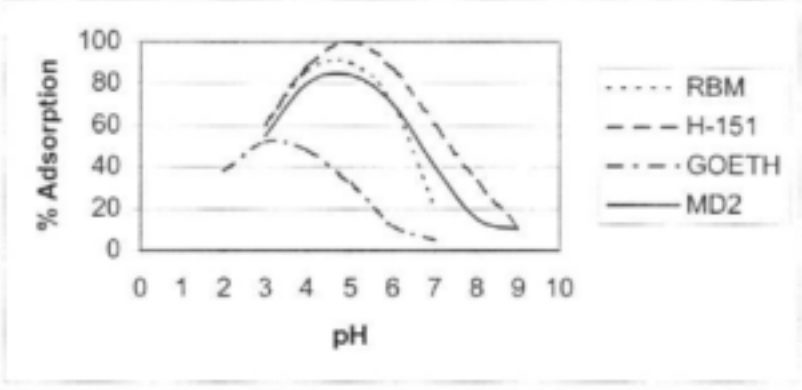

Figure 4.4 The pH dependence of F^- adsorption for different mineral sorbents: RBM = amorphous Al_2O_3; H-151 = activated alumina type H-151; GOETH = goethite; MD2 = gibbsite/goethite

Clearly the adsorption capacity is determined by the structure of the clay and in particular the surface charge distribution as a function of pH. The adsorption capacity seemed to increase with increasing Al and Fe oxide content. Thus, the more basic the surface and the more easily it can be protonated at pH values above 3 the better were the adsorption characteristics of the clay. At pH values below 3, F^- is completely protonated to form neutral HF and therefore rapidly loses its ability to adsorb onto positive surfaces.

(d) Effect of chemical and physical pretreatment on adsorption capacities

A few of the clay types that showed above average F^- adsorption tendencies were selected to determine the effect of chemical and physical treatment on the possible enhancement of adsorption capacity. The selected clay types were: gibbsite-goethite (MD2), palygorskite-dolomite (CAL), kaolinite-goethite (SLV), and amorphous Al_2O_3 (RBM). Activated alumina (ALU) was included for comparison.

For clay sample MD2, consisting mainly of gibbsite and a minor amount of goethite, a slight increase in adsorption capacity was observed with increasing heat treatment temperature up to 600°C followed by a decrease at temperatures above 600 °C as shown in Figure 4.5. Similar results can be found in the literature (Hauge et al, 1994) for clays with high concentrations of Al oxides. The decline in adsorption capacity above 600°C can be attributed to the gradual conversion of gibbsite into α-Al_2O_3 that has a smaller tendency to adsorb F^-.

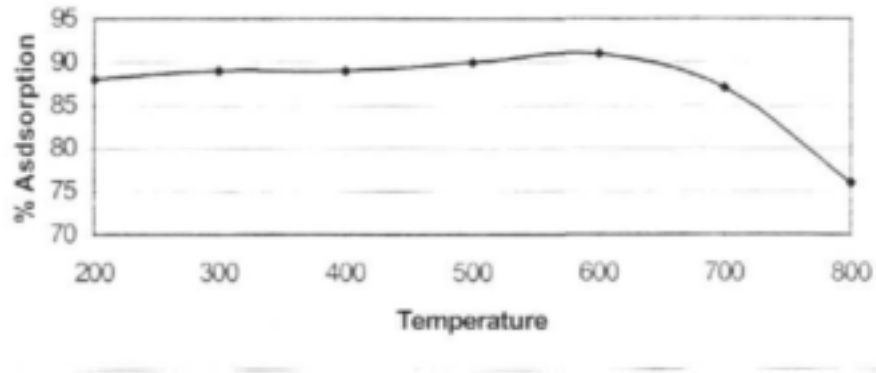

Figure 4.5 Percentage adsorption for the bauxitic clay (MD2) as a function of heat-treatment temperature

In the case of goethites similar reduction in adsorption capacities after heat treatment at temperatures above 600°C were observed (Wang and Reardon, 2001). This may be attributed to the formation of magnetites, a form of iron oxide which show little tendency to adsorb F^-. The temperature of 600°C therefore represents an upper limit above which F^- adsorption decreased for the clay types containing Al and Fe oxides. Should clays be used as substrates for F^- removal, lower temperatures could be used without significantly changing adsorption capacities.

The dolomite in samples such as CAL can also play a role in F^- adsorption. It was found that adsorption increased after these clays were heated to 600°C. This could be attributed to the conversion of calcium and magnesium carbonates into oxides of these metals. Subsequent exposure of the freshly formed CaO to F^-, could result in the formation of CaF_2. This process could contribute to F^- removal from the solution through a precipitation mechanism rather than an adsorption or ion exchange mechanism.

Figure 4.6 summarises the effect of heat treatment and chemical treatment on the adsorption capacities of the selected clay types. Chemical treatment had a significant effect on the adsorption capacities of certain clays such as palygorskite-dolomite (CAL), kaolinite-goethite (SLV), and amorphous Al_2O_3 (RBM), but little change was observed for gibbsite-goethite clay (MD2). Activated alumina was included as a reference. The pre-treatment procedures were not expected to affect the adsorption characteristics of this sorbent.

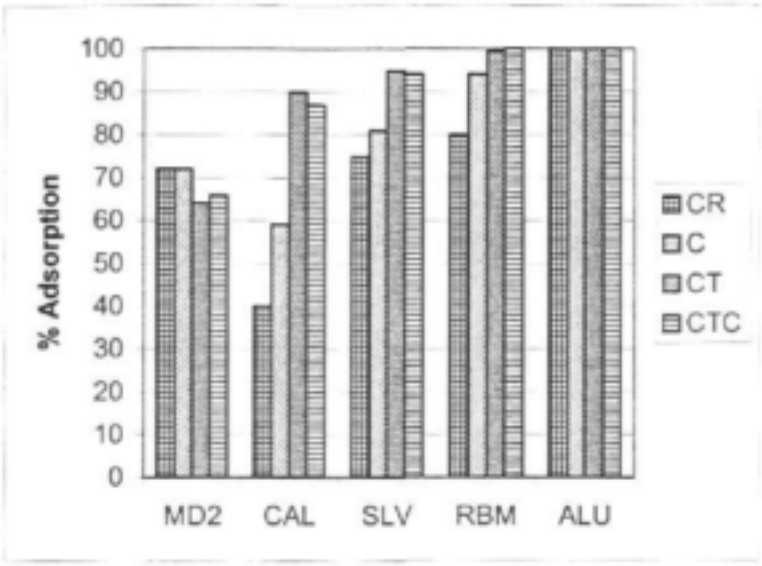

Figure 4.6 The effect of heating and chemical treatment on adsorption capacities of selected samples. CR = clean raw, C = heated for 1 h at 600°C , CT = chemically treated with 1% Na_2CO_3 and 1% HCl, CTC = heated and followed by chemical treatment

X-ray diffraction data for heated and non heated clays provide an insight into the crystallographical changes that take place during heating and can be used to explain why heating at 600°C increase adsorption capacities for certain clays. The X-ray diffractograms given in Figures 4.7 to 4.10 show the structural changes that occur in:

- CAL, (Figure 4.7) where the dolomite structure is decomposed and $CaCO_3$ and $MgCO_3$ are converted into Mg and Ca oxides. The dolomite peaks disappear on heating while MgO peaks appear. A dramatic increase in adsorption capacity was observed after treatment probably reflecting the formation of CaF_2 during the adsorption process.
- RBM, (Figure 4.8) where the amorphous or microcrystalline structure is too small for proper XRD structural identification. RBM consist partly of amorphous Al oxide, a mixture of α- and γ-Al_2O_3 which do not undergo any change on heating at this temperature. Its adsorption characteristics are therefore unchanged.
- MD2, (Figure 4.9) where gibbsite is converted into aluminium oxide and goethite into hematite, these changes do not influence the adsorption characteristics.
- SLV, (Figure 4.10) where koalinite is decomposed and probably converted into Al and Si oxides. The released Al oxides, probably γ-Al_2O_3, then contributes to improved adsorption characteristics.

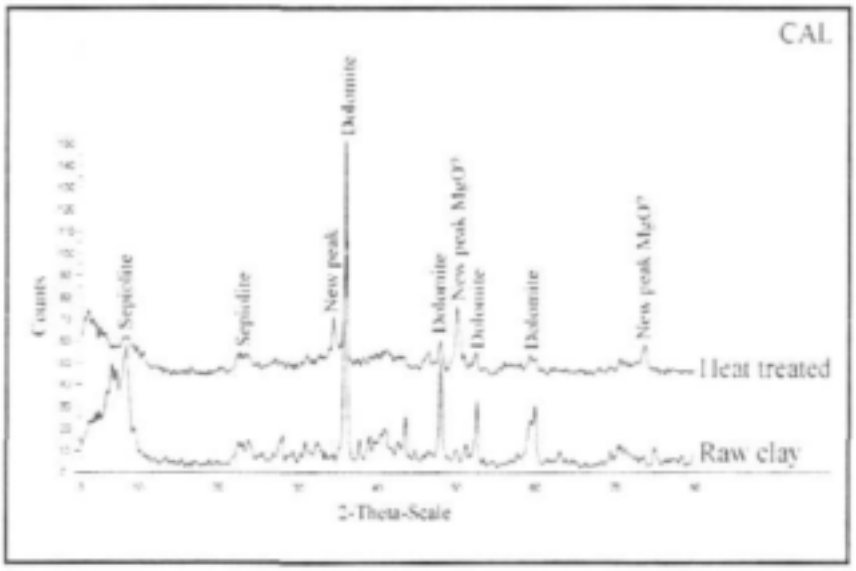

Figure 4.7 X-ray diffractogram for CAL showing structural changes after heating at 600°C for 2 h

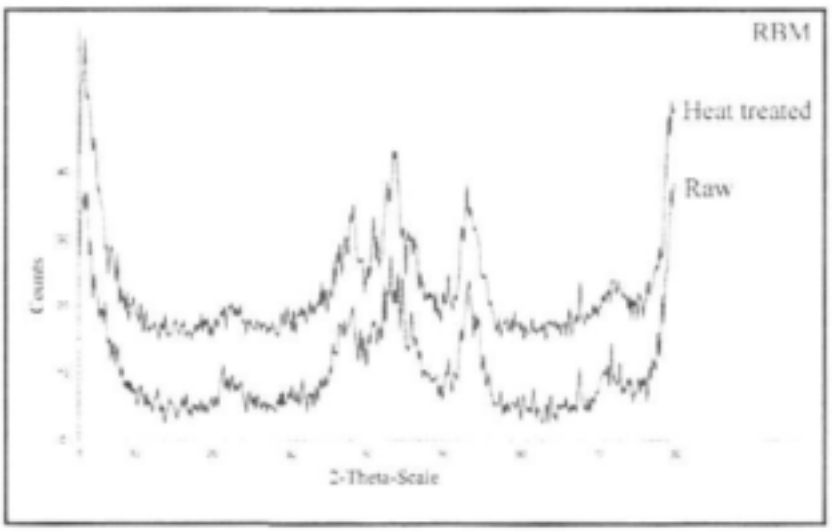

Figure 4.8 X-ray diffractogram for RBM showing structural changes after heating at 600°C for 2 h

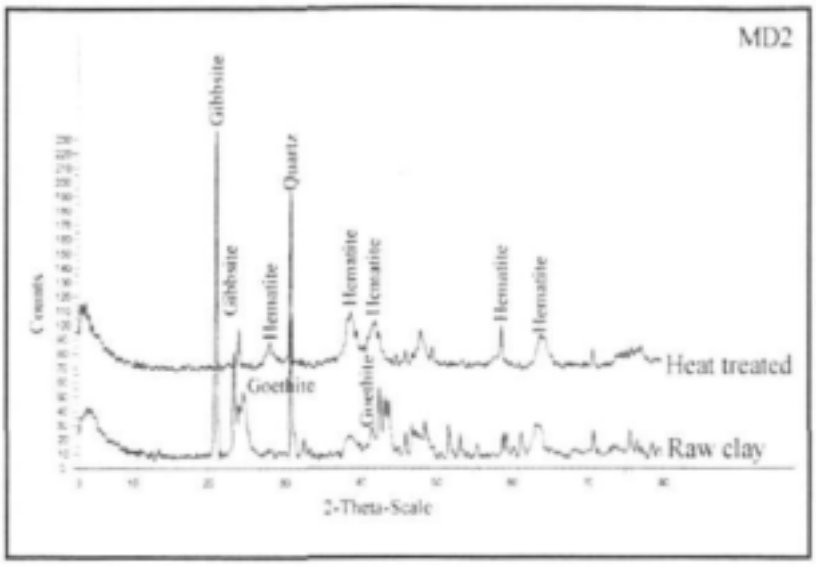

Figure 4.9 X-ray diffractogram for MD2 showing structural changes after heating at 600°C for 2 h

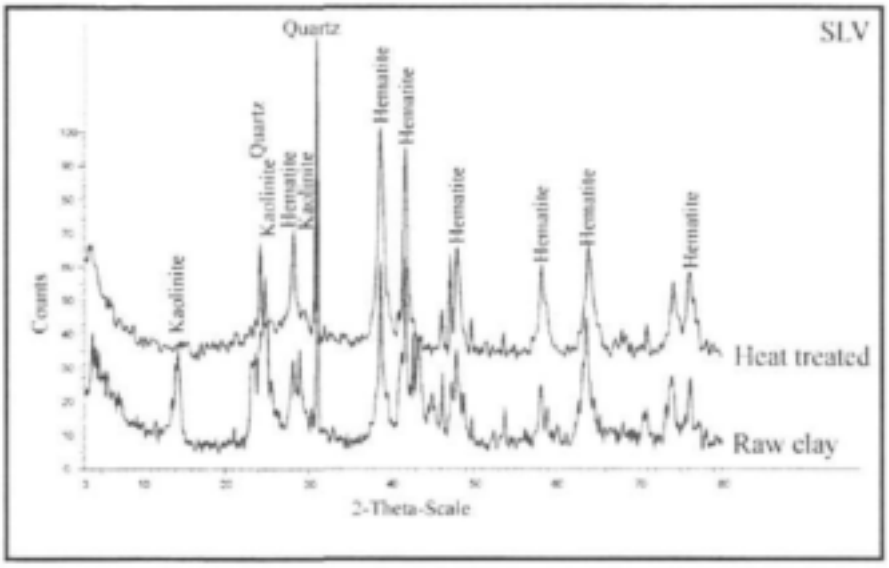

Figure 4.10 X-ray diffractogram for SLV showing structural changes after heating at 600°C for 2 h

(e) Interpretation of adsorption capacities in terms of structure and elemental composition

To assess the contribution of amorphous components to the overall F^- adsorption capacity of clays, an ammonium oxalate extraction was performed. The F^- adsorption capacity was determined before and after the extraction. The clays MD2 and SLV contain gibbsite and

goethite and are therefore likely to also have substantial amounts of amorphous aluminium and iron oxides as a result of weathering. The results show a drop of ca. 70% in the adsorption capacity for MD2 at pH6 and a drop of ca. 80% for SLV after extraction. This would indicate that amorphous Al and Fe oxides play a very important role in the adsorption capacities of the clays. Ammonium oxalate is used to dissolve by complexation Al and Fe from amorphous phases in clays and soils (Parfitt, 1989).

The major element composition of selected clay samples was determined by XRF by Set Point Technologies. The results given as % metal oxide are given in Table 4.5. and provide support for the positive correlation between adsorption capacity and the amount of Al and Fe oxides present in the clays.

TABLE 4 .5 Major element composition of selected clay samples and adsorption capacity (% metal oxide)

Oxide	ALU	RBM	MD2	CAL	SLV
% Ads	100	80	80	60	67
SiO_2	0	0	9.7	25.3	25.5
Al_2O_3	100	92.9	32.0	2.2	17.5
Fe_2O_3	0	0.04	31.1	1.24	41.5
TiO_2	0	0	3.04	0.11	2.61
CaO	0	0.03	0	14.2	0.02
MgO	0	0	0	21.6	0
LOI	0	6.34	23.0	34.6	12.1

The data clearly show that the adsorption capacity decreases as the Al and Fe oxide content decrease. In the case of CAL, the Al and Fe oxide content is low but the adsorption capacity is still relatively high. CAL is a dolomitic clay and the high Ca and Mg content provides an alternative mechanism for F removal from the solution as discussed above. The high loss on ignition (LOI) of 35% reflects the decomposition of Ca and Mg carbonates in their respective oxides and the concomitant release of CO_2.

(f) Leaching of impurities from substrates during adsorption

Leaching of impurities from clays during adsorption could have adverse health effects if these impurities are of a toxic nature, Al being potentially the most problematic. The metals Al, Fe, Cu, Ca, Mg, Cr, Mn, Ni, Zn, and As were determined in leachates by ICP-OES (see Section 9 of Appendix B) after 5 g of clay was extracted with water and 10 $mgF.L^{-1}$ solutions for 2 h. The results are summarised in Table 4.6 for clays washed with water only and clays that were chemically pretreated.

TABLE 4.6 Metal impurities ($mg.L^{-1}$) in clay leachates extracted with 10 $mg.L^{-1}$ fluoride solutions before and after chemical pre-treatment with 0.1 M Na_2CO_3 and 1% HCl

Metal	DL*	ALU Before	ALU After	RBM Before	RBM After	MD2 Before	MD2 After	SLV Before	SLV After	CAL Before	CAL After
Al	0.10	**1.15**	< DL	**3.67**	< DL	< DL	< DL	< DL	< DL	**0.71**	**1.68**
As	0.05	< DL	< DL	< DL	< DL	< DL	< DL	< DL	< DL	< DL	< DL
Ca	0.05	**2.68**	**0.23**	< DL	< DL	**0.18**	< DL	**1.4**	< DL	**4.64**	**115**
Cr	0.05	< DL	< DL	< DL	< DL	< DL	< DL	< DL	< DL	< DL	< DL
Cu	0.02	< DL	< DL	< DL	< DL	< DL	< DL	< DL	< DL	**0.02**	< DL
Fe	0.05	< DL	< DL	< DL	< DL	< DL	< DL	< DL	< DL	**0.51**	< DL
Mg	0.05	**0.11**	< DL	< DL	< DL	**0.06**	< DL	**0.58**	< DL	**10.9**	61.5
Mn	0.02	< DL	< DL	< DL	< DL	**0.23**	< DL	< DL	< DL	< DL	< DL
Ni	0.05	< DL	< DL	< DL	< DL	< DL	< DL	< DL	< DL	< DL	< DL
Zn	0.05	< DL	< DL	< DL	< DL	< DL	< DL	< DL	< DL	< DL	< DL

*DL is detection limit of analytical method

It is clear that in the case of ALU and RBM, both being aluminium oxide containing substrates, chemical pre-treatment reduced the amount of Al leached out to below the detection limits of the analytical method. The reverse result was obtained for CAL, a dolomitic clay, where chemical pre-treatment increased the release of Al. The use of dolomitic clays for fluoride removal is therefore not advisable since Al levels in the leachate before and after chemical treatment are too high. For the other substrates chemical treatment effectively cleans the material to such an extent that metal impurities in the leachate are neglible.

4.5 LABORATORY SCALE COLUMN DEFLUORIDATORS

(a) Introduction

Mini columns packed with sorbent were used to study the suitability of selected clays to be used in defluoridation columns. The main objective was to compare the results obtained using the batch type adsorption procedure discussed above with that from the dynamic type adsorption conditions found in column adsorption. Important factors that were studied included: the rate of $F^- - OH^-$ exchange relative to flow rate through the column, column capacity, regeneration efficiency, and the effects of flow rate, pH and concentration on column performance.

(b) Column design and operational conditions

Mini columns consisted of 180 x 14 mm glass tubes fitted with no 1 porosity frits on both ends. The columns were connected to a Gilson Minipuls 3 peristaltic pump using Tygon tubing. Columns were typically packed with 4 g sorbent. The flow direction was from bottom to top. The pH of F^- feed solutions were adjusted to pH 6 to ensure proper conditions for adsorption to occur. A description of the procedure is given in Appendix B Section 10.

Clay samples were washed with deionised water until F^- free, dried at 105°C, compacted in a Perkin Elmer pellet press at 5t (pellet diameter was 35 mm), heat treated at 600°C for 2 h, cooled in a desiccator, and crushed in a Siebtechnik mill to particle size < 2 μ. This procedure was followed to stabilise the clay samples to prevent loss of small particles during column operation.

(c) Breakthrough volumes and column capacities

Breakthrough volumes and column capacities were determined for activated aluminium (ALU) samples at different flow rates using a 4 g column packing and a 10 $mg.L^{-1}$ F^- feed solution.

Column capacities given in Table 4.7 were calculated from the breakthrough volumes determined from curves for residual F^- vs time curves shown in Figure 4.11.

TABLE 4 .7 Breakthrough volumes, residual F concentrations in non-saturated columns, and columns capacities for a column with 4 g activated aluminium and a 10 $mg.L^{-1}$ F^- test solution. Flow rate 4 $mg.L^{-1}$

Flow rate ($mL.min^{-1}$)	**Residual [F^-] ($mg.L^{-1}$)**	**Breakthrough time (m)**	**Breakthrough vol (mL)**	**Adsorption capacity ($mg.g^{-1}$)**
2	0.6	520	1040	2.7
4	0.8	260	1040	2.7
8	1.0	100	800	2
10	1.2	75	750	1.9

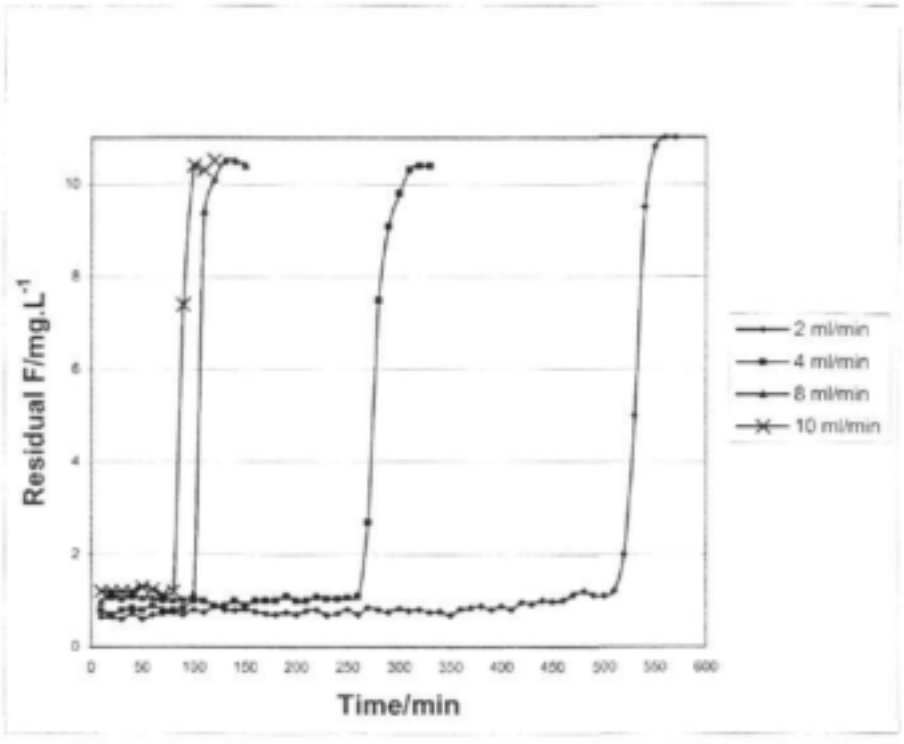

Figure 4.11 Residual F^- concentration vs time after passage of a 10 $mg.L^{-1}$ F^- feed solution through a 4 g activated alumina column at different flow rates.

The curves show that the residual concentrations for non saturated columns increased with flow rate from about 0.5 to 1.2 $mg.L^{-1}$ – a clear indication that exchange kinetics required a limit to the flow rate at about 2 $mL.min^{-1}$ in order to maintain a F^- at the ideal level at 0.6 $mg.L^{-1}$. The drop in adsorption capacity as the flow rate increased also point to a limitation on flow rates because of kinetic considerations.

(d) Concentration limitations

The effect of F^- concentration in the feed solution on column capacity and column efficiency was studied for an activated aluminium column. The results are given in Table 4.8 and Figure 4.12.

TABLE 4.8 Breakthrough volumes, residual F^- concentrations in non-saturated columns, and column capacities for a column packed wit 4 g activated aluminium at different feed solution concentrations. Flow rate 4 $mL.min^{-1}$.

Feed [F^-] ($mg.L^{-1}$)	Residual [F^-] ($mg.L^{-1}$)	Breakthrough time (m)	Breaktrough vol (mL)	Adsorption capacity ($mg.g^{-1}$)
5	0.8	560	1020	2.6
10	0.9	260	1040	2.7
20	1.6	120	480	2.8
50	2.5	70	280	3.5

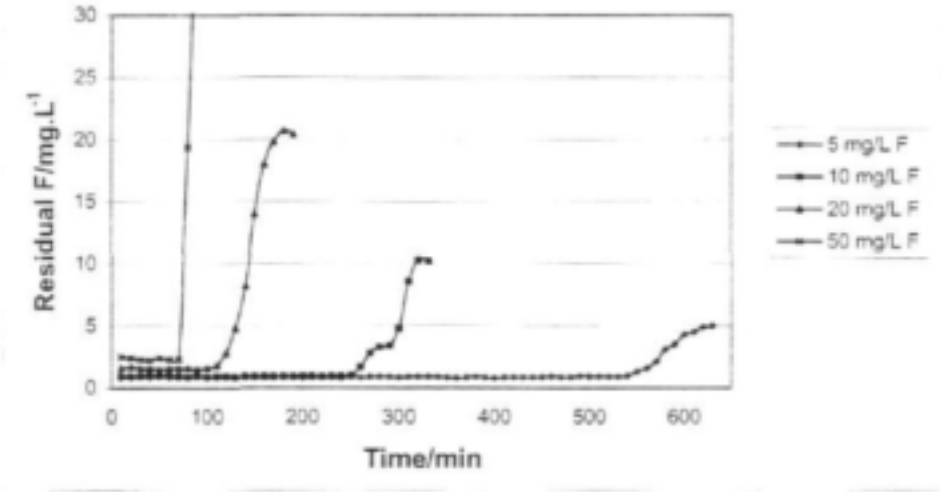

Figure 4.12 Residual F^- concentration vs time after passage of different feed solution concentrations through a 4 g activated alumina column at a flow rate of 4 $mL.min^{-1}$

As was expected the concentration of the feed solution is a determining factor in the efficiency of the column. Residual F^- concentrations for non-saturated columns increased from 0.8 to 2.5 $mg.L^{-1}$ as the feed concentration increased from 5 to 50 $mg.L^{-1}$. At a flow rate of 4 $mL.min^{-1}$ a feed volume concentration limit of ≤ 10 $mg.L^{-1}$ is required to maintain a residual F^- concentration below 1 $mg.L^{-1}$.

(e) Regeneration procedures

The efficiency of column regeneration with 0.1 M Na_2CO_3 and 1% HCl was studied using activated alumina (ALU) and aluminium oxide (RBM) packings of 2 g, flow rates of 4 $mL.min^{-1}$ and feed concentrations of 10 $mg.L^{-1}$. The procedure is described in Appendix B. The results obtained after successive regenerations are shown in Figure 4.13 for ALU and Figure 4.14 for RBM. It is evident that even after 10 regenerations the breakthrough volumes and hence the adsorption capacities of the columns did not deteriorate very much. In Table 4.9 the column capacities and residual F^- concentrations are given for successive regenerations. Residual F^- concentrations show only a small increase after each regeneration, about 20% for ALU and 30% for RBM. Adsorption capacities show the same trend namely a 15% decrease for ALU and a 30% decrease for RBM, after successive regeneration.

TABLE 4.9 Column capacities and residual F concentrations for successive regenerations of 2 g packings of ALU and RBM. Flow rate 4 mL.min^{-1}. FEED [F$^-$] = 10 mg.L^{-1}

Regeneration no.	ALU Residual [F$^-$] (mg.L^{-1})	RBM Residual [F$^-$] (mg.L^{-1})	ALU Breaktrough vol (mL)	RBM Breaktrough vol (mL)	ALU Adsorption capacity (mg.g^{-1})	RBM Adsorption capacity (mg.g^{-1})
1	0.95	1.0	480	400	2.4	2.0
2	0.90	1.2	480	400	2.4	2.0
3	1.01	1.1	440	360	2.2	1.8
4	0.95	1.2	520	360	2.6	1.8
5	1.11	1.3	440	400	2.2	2.0
Ave 1st 5	**0.98**	**1.2**	**472**	**384**	**2.4**	**1.9**
6	1.20	1.1	400	360	2.0	1.8
7	1.12	1.3	400	240	2.0	1.2
8	1.20	1.4	480	320	2.4	1.6
9	1.18	1.4	480	240	2.4	1.2
10	1.20	1.3	440	200	2.2	1.0
Ave 2nd 5	**1.18**	**1.3**	**440**	**272**	**2.2**	**1.4**

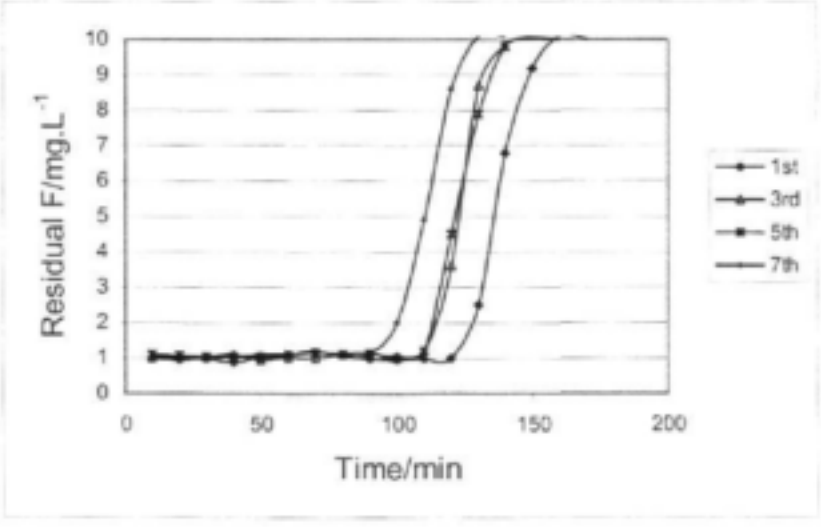

Figure 4.13 Residual F$^-$ concentration vs time after passage of a 10 mg.L^{-1} F$^-$ feed solution through a 2 g activated alumina (ALU) column at a flow rate of 4 mL.min^{-1} after successive regenerations.

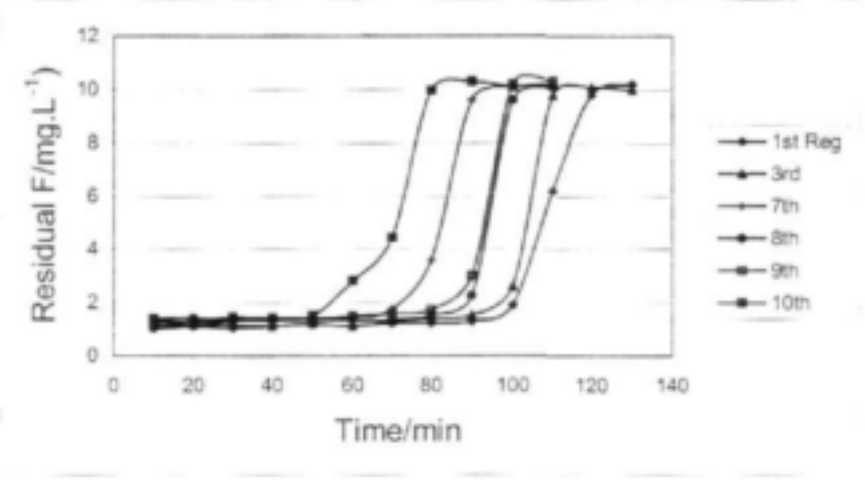

Figure 4.14 Residual F^- concentration vs time after passage of a 10 $mg.L^{-1}$ F^- feed solution through a 2 g aluminium oxide (RBM) column at a flow rate of 4 $mL.min^{-1}$ after successive regenerations.

(f) Column capacities for selected clay packings

The suitability of selected clay packings for use in defluoridation columns was compared by determining adsorption capacities and residual F^- concentrations for non saturated columns. Table 4.10 compares the adsorption capacities and residual F^- concentrations for 4 g sorbent and a feed solution of 10 $mg.L^{-1}$ F^- passed through a column at 4 $mL.min^{-1}$. Breakthrough curves for ALU, RBM, CAL, SLV, MD2, MD4 and RYE are shown in Figure 4.15. It is clear that the ability of natural sorbents to remove F^- from solution is not nearly comparable with the activated alumina here used as benchmark. RBM, amorphous aluminium oxide, however has excellent F^- removal characteristics, not too much different from that of activated alumina. This oxide is obtained from processed Australian bauxite ore, and is available in large quantities at Richardsbay Minerals where it is used as feedstock for the aluminium smelter. It is a relatively cheap and easily available substance. Of the South African clays only MD2 which is a low grade bauxite, shows any potential as sorbent for F^- removal. Its performance is similar to that of SLV, the Sri Lankan clay used in clay brick defluoridation in that country. The residual F^- concentrations are ranging from 0.8 for ALU through 1.2 for RBM, 1.4 for MD2 and 1.8 for SLV to totally unacceptable levels of 4.5 $mg.L^{-1}$ for MD4 and RYE. MD4 is a low grade South African bauxite from the same area as MD2. This result emphasises the local variability of clays taken from the same deposit. RYE is a laterite with a significant Fe oxide component.

TABLE 4.10 Breakthrough volumes, residual F^- concentrations in non-saturated columns, and column capacities for a column packed with 4 g of different clay sorbent. Feed solution concentrations 10 $mgF.L^{-1}$. Flow rate 4 $mL.min^{-1}$.

Clay ID	Residual [F^-] ($mg.L^{-1}$)	Breakthrough time (m)	Breakthrough vol (mL)	Adsorption capacity ($mg.g^{-1}$)
ALU	0.8	250	1000	2.5
RBM	1.2	180	720	1.8
MD2	1.4	100	400	1.0
CAL	2.1	90	360	0.9
SLV	1.8	70	280	0.7
MD4	4.5	40	160	0.4
RYE	4.2	20	80	0.2

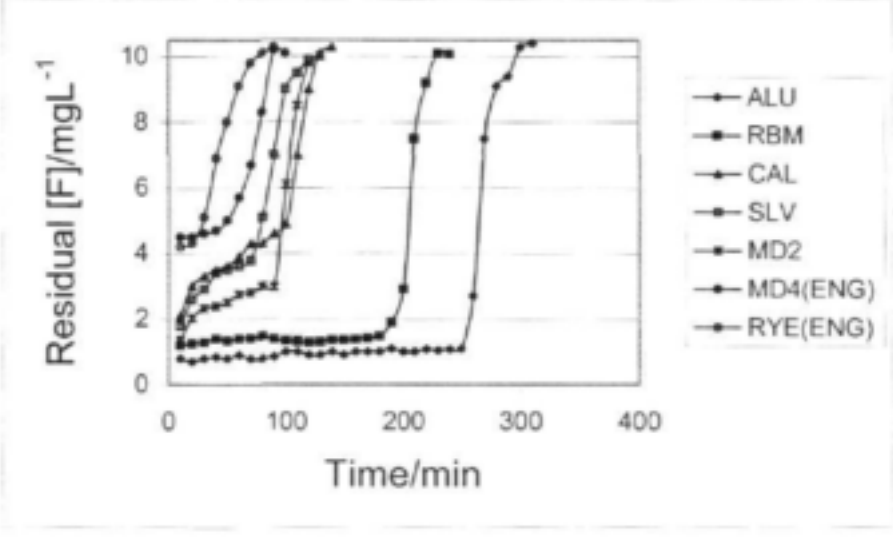

Figure 4.15 Residual F^- concentration vs time after passage of a 10 $mg.L^{-1}$ F^- feed solution through 4 g of different clay sorbents at a flow rate of 4 $mL.min^{-1}$

4.6 DISCUSSION

This study shows that clay types can differ enormously in their adsorption capacities for F^-. Big differences also occur within a specific clay type, even if taken from the same deposit. A trend in adsorption capacity related to clay structure can, however, be observed. Adsorption capacity decreases as the concentration of exchangeable OH groups decreases. Clay types consisting of the metal oxides of Fe and Al were found to have the best potential as sorbents for F^- from aqueous solutions.

Chemical and physical pre-treatment increased the adsorption capacity in some clay types where the protonation of the surface during acid treatment could create a surface with positive charge.

The bauxitic clays and a processed bauxite (amorphous aluminium oxide) showed the best overall potential to be used as defluoridation sorbents.

4.7 REFERENCES

BÅRDSEN A and BJORVATN K (1995). Fluoride sorption isotherm on fired clay. Proc. 1st Int. Workshop on fluorosis and defluorication of water. *Publ. Int. Soc. Fluorid Res.* 46-49.

BARNARDO DJ (1998). Aluminium. In: Wilson MGC and Anhaeusser CR (eds.) *The mineral resources of South Africa.* Handbook, Council for Geoscience **16**, 46-52.

BOWER CA and HATCHER JT (1967). Adsorption of fluoride by soils and minerals. *Soil Sci.* **103**, 151-154.

BROWER ID, BACKER DO, DE BRUIN A and HAUTVAST JGAJ (1988). Unsuitability of WHO guidelines for fluoride concentrations in drinking water in Senegal. *The Lancet* **1**(8579), 223-225.

CHATURVEDI AK, PATHAK KC and SINGH VN (1988). Fluoride removal from water by adsorption on China clay. *Appl. Clay Sci.* **3**, 337-346.

CHATURVEDI AK, YADAVA KP, PATHAK KC and SINGH VH (1990). Defluoridation of water by adsorption on fly ash. *Water, Air and Soil Pol.* **49**, 51-61.

CHHABRA R, SINGH A and ABROL IP (1980). Fluorine in sodic soils. *Soil Sci. Soc. AM. J.* **44**, 33-36.

FOSS PJ and PITTMAN JM (1986). Efficacy of fluoride on dental caries reduction by means of a community water supply. *J. Dent. Child.* **53**, 219-222.

HAO OJ, ASCE AM, HUANG CP and ASCE M (1986). Adsorption characteristics of fluoride onto hydrous alumina. *J. of Environ. Eng.* **112(6)**, 1054-1069.

HAUGE S, ÖSTERBERG R, BJORVATN K, SELVIG KA (1994). Defluoridation of drinking water with pottery: effect of firing temperature. *Scand. J. Dent. Res.* **102**, 329-333.

HORN GFJ and STRYDOM JH (1998). Clay. In: Wilson MGC and Anhaeusser CR (eds.) *The mineral resources of South Africa.* Handbook, Council for Geoscience **16**, 46-52.

KAU PMH, SMITH DW and BINNING P (1997). Fluoride retention by kaolin clay. *Journal of Contam. Hydrol.* **28**, 267-288.

McCAFFREY LP and WILLIS JP (2001). Distribution of fluoride-rich groundwater in the Eastern and Mogwase regions of the Northern and North West Provinces. *WRC Report No 526/1/01.*

MOGES G, ZEWGE F and SOCHER M (1996). Preliminary investigations on the defluoridation of water using fired clay chips. *J. of Afr. Earth Sci.* **21**(4), 479-482.

OMUETI JAI and JONES RL (1977) Fluoride adsorption by Illinois soils. *J. of Soil Sci.* **28**, 546-572.

PADMASIRI JP and ATTANAYAKE MASL (1991) Reduction of iron in groundwater using a low cost filter unit. *J. of the Geol. Soc. of Sri Lanka* **3**, 68-77.

PUKA LR (2003) Fluoride adsorption modelling and the characterisation of clays for defluoridation of natural waters. MSc Thesis (RAU).

SCHOEMAN JJ and MACLEOD H (1987). The effect of particle size and interfering ions on fluoride removal by activated alumina. *Water SA* **13**(4), 229-234.

SCHOEMAN JJ and STEYN A (2000). Defluoridation, denitrification and desalination of water using ion-exchange and reverse osmosis technology. *WRC Report TT* 124/00.

SRIMURALI M, PRAGATHI A and KARTHIKEYAN J (1998). A study on removal of fluorides from drinking water by adsorption onto low-cost materials. *Environ. Pollut.* **99**, 285-289.

WANG Y and REARDON EJ (2001). Activation and regeneration of a soil sorbent for defluoridation of drinking water. *App. Geochem.* **16**, 531-539.

ZEVENBERGEN C, VAN REEUWIJK LP, FRAPPORTI G, LOUWS RJ and SCHUILING RD (1996). A simple method for defluoridation of drinking water at village level by adsorption on Ando soils in Kenya. *Sci. of the Total Environ.* **188**, 225-232.

CHAPTER FIVE

PREPARATION OF CLAY PELLETS

5.1 SELECTION AND DESCRIPTION OF CLAYS

A key requirement for any defluoridation technology based on clay, is that the clay must be effectively immobilised. In other words, it has to prepared in such a way that it will not impart turbidity, colour, taste or any other offensive impurities to the water. In order to conduct a systematic investigation into this immobilisation process, as well as the defluoridation efficiency of the immobilised clay, a large stockpile of each clay had to be prepared which would provide a consistent supply throughout the duration of the project.

Following the extensive survey and testing of clays reported in the preceding chapters, four clays were selected for large-scale testing:

- MD2 – obtained from near Mooi River in Natal. It is a bauxitic clay of dry red appearance with a fine powdery structure.
- KOP – obtained from near Koppies in the Freestate. It is a bentonitic clay, greenish in its natural state and brownish white after baking. It is slightly moist with a loose granular structure.
- RYE – named after the farm from which it was obtained in Limpopo. It is a lateritic clay, red rusty in appearance. The material is coarse, brittle and hard with large particles in its natural state.
- ZEB – obtained from near the Zebediela estate in Limpopo. It is a white palygorskite with a dry, loose, granular structure.

Approximately one tonne of each of these clays were excavated and brought by road transport in bags to the campus of the Rand Afrikaans University.

5.2 DRYING, CRUSHING AND SIEVING

Upon delivery, all the clays were spread out on plastic sheets in thin layers and left for about one week in the sun. All roots, larger stones and other debris were hand-picked from the layers and discarded.

The clays were then put into a concrete mixer in smaller batches together with three large steel balls to resemble a rudimentary ball mill. After about ten minutes of rotation, the clay was ejected and sieved through a sheet sieve with apertures of 4,36 mm. In the case of RYE, the clay had to be milled much longer in the concrete mixer before the clay lumps were significantly broken down. Both the "through" and the "retained" fractions were then stored in sealed 200 litre steel drums. The "through" fraction was between about 20% and 50% of the total clay volume. The "retained" fractions were kept as backup should more clay be required, but it was not necessary. All the clay requirements of the project could be met from the initial "through" fractions.

Upon removal from the stockpiles, the smaller quantities of clay used for laboratory testing were finally sieved by hand through a standard 1,18 mm sieve used for geotechnical sieve analyses, to obtain a reasonably homogeneous material for compression, baking and other laboratory analyses.

5.3 OPTIMAL PELLET MANUFACTURING CONDITIONS

5.3.1 Optimal baking conditions

The baking of clay is a common industrial process and well described. Upon heating, the first chemical reaction occurs at about 350°C when the water combines with the silica in the clay. At 500°C the dehydration process is complete and the chemical composition of the clay is permanently altered. After 500°C vitrification starts which makes the clay hard, glossy and non-porous (Reader's Digest, 1979).

Initial tests at a baking temperature of 400°C produced, for all the clays, an unstable product which crumbled upon handling. A fixed baking temperature of 600°C was then adopted, a temperature choice which is also supported by work reported in an earlier chapter.

A final concern related to the baking process is the rate at which the clay is heated. The temperature should be increased slowly to allow moisture pockets to evaporate without forming steam, otherwise the clay structure will be damaged by the rapid release of steam. Practical guidelines suggest a heating rate of no more than 10°C/minute. For the duration of this project, the kiln was programmed to raise the temperature to 600°C over a period of two hours, or an equivalent rate of about 5°C/minute. The temperature was then maintained for two hours, after which the kiln was allowed to cool down naturally. Ambient temperatures were typically reached after a cooling down period of four hours.

5.3.2 Manufacture of pellets

During the first series of tests, a hydraulic press was used to compress the clay into flat discs with a diameter of 64 mm and thickness of about 8 mm. Pressures of 5, 10 and 15 MPa were used. During the second series of tests, a compression method was developed which could conceivably also be used for full-scale production should the method be later applied in a rural setting. This method entailed the use of a screw press where the pressure is applied through a torque wrench. With this method, the pressure is limited by the physical strength of the operator. By calibration of the screw press and the design of a series of special moulds, pressures of 8,5 MPa and 11,7 MPa could be applied on discs 40, 25 and 12 mm in diameter.

The easiest, simplest manufacturing method is obviously when the clay is simply pressed and baked without any additives – the sundried clay is then simply put into the moulds and pressed. This worked fine for the clays MD2 and KOP. For RYE and ZEB, however, this process did not yield stable pellets and it was clear that some additives were required.

At this point of the investigation, adsorption tests by the Department of Chemistry showed ZEB to have inadequate adsorption potential and this clay was therefore omitted from all further work.

The lack of stability for RYE was found to be its lack of plasticity, as determined by a standard geotechnical test (NITRR, 1986). The plasticity index of RYE was –2 (practically zero), compared to values of +6 for MD2 and +36 for KOP. Some tests were therefore conducted with water (between 2% and 4%) and cement (8%) as stabilisers. Although some stability was gained, the products imparted a yellowish tinge to water upon contact, which was not acceptable. Further tests with water alone did provide stability, provided the moisture content was closely kept between 7% and 8%. At 5% the product disintegrated upon contact with water, and at 10% the pellets crumbled upon release from the mould.

The final preparation methods adopted were:

- For KOP, there is no need for water. The clay is easily compressible and remains stable after compression and baking.
- For MD2, there is also no need for water. Its fine structure causes the clay to cling to the mould, necessitating frequent cleaning.
- For RYE, the optimum moisture content is 8%, which should be strictly adhered to if the pellet is to remain intact after compression and baking.
- In all cases, compression at about 10 to 12 MPa leads to good results.

5.4 PROPERTIES OF CLAY PELLETS

5.4.1 Consolidation

In all cases, the moulds were filled with loose clay, scraped level en then compressed. As the pressure is applied, there is rapid initial consolidation at first with slower consolidation towards the end. At a pressure of 11,7 MPa, the consolidation was 41% for MD2, 37% for KOP and 24% for RYE.

5.4.2 Water adsorption

It is important that the pellets have a fairly high internal porosity to provide the micropores necessary for efficient adsorption. A simple test was devised whereby the pellets were cooled overnight, weighed and then immersed in water for 24 hours. The surfaces were then dried by blotting paper and the pellets reweighed. The weight increase is then an indication of the internal porosity.

There are only small differences in weight increase over the pressure range 5 to 15 Mpa. At a pressure of 11.7 MPa, the mass increase ranged between 24% to 32% for all the clay types, indicating a fairly open pore structure.

5.4.3 Effect on water quality by leaching

The water to which the pellets were exposed for 24 hours in the water adsorption test described above, was tested for turbidity. Although all tests were preformed in triplicate, the turbidity values were erratic and did not follow a clear trend with either clay type or pressure. In general, the turbidity values were between 1 and 5 NTU. This may seem quite high, but it is more reliably measured in a larger household scale column, as will be reported in the next chapter.

5.4.4 Effect on water quality by abrasion

The pellets, after the water adsorption test, were suspended in a beaker directly above a magnetic stirrer bar for a predetermined time at a predetermined speed. After the test, the water was tested for turbidity. The hypothesis was that this is a much more vigorous test than leaching and that a larger response would be measured.

Surprisingly, very lower or comparable with the leaching values were measured, indicating that the pellets, which were quite fragile during handling, are surprisingly stable once they are firmly positioned in water.

5.5 DISCUSSION

Water defluoridation by clay can only work if the clay can be effectively immobilised to keep the water clean and potable after treatment. A significant part of the total effort was thus devoted to a systematic investigation into the best and easiest way to achieve this. Although the emphasis of this project is to demonstrate the *technical feasibility* of water defluoridation by clay and not necessarily to develop the technology to a *practical, economical* and *sustainable* level, the results of this chapter nevertheless are also promising pointers towards full-scale implementation. The main findings of this chapter are:

- Of the three remaining candidate clays (after adsorption tests eliminated the fourth), practical methods could be developed to produce clay pellets that were stable.
- This could be achieved by using two of the clays directly in a sun-dried form, and by adding only water to the third.
- The compression could be done with a manual press requiring no other power source and a simple set of moulds.
- The baking required a sustained temperature of 2 hours at about 600°C.
- The pellets produced had a fairly high internal porosity, which boded well for its eventual adsorption capacity.
- There was no serious turbidity increase of the water exposed to the pellets, and tests in larger, more quiescent reactors may have smaller effects.

5.6 REFERENCES

Petersen, Z.G. (2002) The Stabilisation of Clay Pellets Used for Water Defluoridation. Undergraduate Thesis, submitted to the Department of Civil Engineering, Rand Afrikaans University.

CHAPTER SIX

DEFLUORIDATION EFFICIENCY

6.1 EXPERIMENTAL DESIGN

The final part of the investigation measured the defluoridation efficiency of clay pellets under simulated household conditions. Three questions had to be answered:

- How is the defluoridation efficiency affected when the clay powder is compressed to clay pellets? This question was answered by conducting conventional isotherm tests on the clay powder (baked at different temperatures) as well as through a specially devised test to attain equilibrium with a number of clay pellets.
- How well do clay pellets perform in a pipe reactor under simulated household conditions? This question was addressed by two extended tests in a long pipe reactor similar to that used in Sri Lanka – termed the Type 1 reactor.
- How is the defluoridation efficiency affected by pellet size and pH? This question was addressed with a number of accelerated tests in short pipe reactors – termed the Type 2 reactor.

A stockpile of clay pellets was manufactured according to the procedures developed in the previous chapter and used alongside the original clay stockpiles for all the tests performed in this chapter. The column testing was done over a period of approximately six months, running the reactors continuously.

The initial intention was to conduct all the column tests with a long Type 1 reactor. This reactor, however, contains a large number of pellets with a large adsorption capacity which had to be operated for a month or longer to get a conclusive result. After two of these experiments, another alternative had to be adopted to be able to include a larger matrix of variables within the time available for this project. The columns were therefore significantly reduced in size to a Type 2 reactor (thereby limiting the adsorption capacity of the pellets) and higher fluoride concentrations were fed to the reactors (to exhaust the adsorption capacity more rapidly). The latter number of experiments were therefore all done with the Type 2 reactors.

6.2 ANALYTICAL METHODS

6.2.1 Solutions

In all cases laboratory reagents were utilized. The test solution was made by diluting sodium fluoride with tap water and made to concentrations of 30 and 50 mg/l. The concentrated solutions were utilized in order to speed up the time it took to exhaust the clay media. In the fluoride determinations, TISAB IV solution was utilized as prescribed in Standard Methods (No. 1551).

6.2.2 Analytical Equipment

For the fluoride determination, an ORION Ion Selective Electrode coupled to a Phillips pH/mV meter was utilized. pH determinations were done using an ORION meter which had

its input fed from a pH probe. Reagent mass determinations were carried out using Phillips mass balance (.000g resolution). Turbidity was measured with a HACH RATIO turbidimeter.

6.2.3 Isotherm Tests

For the tests done with powdered clay, the material was crushed and sieved through a 1,18 mm sieve. Quantities of 25g, 50g, 75, and 100g were placed in 300ml beakers to fluoride solutions of 250ml each. The suspensions were then agitated for 3 hours on a shaker table. A small volume of each suspension was filtered and 5ml used for the measurement of the remaining fluoride concentration. Except for one test, the pH of the water was not adjusted and stayed at about pH 8,2.

To obtain isotherms for the clay pellets, a different strategy had to be followed. In this case, a number of pellets (total mass 135,5 g) were placed in a small column. A fixed volume of 1000 ml of a known fluoride concentration was then continuously circulated through the column with a pump. After 24 hours, the remaining fluoride concentration was measured. This provided one data point. Three data points, each with a different starting fluoride concentration, were thus obtained for each clay.

The 24 h circulation time of the fluoride solutions was empirically determined. One test for each clay was continued for almost two days and the remaining fluoride concentration measured intermittently. The results are shown in Figure 6.1 below. From this graph, a standard circulation time of 24 h was then adopted for all subsequent tests.

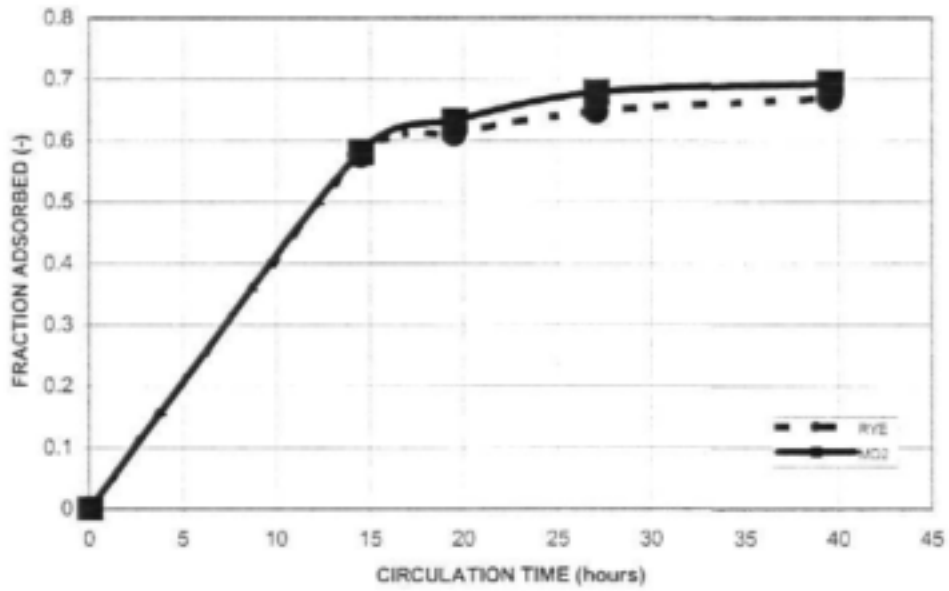

Figure 6.1 Determination of circulation time of 24 hours

6.2.4 Column Tests

Figure 6.2 depicts a schematic of the experimental setup used. Hundred litres of fluoride-rich water was then pumped through a column packed with the pellets under study. Product water from the column was led (initially) to an automatic sampler, which had 24 sample bottles. The auto sampler was programmed to take a 50 ml sample at hourly intervals. On later experiments, product water was piped into small plastic containers that had been slit at their

50 ml mark. This means that a sample collected would have been continuously averaged over a 24 hour's interval.

In order to achieve the retention times required to achieve the desired adsorption effect, the pump(s) were governed through a computer program that enabled a power supply lasted a few seconds every 6 hourly interval (for example 90 seconds on; 5 hr, 58 mins 30 secs off). This implies that the flow through the system was only semi-continuous.

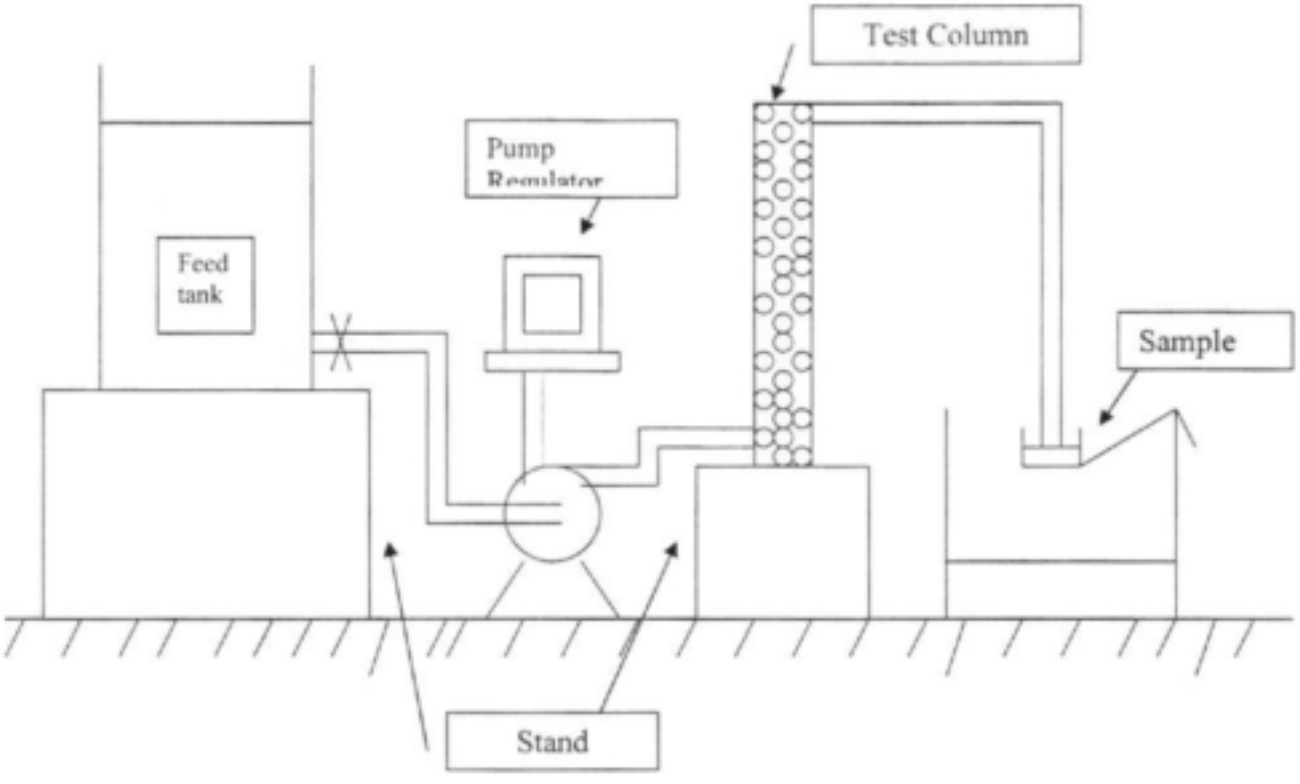

Figure 6.2 Typical Arrangement for Column Tests

6.3 ISOTHERM TESTS WITH POWDERED CLAY

The first tests were done with powdered MD2 and RYE to demonstrate the effect of baking temperature on the adsorption capacity. The results are shown in Figure 6.3 for MD2, and on Figure 6.4 for RYE. The temperature has different effects on the two clays. In the case of MD2, there is a progressive deterioration in adsorption capacity as the baking temperature is increased towards 600°C. For RYE, the adsorption capacity increases as the temperature is raised up to 500°C, and then deteriorates again at 600°C.

The isotherms in Figures 6.3 and 6.4 can be used directly to determine the adsorption capacity of the clay. When the maximum tolerable fluoride concentration is known, the relevant loading capacity of the clay can be read off the graph. The following example is for illustration:

> A water source has a fluoride concentration of 5 mg/l. If the permissible fluoride concentration is 2 mg/l, how much water can be treated by 3 kg of MD2 clay powder baked at 600°C?

From Figure 6.2, it can be seen that 2 mg/l corresponds to a loading of about 0,0001 mg/mg, or 300 mg for every 3 kg of powder. Each litre of water contributes (5-2) = 3 mg to the clay loading. A total of 100 litres can thus be treated.

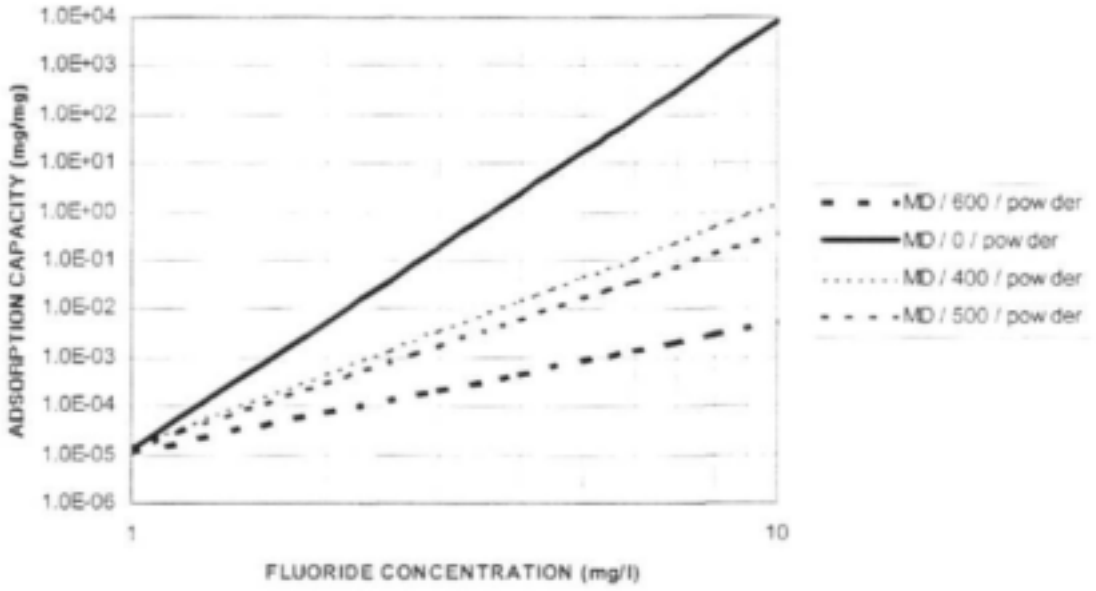

Figure 6.3 Isotherms of MD2 clay powder baked at different temperatures

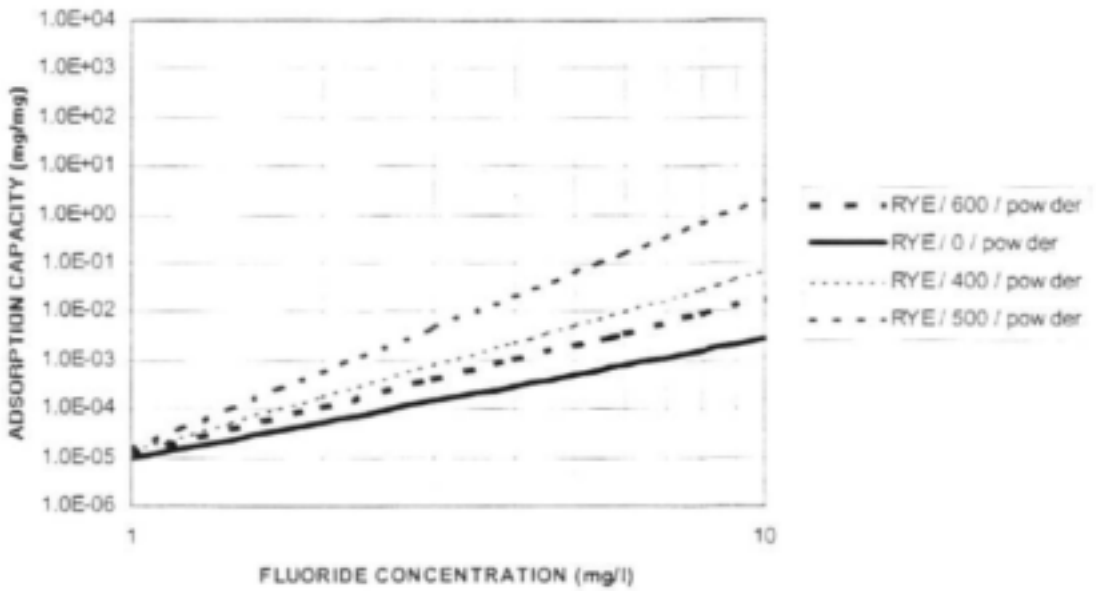

Figure 6.4 Isotherms of RYE clay powder baked at different temperatures

A single test was performed to verify the commonly reported finding that adsorption improves with a reduction in pH. An isotherm was thus determined for MD2 clay powder baked at 600°C for a fluoride solution where the pH was adjusted to pH 5,2 - it would have been about pH 8,2 otherwise. As expected, there was a marked increase in adsorption capacity, as shown below in Figure 6.5.

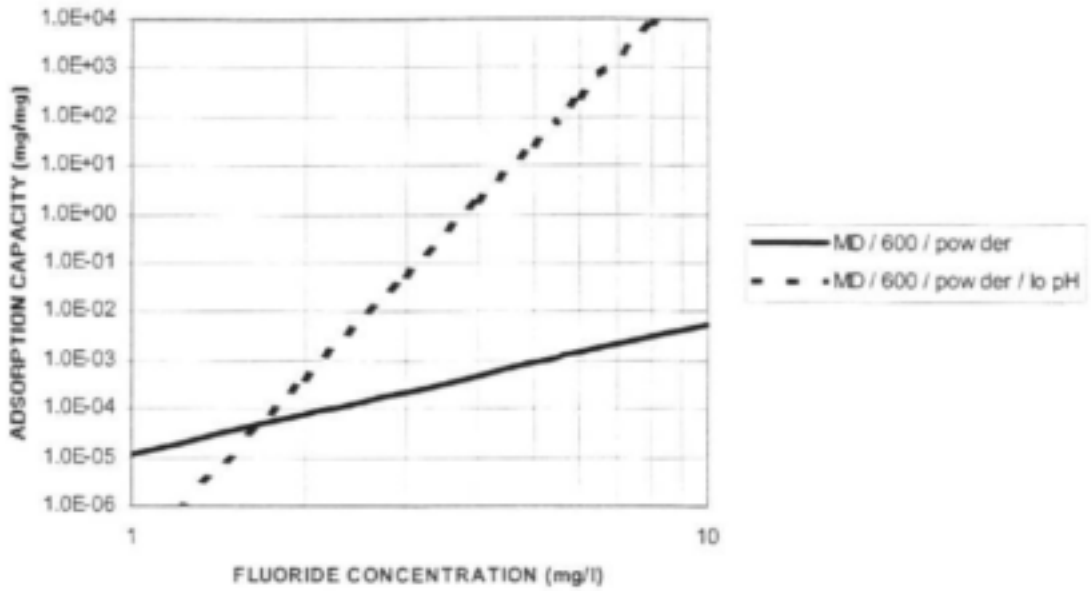

Figure 6.5 Isotherms for MD2 at pH8,2 and pH5,2 respectively

6.4 ISOTHERM TESTS WITH PELLETED CLAY

The test now proceeded to determine the effect of the pelletisation of the clay on its adsorption capacity. Isotherms were thus determined for both MD2 and RYE, on clay pellets baked at 600°C as well as on the same pellets ground back to powder. The comparative results are shown on Figure 6.6.

There are two important points to consider on Figure 6.6. In the first place, there is a decrease in adsorption capacity as one would expect given the extra diffusion step required to move the fluoride to within the macropores of the pellets. In the second place, the fairly large difference in adsorption capacity between the two clay powders are practically eliminated when the pellets are compared. The final line on Figure 6.6 is the adsorption capacity of undisturbed, unbaked RYE lumps which were simply obtained by taking the size fraction between 4,36 mm and 9,6 mm sieve sizes. This was an option pursued in the light of the difficulty to immobilise the RYE clay after milling, but the poor adsorption capacity of the unground lumps sunk this option.

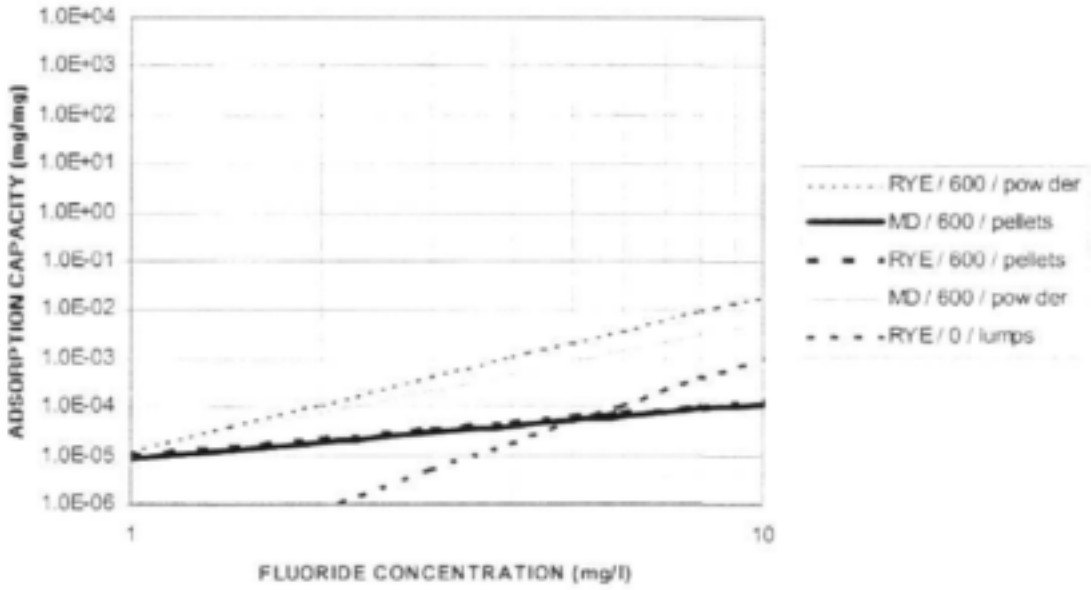

Figure 6.6 Isotherms to show the effect of pelletisation

6.5 COLUMN TESTS WITH THE TYPE 1 REACTOR

Figure 6.7 shows a graph detailing the residual fluoride concentration on the product water discharged from the large cylinder (henceforth referred to a Reactor Type 1). Table 6.1 below summarizes some key parameters pertaining to the reactor.

Table 6.1 Summary of Reactor Parameters for experiment shown in Figure 6.7

Reactor Size	Type I (long column)
Clay Type	MD2
Pellet Size	40 mm
No. of Pellets Packed	50
Void Space	67%
Retention Time	24 hrs
Feed F- Concentration	15 mg l

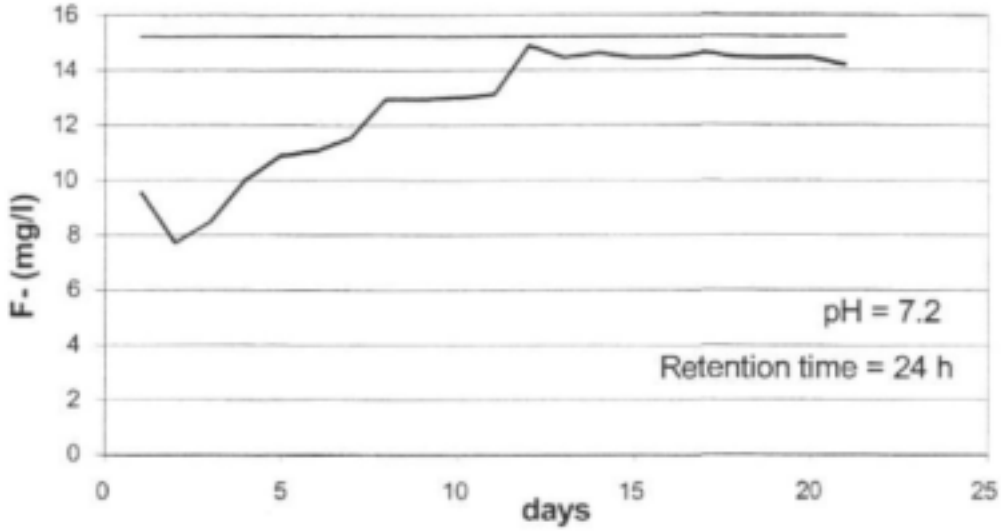

Figure 6.7 Residual fluoride concentration in Reactor Type 1 (clay type = MD2, pH = 7,2, retention time = 24 h, feed concentration 15,2 mg/l)

It can be seen from the figure above that the slight dip over days 2 and 3 can be attributed to the system still rinsing up till the reactor exhibits best performance at about 55% removal. At a feed concentration of 15.2 mg/l, and a retention time of approximately 24 hours, media exhaustion is achieved between day 12 and day 14.

A similar experiment is reported in Figure 6.8. The experimental conditions were similar in terms of the equipment, and clay type. The only difference is that the clay pellets have been filled to slightly more than two thirds of the column volume. As to be expected, with the lower exchange surface area as well as adsorption sites, the initial adsorption performance reduces to about 50%. The general shape of the curve, however, remains similar.

Table 6.2 Summary of Reactor Parameters for experiment shown in Figure 6.8

Reactor Size	Type I (long column)
Clay Type	MD2
Pellet Size	40 mm
No. of Pellets Packed	36
Void Space	67%
Retention Time	24 hrs
Feed F- Concentration	30 mg/l

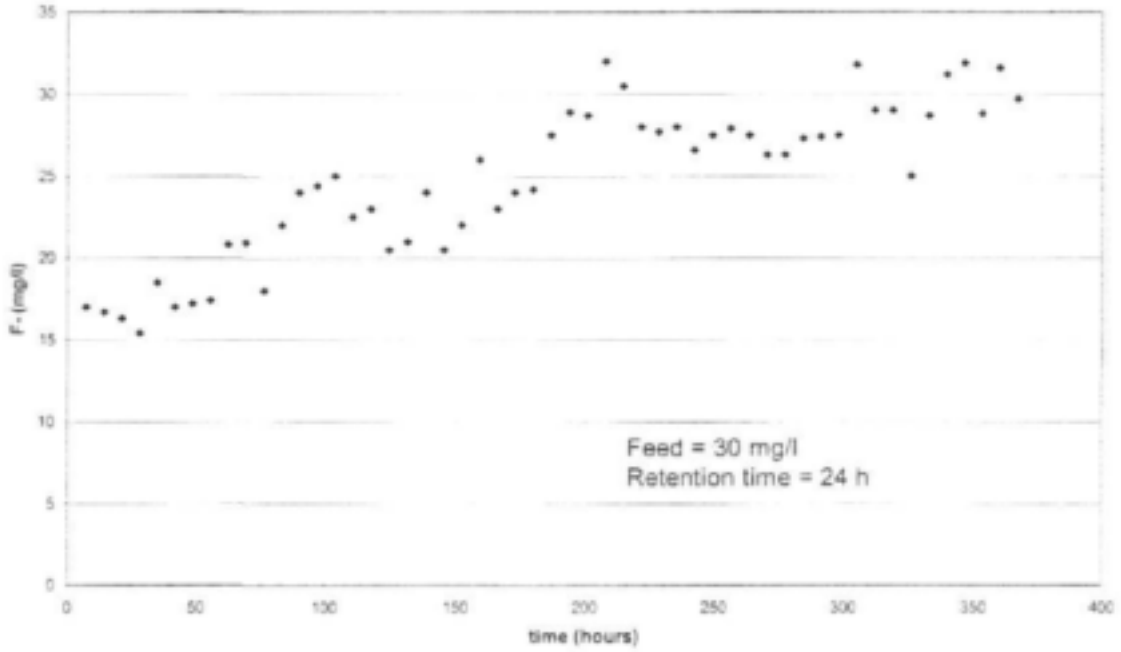

Figure 6.8 Residual fluoride concentration in Reactor Type 1 (clay type = MD2, pH = 7.2, retention time = 24 h, feed concenration 30 mg/l)

6.6 COLUMN TESTS WITH THE TYPE 2 REACTOR

6.6.1 Effect of pellet size

The next tests carried out investigated the comparative adsorptive capacities of the MD2 pellets when packed in different sizes (ie, 12, 25 & 40 mm). The results are shown in Figure 6.9. As expected, the smallest size considerably outperformed the rest at an initial F- reduction of slightly more than 70% (a residual F- content of 13 mg/l from a feed of 50 mg/l). The 25 and 40 mm pellets had curves that reflect an initial adsorption of 50% and 20%, respectively. The adsorption cycles were 9, 6 and 2 days for the smallest to the largest pellet. This suggests that surface adsorption is the more dominant defluoridation mechanism compared to intra-media sorption. The same large pellets, however, took considerably longer to exhaust when packed in the longer columns in figures 6.7 and 6.8 (bearing in mind that the feed concentrations in those experiments were lower).

Figure 6.10 shows the adsorption of fluoride into KOP clay. The initial sorption capacity for the 12 mm pellet (which is the best performing) is more than 70%. The exhaustion period is about 15 days for this clay at the retention time of 24 hours. The KOP clay generally performs better than the MD2 throughout the adsorption cycle. In addition, its exhaustion period extends from 13 days (at a 30 mg/l feed concentration) to longer periods of time for the best performing particle sizes, at least. Unfortunately, these tests do not yield data on the eventual exhaustion time for the smaller pellets beyond 13 to 15 days which is when their counterpart 40 mm diameter pellets start to lose their fluoride removal ability.

In both cases, a minimum removal efficiency of >70% is achieved for the 12 mm pellets.

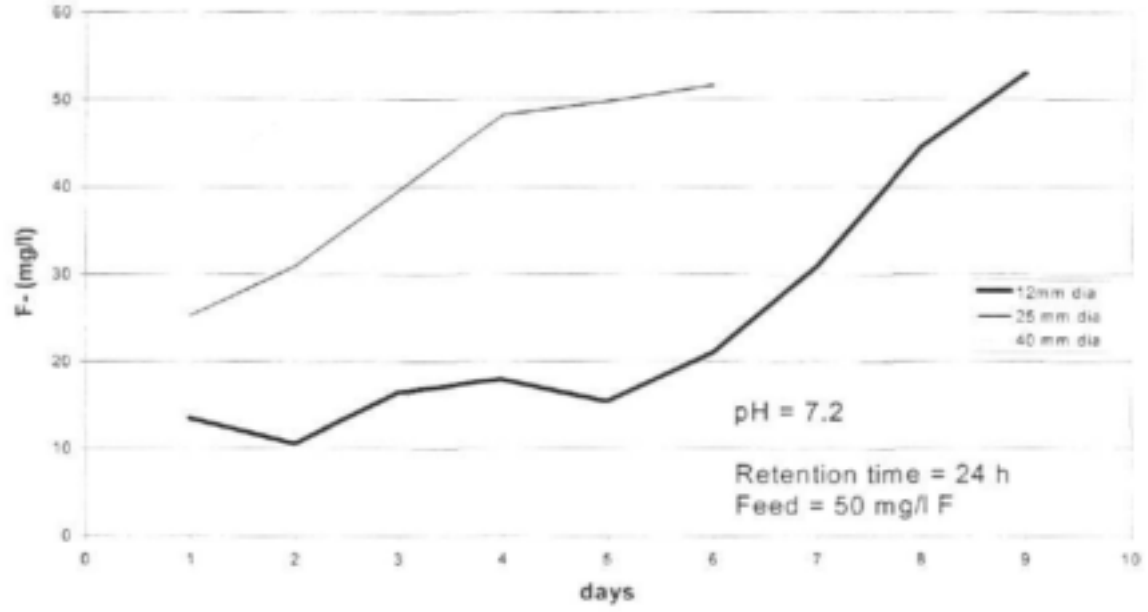

Figure 6.9 Residual fluoride concentration in Reactor Type 2 (clay type = MD2, pH = 7.2, retention time = 24 h, feed concentration = 50 mg/l)

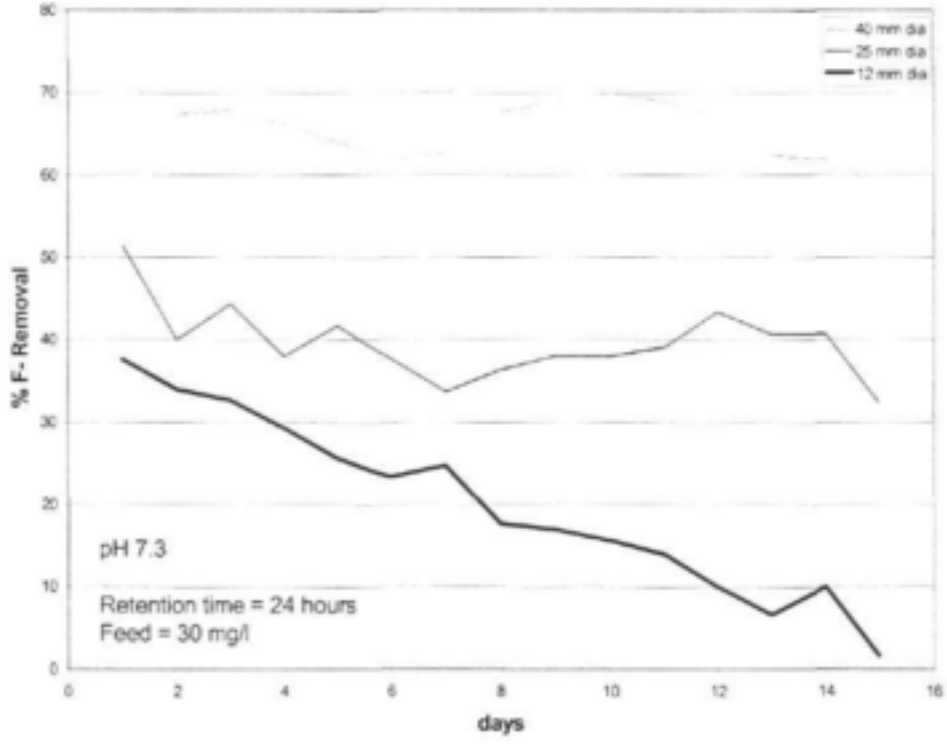

Figure 6.10 Fluoride removal in Reactor Type 2 (clay type = KOP, pH = 7.3, retention time = 24 h, feed concentration = 30 mg/l)

Table 6.3 Summary of Reactor Parameters experiment shown in Figure 6.10

Reactor Size	Type II (ie. short column)
Clay Type	KOP
Pellet Size	12, 25 & 40 mm
No. of Pellets Packed	160, 16 & 6 respectively
Void Space	67%, 62% &55% respectively
Retention Time	24 hrs
Feed F- Concentration	30 mg l

Figure 6.11 shows the fluoride adsorption performance of the RYE clay. Predictably and in line with the other clays, the smallest pellet considerably outperforms the other larger pellets. Interestingly, the performance of the 12 mm and the 25 mm pellets is almost the same over the duration of the test run.

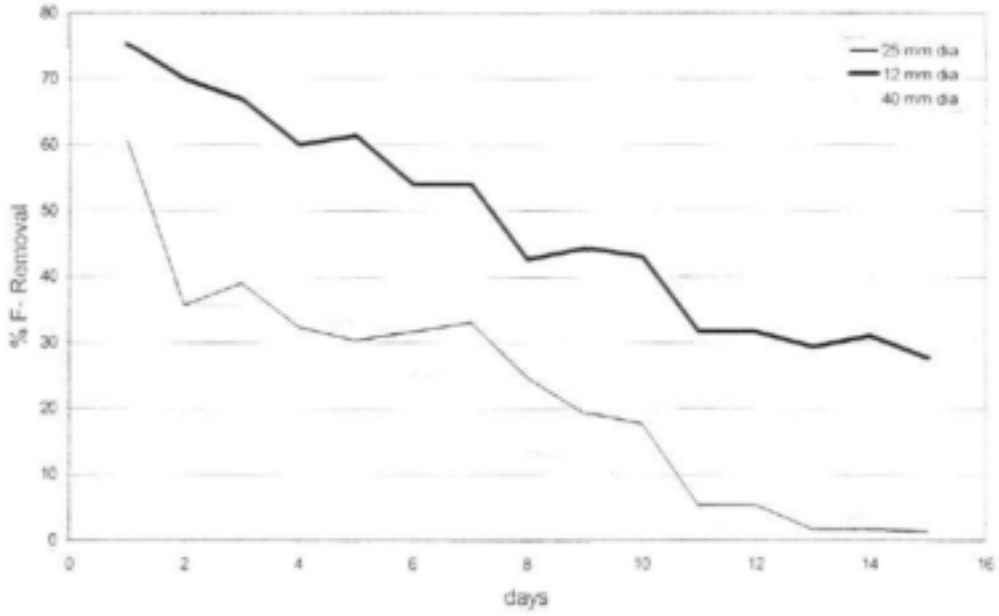

Figure 6.11 Fluoride removal in Reactor Type 2 (clay type = RYE, pH = 7.3, retention time = 24 h, feed concentration = 30 mg/l)

6.6.2 Effect of pH

Figure 6.12 below illustrates the effect pH has on the removal efficiency of clay media. In this case 12 mm MD2 clay pellets were used. Whilst at pH 5.25 there is a general increase in the removal of fluoride compared to pH 7.5, it would appear that more data points are needed over a wider pH range to get a clearer picture. According to the literature (for example Moges *et al*, 1996), the pH range of 5 to 7 presents the optimal adsorption conditions for clay media. This is convenient as it overlaps with the area where typical drinking water pH is found. In explanation: The lower efficiency of defluoridation in the alkaline region is to be expected due to competition from hydroxyl ions, since OH- and F- have the same charge and ionic radii. A lower defluoridation efficiency in the acidic region, on the other hand, can possibly

be attributed to the protonation of fluoride, thus reducing the concentration of free fluoride available for adsorption.

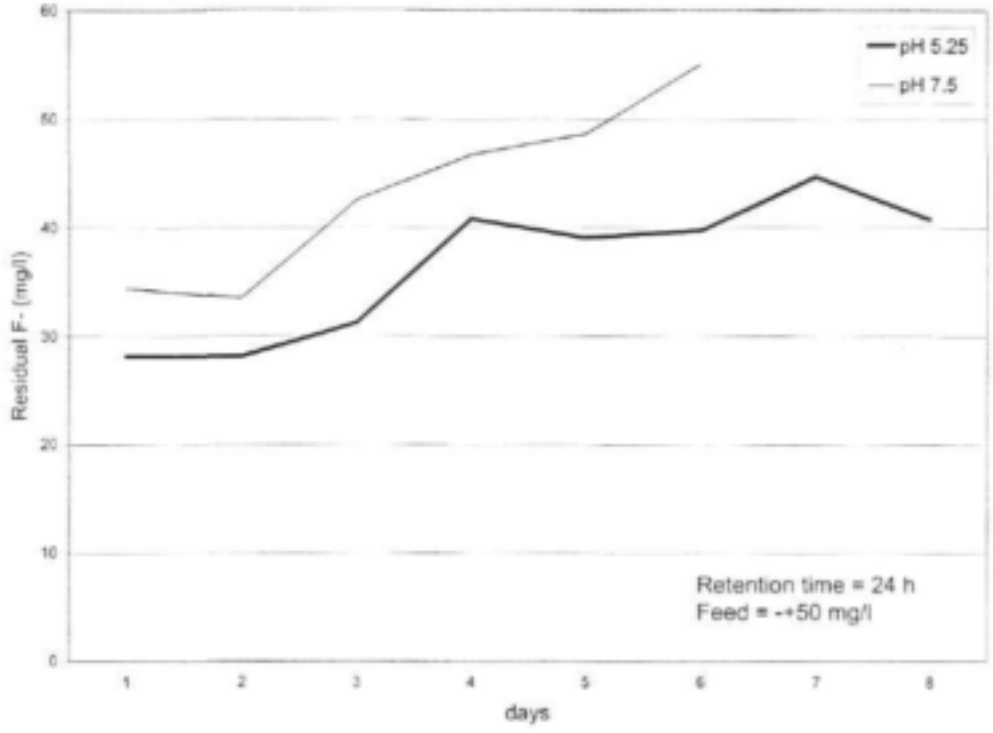

Figure 6.12 Effect of pH on residual fluoride concentration in Reactor Type 2 (clay type = MD2, pellet size = 12 mm, pH = 7,5 and 5,25 respectively, retention time = 24 h, feed concentration = 50 mg/l)

6.7 OTHER WATER QUALITY PARAMETERS

One normally would pack a long column by filling it with water first, and then allowing the pellets to fall through the water into position. During this process, less than 5% of the pellets disintegrated on their path through the water. Upon disintegration, the aesthetic water quality did not deteriorate, which was most likely due to the quiescent conditions in the column. The colour of the water was consistentle below 5 Haxen units and the nephelometric turbidity was consistently below 1 NTU.

6.8 DISCUSSION

The findings of this chapter are:

- Upon baking, the adsorption capacity of the MD (bauxitic) clay is reduced, but the adsorption capacity of the RYE (lateritic) clay is slightly enhanced.
- The adsorption capacity of MD clay is significantly enhanced when the pH is dropped from pH 7,2 to pH 5,5 – in line with the fundamental work reported in Chapter 3.
- When the clay is pelleted, there is a further reduction in adsorption capacity. After pelletisation, the adsorption capacities of the MD and RYE clays are approximately the same.

- The full adsorption capacity of the pellets is utilised after about 24 hours of contact with the water.
- A column filled with larger pellets has a lower adsorption capacity than a similar column filled with smaller pellets – an effect found with all three clays tested.
- Typical columns, subjected to household type flow rates, achieve initial fluoride removal rates of about 70% and are exhausted after about two weeks of continuous operation.

6.9 REFERENCE

Moges G, Zewge F and Socher M, Preliminary Investigations on the Defluoridation of Water Using Fired Clay Chips, Journal of African Earth Sciences 21 (1996) 479-482

CHAPTER SEVEN

CONCLUSIONS AND RECOMMENDATIONS

7.1 SUMMARY

This project is the culmination of a series of three projects, which progressed as follows:

- A first project during 1999 stressed the need for rural solutions to the commonly encountered problems of nitrate and fluoride, reviewed the sustainability of the commonly used technologies in rural context and came to the conclusion that new and more appropriate solutions need to be developed.
- A second project during 2000 took a closer look at a simple method reported from Sri Lanka where fluoride was successfully removed at domestic level with brick chips. A visit was made to Sri Lanka, the sketchy literature on this technology was systematically reviewed and some preliminary laboratory tests were conducted. The promising potential of this technology for South African conditions was confirmed.
- This third project, carried out over a period of 30 months, systematically continued the investigation of clay-based defluoridation in four main parts. Firstly, a broad sample of South African clays were sampled and tested. Secondly, the fundamental adsorption mechanisms of fluoride onto clay were studied. Thirdly, methods were developed to immobilise the clay into pellets which could be exposed to water without decomposition. Fourthly, adsorption studies were conducted in laboratory columns which approached the domestic units used in Sri Lanka.

The Sri Lankan case study was studied in detail, by means of the available literature as well as a site visit. Its main features, relevant to possible local application, are:

- The project is deemed to be successful with 1400 households in 60 villages participating, with the support of the WHO. The extension of this project to further phases seems likely.
- The units are only installed in homes where infants less than three years old reside, possibly pointing to some resistance if the units have to be maintained indefinitely.
- The clay used is mainly kaolinitic and similar clays are available in South Africa.
- The clay is fired into bricks by low-temperature wood-fuelled fire, and the brick fragments from the kilns are used in the defluoridators.
- The removal is very good and units run for about two months or more before they have to be recharged with fresh brick chips.
- There is no attempt to regenerate the chips – they are simply discarded and replaced.
- Although good empirical research supports the findings, there is little fundamental work reported on the adsorption mechanisms.
- The literature search indicated research on fluoride adsorption onto clay by a number of other researchers from Africa and elsewhere.
- The only forum where these experiences are shared seems to be the International Society for Fluoride and Fluorosis (ISFF), which has had three international meeting up to now.
- An interest has been expressed by the ISFF organisers to have a future meeting hosted in South Africa.

A fundamental analysis of fluoride adsorption onto clay was undertaken first, with the following results:

- A theoretical model was derived based on chemical equilibrium and verified by successfully fitting experimental adsorption data, both obtained in this study and taken from the literature.
- Results obtained in this chapter support the exchange mechanism for F^- adsorption. The accurate determination of pH changes during adsorption and a thorough investigation of the acid-base properties of the substrate and its effect on the ion exchange properties, provided enough evidence to resolve uncertainties in the literature with regard to the nature of the F^- adsorption mechanism. This work confirms that a rise in pH should accompany the adsorption of F^- as predicted by the ion exchange model.
- Adsorption modelling based on thermo-dynamic considerations, i.e. the thermo-dynamic constants for the different equilibria in the adsorption process, proved to be successful in predicting adsorption curves for metal oxide substrates. Since metal oxides of Fe and Al are the predominant mineral structures found in clays showing F^- adsorption potential, the model provides a useful tool for the interpretation and prediction of adsorption behaviour of substrates under different pH conditions.

An extensive survey and testing programme of 23 South African clay samples was conducted next, as well as a bauxite sample from Australia and a Sri Lankan clay sample. The main findings were:

- Clay types can differ enormously in their adsorption capacities for F^-.
- Big differences also occur within a specific clay type, even if taken from the same deposit a small distance apart. This suggests that sampling for future work should possibly allow for multiple samples within the same deposit to obtain the optimal procust.
- A trend in adsorption capacity related to clay structure can, however, be observed. Adsorption capacity decreases as the concentration of exchangeable OH groups decreases.
- Clay types consisting of the metal oxides of Fe and Al were found to have the best potential as adsorbents for F^- from aqueous solutions.

Water defluoridation by clay can only work if the clay can be effectively immobilised to keep the water clean and potable after treatment. A significant part of the total effort was thus devoted to a systematic investigation into the best and easiest way to achieve this. Although the emphasis of this project is to demonstrate the *technical feasibility* of water defluoridation by clay and not necessarily to develop the technology to a *practical, economical* and *sustainable* level, the results of this chapter nevertheless are also promising pointers towards full-scale implementation. The main findings of this work were:

- Of the three remaining candidate clays (after adsorption tests eliminated the fourth), practical methods could be developed to produce clay pellets that were stable.
- This could be achieved by using two of the clays directly in a sun-dried form, and by adding only water to the third.
- The compression could be done with a manual press requiring no other power source and a simple set of moulds.
- The baking required a sustained temperature of about 600°C for a period of 2 hours.

- The pellets produced had a fairly high internal porosity, which boded well for its eventual adsorption capacity.
- There was no serious turbidity increase of the water exposed to the pellets, and tests in larger, more quiescent reactors may have even smaller effects.

Three clays – KOP, RYE and MD2 were evaluated for performance in long term tests using cylindrical reactors for fluoride removal. The conclusions drawn were as follows:

- All three clays performed very well recording removal efficiencies of more than 70% for the smallest sized pellets.
- Predictably, the smallest sized pellet (12 mm dia) out-performed the other pellets of sizes 25 mm and 40 mm dia. The 25 mm pellet performed slightly better than the larger pellet.
- Structurally, the pellets proved to be sufficiently rugged and stable not to impart colour and turbidity to the product water. In the cases where the pellets collapsed, the failed clay particles invariably settled at the bottom of a column (this can be attributed, of course, to the relatively quiescent conditions prevailing in the columns due to the long contact times employed).
- No discernible or adverse odour was detected on the product water. In the product water, colour was consistently less than 5 Hazen units and nephelometric turbidity was consistently less than 1 NTU.
- Fluoride - spiked water to very high concentrations (30 mg/l and 50 mg/l) exhausted a full-scale column between 8 days and about 18 days.
- The initial fractional removal of fluoride, for the clay samples and pellet manufacturing conditions used, was about 70% which indicates good potential for further development and refinement.

7.2 ACCOMPLISHMENT OF RESEARCH OBJECTIVES

The contract stated five specific objectives:

- Survey South African clay deposits and select the most promising deposits for further work in the laboratory. *This objective was accomplished.*
- Conduct a fundamental study into the nature of the adsorption mechanisms controlling fluoride adsorption onto clay. *This objective was accomplished.*
- Develop a method to immobilise the clay into pellets which can be used in full-scale defluoridators. *This objective was accomplished.*
- Develop and test a laboratory prototype similar to what would be used in practice. *This objective was accomplished.*
- Build a field prototype and evaluate at village level, where fluoride is a known problem. *This objective was not accomplished, as agreed with the steering committee. The last part of the project was used to rather improve the defluoridation efficiency of the clay pellets from about 50% to 70%.*

7.3 CONCLUSIONS

- There is a need for a practical, simple defluoridation technology which will be sustainable for rural villages with limited monetary and manpower resources.
- The use of discarded brick fragments as piloted in Sri Lanka, is a promising technology with a proven track record at hundreds of households.
- The adsorption of fluoride onto clay was modelled successfully in this project and a rational basis for this technology therefore exists.
- Clay deposits in South Africa could be potentially be just as successful, but great variations exist even within the same deposits. Careful mining of the deposits is an important prerequisite.
- A practical, simple method of compression and baking was developed which will effectively immobilise the clay as pellets to ensure good water quality, while still attaining good defluoridation efficiency.
- The initial defluoridation efficiency of domestic units using these pellets was measured at about 70%.

7.4 RECOMMENDATIONS FOR FURTHER RESEARCH

The groundwork had been done to expand this project to field-scale testing, with adequate demonstration of its potential to warrant further attention. This will require the following main elements:

- The location of the test sites, after which the most appropriate clay pits can be surveyed.
- A semi-automated method of pellet manufacture to produce adequate pellets for testing. During this project, pellets were produced manually which will not be practical for full-scale testing.
- A multi-disciplinary approach which should not only include the technical aspects covered in this project, but also sociologists and health professionals to explain the relevance of the technology to the community, and to evaluate its success and acceptance.

CHAPTER EIGHT

BIBLIOGRAPHY

8.1 PAPERS FROM THE FIRST INTERNATIONAL WORKSHOP ON FLUOROSIS AND DEFLUORIDATION OF WATER HELD AT NGURGOTO, TANZANIA (1995)

BARDSEN A and BJORVATN K. Fluoride Sorption Isotherm on Fired Clay.

BHARGAVA DS. Optimum Operation of Counter-Current Water Defluoridation System.

BJORVATN K and BARDSEN. A Use of Activated Clay for Defluoridation of Water.

BREGNHOJ H and DAHI E. Kinetics of Uptake of Fluoride on Bone Char in Batch.

BREGNHOJ H, DAHI E and JENSEN M. Modeling Defluoridation of Water in Bone Char Columns.

DAHI E and BREGNHOJ H. Significance of Oxygen in Processing of Bone Char for Defluoridation of Water.

DAHI E, BREGNHOJ H and ORIO L. Sorption Isotherms of Fluoride on Flocculated Alum.

DAHI E, SINGANO JJ and NIELSEN JM. Kinetics of Defluoridation of Water by Calcined Magnesia and Clay.

GUMBO FJ and MKONGO G. Water Defluoridation for Rural Fluoride Affected Communities in Tanzania.

HE GL, CHANG Y and JI RD. Mechanisms of Defluoridation of Drinking Water by Tricalcium Phosphate.

IBRAHIM Y, AFFAN AA and BJORVATN K. Fluoride and Fluorosis in the Sudan.

MABELYA L, VAN'T HOF MA, *et al.* Suitability of The TF-Dental Fluorosis Index for Detection of Fluoride Sources.

NIELSEN JM and DAHI E. Measurement of Fluoride in Magadi.

NIELSEN JM, and DAHI E. The Occurrence of Fluoride Contaminated Magadi (Trona) in Kenya and Tanzania.

RAJCHAGOOL S. The Applied Icoh Defluoridator.

SINGANO J J, MASHAURI DA *et al.* Effect of pH on Defluoridation of Water by Magnesite.

TEKLE-HAIMANOT R, FEKADU A, *et al.* Fluoride Levels in Water and Endemic Fluorosis in Ethiopian Rift Valley.

VAN PALENSTEIN HELDERMAN WH, MKASABUNI E, *et al.* Severe Fluorosis in Children Consuming Fluoride Containing Magadi.

8.2 PAPERS FROM THE SECOND INTERNATIONAL WORKSHOP ON FLUOROSIS AND DEFLUORIDATION OF WATER HELD AT NAZRETH, ETHIOPIA (1997)

ASTROM AN, AWADIA AK and CHANDE O. Information About Oral Health among Women attending Health Clinics in Arusha.

AWADIA A K, BJORVATN K, BIRKELAND JM and HAUGEJORDEN O. Dental Fluorosis with Special Reference to Incisors and Molars of Tanzanian School Children, Bergen, Norway.

BAPURAO S (1997) Fluoride and Silicon Content in Drinking Water.

BARDSEN A and BJORVATN K. Dental Fluorosis in Subjects Exposed to Fluoride Containing Drinking Water at Different Age.
BHARGAVA DS. Economical Technology of Fluoride Removal using Fishbone Charcoal Columns at Domestic Level.
BJORVATN K, BARDSEN A, TEKLE-HAIMANOT R. Defluoridation of Drinking Water by the Use of Clay/Soil, Bergen.
BREGNHOJ H. Critical Sustainability Parameters in Defluoridation of Drinking Water.
DAHI E. Development of The Contact Precipitation Method for Appropriate Defluoridation of Water.
FANTAYE W, SHIFERA G and TEKLE-HAIMANOT R. Prevalence of Dental Fluorosis in the Wonji Shoa Sugar Estate.
JACOBSEN P and DAHI E. Bone Char Based Bucket Defluoridator in Tanzanian Households.
JACOBSEN P and DAHI E. Charcoal Packed Furnace For Low-Tech Charring of Bone.
JACOBSEN P and DAHI E. Effect of Calcium Addition on the Defluoridation Capacity of Bone Char.
KARTHIKEYAN G, APPARAO BV and MEENAKSHI S. Defluoridation Properties of Activated Alumina.
KARTHIKEYAN G, PIUS A and APPARAO BV. A Simple Method for Determination of Total Fluoride Intake.
KVALHEIM A, BJORVATN K, BARDSEN A and TEKLE-HAIMANOT R. Significance of Elevation on Fluoride Binding Capacity of Ethiopian Soils.
LAKSHMAIAH N, PARANJAPE PK and MOHAN PM. Biodefluoridation of Fluoride Containing Water by a Fungal Biosorbent.
LOUW AJ and CHIKTE UME. Fluoride and Fluorosis, The Status of Research in South Africa, Tygerberg, South Africa.
MALDE M K, BJORVATN K and JULSHAMN K. Analytical Problems in Assessment of Fluoride in Food.
MANOHAR SP and DE GROOT CPM. Fluorosis Control in the Rural Drinking Water Supply and Sanitation Project.
MEKLAU Z, TEKLE-HAIMANOT R, SHIFERA G. Prevalence of Low Back Pain at an Agro-industrial Community in the Rift Valley.
NIELSEN JM and DAHI E. Fluoride Contamination and Mineralogical Composition of East African Magadi Trona.
NIELSEN JM and DAHI E. Household Purification of Fluoride Contaminated Magadi (Trona).
PADMASIRI JP. Low Cost Domestic Defluoridation, Peradeniya, Sri Lanka.
PUANGPINYO W and OSIRIPHAN N. Preparation of Bone Char By Calcination.
RAJCHAGOOL S and RAJCHAGOOL C. Solving the Fluorosis Problem in a Developing Country.
RWENYONYI MC, BJORVATN K, BIRKELAND JM and HAUGEJORDEN O. Dental Fluorosis in Relation to Altitude and Fluoride in Drinking Water in Uganda, Bergen, Norway.
SHIFERA G and TEKLE-HAIMANOT R. A Review of the Defluoridation Program of Drinking Water Supplies of an Ethiopian Estate.
SHIFERA G, MELAKU Z, ASEFFA G and TEKLE-HAIMANOT R. Skeletal Fluorosis among Retiring Employees of Wonji Shoa Sugar Factory.
SINGANO JJ, MASHAURI DA, MTALO FW and DAHI E. Kinetics of Sorption of Fluoride on Calcined Magnesite in Batch.
VENKOBACHAR C, LYENGAR L and MUDGAL AK. Household Defluoridation of Drinking Water Using Activated Alumina.
WANDERA M, MALDE MK and BJORVATN K. Assessment of the Fluoride Content of Weaning Food Items in Western Uganda.

8.3 PAPERS FROM THE THIRD INTERNATIONAL WORKSHOP ON FLUOROSIS AND DEFLUORIDATION OF WATER HELD AT CHIANG MAI, THAILAND (2000)

ALBERTUS J, BREGNHOJ H and KONGPUN M. Bone Char Quality and Defluoridation Capacity in Contact Precipitation.

AMIRTHANATHAN GE and PADMASIRI JP. Extended Kinetic Model for Simulation of Domestic Defluoridators used in Sri Lanka.

BAILEY K, CHILTON J, *et al.* Fluoride in Drinking Water.

BHARGAVA DR and SWAROOP D. Nomographs for Instant and Efficient Field Defluoridation.

FANGSREKAM N, WATANESK S, *et al.* Adsorption Study for Defluoridation by Bone Char.

GORACCI G, BAZZUCCHI M. New Classification of Fluorosis and Results of Fluoride Application on Human Dental Structures.

NOPPAKUN W, RATANASTHEIN B, *et al.* Impact Assessment of Geothermal Source to Fluorosis in Doi Hang Subdistrict, Muang District, Chiangrai Province.

PADMASIRI JP. Effectiveness of Defluoridation of Drinking Water in Kekirawa.

SAPARAMADU DG. An Overview of the De-fluoridation project in Sri Lanka – Some Experiences.

SUSHEELA AK and BHATNAGAR M. Prevention and Control of Fluorosis: Impact of Interventions.

TANSUKANUN W. Community Decision Making on Fluorosis Problem Solving in Mae-Son Subdistrict, Lampang, Thailand.

TSEWAMESKEL S. The Correlation of Fluoride and Iron Concentrations in Groundwater of Jimma.

VAISH AK and VAISH P. Fluoride Contamination, Fluorosis and Defluoridation at Domestic Level: A Case Study from Dungarpur District, Rajasthan, India.

VAISH P and VAISH AK. Key Factors for Sustainability of Fluoride Management Programme with Special Reference to Rajasthan, India.

8.4 PAPERS FROM INTERNATIONAL JOURNALS

2002 BALCI S and GOKCAY E Effects of Drying Methods and Calcination Temperatures on the Physical Properties of Iron Intercalated Clays. *Materials Chemistry and Physics* **vol 76** 46-51.

1979 KAU PMH, SMITH DW, and BINNING P Fluoride Retention by Kaolin Clay. *Journal of Contaminant Hydrology* **vol 28(6)** 267-288.

1960 ANDREW RW, JACKSON ML, and WODA K (1960) Intersalation as a Technique for Differentiation of Kaolinite from Chloritic Minerals by X-ray Diffraction. *Soil Science Society Proceedings* **vol 24** 422-424.

1964 COLEMAN NT and THOMAS GW (1964) Buffer Curves of Acid Clays as Affected by the Presence of Ferric Iron and Aluminum. *Soil Science Society Proceedings* **vol 28** 187-190.

1966 BOWER CA and HATCHER JT (1966) Adsorption of fluoride by soil and minerals. *Soil Science* **vol 103** 151-154.

1968 HARWOOD JE (1968) The use of an ion selective electrode for routine fluoride analyses on water samples. *Water Research* **vol 3** 273-280.

1977 OMUETI JAI and JONES RL (1977) Fluoride adsorption by Illinois soils. *Journal*

of Soil Science **vol 28** 564-572.

1979 CHHABRA R, SINGH A and ABROL IP (1979) Fluorine in sodic soils. *Soil Science American Society* **vol 44** 33-36.

1979 CHOI W-W and CHEN KY (1979) The removal of fluoride from water by adsorption. *Water Technology* 562-570.

1979 WU YC and ASCE M and NITYA A (1979) Water defluoridation with activated alumina. *Journal of the Environmental Engineering Division* **vol 105** 375-367.

1982 OKOPNAYA NT, ROPOT VM and SOLKAN TN (1982) Defluoridation of water by a mixture of a coagulant and bentonite. *Khimiya Tekhnologiya Vody* **vol 4** 357-359.

1984 LAWLER DF and WILLIAMS DH (1984) Equalization/Neutralization modeling: An application to fluoride removal. *Water Research* **vol 18(11)** 1411-1419.

1985 SCHOEMAN JJ AND BOTHA GR (1985) Fluoride sorption isotherm on fired clay. *National Institute for Water Research* **vol 11** 25-32.

1986 HAO OJ, ASCE AM, HUANG CP and ASCE M (1986) Adsorption characteristics of fluoride onto hydrous alumina. *Journal of Environmental Engineering* **vol 112** 1054-1069.

1986 PARTHASARATHY N, BUFFLE J and HAERDI W (1986) Combined use of calcium salts and polymeric aluminium hydroxide for defluoridation of wastewater. *Water Research* **vol 20** 443-448.

1987 SAMCHENKO ZA (1987) Defluoridation of water by the Al-form of cationites with addition of sodium silicate. *Khimiya Tekhnologiya Vody* **vol 9** 367-1987.

1987 SCHOEMAN JJ AND LEACH GW (1987) An investigation of the performance of two newly installed defluoridation plants in South Africa and some factors affecting their performance. *Water Science Technology* **vol 19** 953-965.

1987 SCHOEMAN JJ and MACLEOD H (1987) The effect of particle size and interfering ions on fluoride removal by activated alumina. *National Institute for Water Research* **vol 13** 229-234.

1987 ZHANG GY, ZHANG NX and YU TR (1987) Adsorption of Sulphate and Fluoride by Variable Charge Soils. *Journal of Soil Science* **38** 29-38.

1988 CHATURVEDI AK, PATHAK KC and SINGH VN (1988) Fluoride removal from water by adsorption on china clay. *Vanarasi, Department of applied chemistry, Institute of Technology, Banaras Hindu University* **3** 337-347.

1988 MOHANRAO NVR and BHASKARAN CS (1988) Studies on defluoridation of water. *Journal of Fluorine Chemistry* **vol 41** 17-24.

1990 CHATURVEDI AK, YADAVA KP, PATHAK KC and SINGH VN (1990) Defluoridation of water by adsorption on fly ash. *India, Kluwer academic publishers* **vol 49** 51-61.

1992 GACIRI SJ and DAVIES TC (1992) The occurrence and geochemistry of fluoride in some natural waters of Kenya. *Journal of Hydrology* **vol 143** 395-412.

1994 HAUGE S, OSTERBERG R, BJORVATN K, and SEVIG KA (1994) Defluoridation of drinking water with pottery: effect of firing temperature. *Norway, Department of Dental Research, University of Bergen School of Dentistry, Bergen* **102** 329-333.

1994 KARTHIKEYAN G, MEENAKSHI S, and APPARAO BV (1994) Defluoridation technology based on activated alumina. *20th WEDC Conference* 1-3.

1994 XU G-X (1994) Fluoride removal from drinking water by activated alumina with CO_2 gas acidizing method. *Journal of Water Separation* **vol 43** 58-64.

1995 BARDSEN A and BJORVATN K (1995) Fluoride sorption isotherm on fired clay. *International Society for Fluoride Research* 46-49.

1996 LAI YD and LUI JC (1996) Fluoride removal from water with Spent catalyst. *Separation Science and Technology* **31(20)**.

1996 MOGES G, ZEWGE F and SOCHER M (1996) Preliminary Investigations on the

Defluoridation of Water Using Fired Clay Chips. *Journal of African Earth Sciences* **21** 479-482.

1996 MOGES G, ZEWGE F and SOCHER M (1996) Preliminary investigations on the defluoridation of water using fired clay chips. *Journal of Earth Sciences* **vol 21** 479-482.

1996 ZEVENBERGEN C, REEUWIJK LP, FRAAPPORTI G, LOUWS RJ and SCHUILING RD (1996) A Simple Method for Defluoridation of Drinking Water at a Village Level by Adsorption on Ando Soil in Kenya. *The Science of the Total Environment* **188** 225-232.

1996 ZEVENBERGEN C, VAN REEUWIJK LP, FRAPPORTI G, LOUWS RJ and SCHUILING RD (1996) A simple method for defluoridation of drinking water at village level by adsorption on Ando soil in Kenya. *The Science of the Total Environment* **vol 188** 225-232.

1997 LOUNICI H, ADDOUR L, BELHOCINE D, GRIB H, NICOLAS S, BARIOU B and MAMERI N (1997) Study of a new technique for fluoride removal from water. *Desalination* **vol 114** 241-251.

1998 KAU PMH, SMITH DW, and BINNING P (1998) Experimental sorption of fluoride by kaolinite and bentonite. *Geoderma* **vol 84** 89-108.

1998 SRIMURALI M, PRAGATHI A and KARTHIKEYAN J (1998) A study on removal of fluorides from drinking water by adsorption onto low cost materials. *Environmental Pollution* **vol 99** 285-289.

1998 WEERASOORIYA R, WICKRAMARATHMA H and Dharmgunawardhane HA (1998) Surface Complexation Modeling of Fluoride Adsorption onto Kaolinite. *Colloids and Surfaces* **144** 267-273.

1998 WEERSOORIYA R, WICKRAMARATHNE HUS and DHARMAGUNAWARDHANE HA (1998) Surface complexation modeling of fluoride adsorption onto kaolinite. *Colloids and Surfaces A: Physicochemical and Engineering Aspects* **vol 144(1-3)** 267-273.

1999 KAILASH CA, GUPTA SK and GUPTA AB (1999) Development of new low cost defluoridation technology (KRASS). *Water Science Technology* **vol 40** 167-173.

1999 KAU PMH, BINNING PJ, HITCHCOCK PW and SMITH DW (1999) Experimental analysis of fluoride diffusion and sorption in clays. *Journal of contaminant hydrology* **vol 36** 131-151.

1999 WEERASOORIYA R and WICKRAMARATHMA H (1999) Modeling Anion Adsorption on Kaolinite. *Journal of Colloid and Interface Science* **213** 395-399.

2000 AZBAR N and TURKMAN A (2000) Defluoridation in drinking water. *Water Science and Technology* **42(1-2)** 403-407.

2000 CASTEL C, SCHWEIZER M, SIMONNOT MO and SARDIN M (2000) Selective removal of fluoride ions by a two-way ion-exchange cyclic process. *Chemical Engineering Science* **vol 55(17)** 3341-3352.

2000 HIEMSTRA T and VAN RIEMSDIJK WH (2000) Fluoride Adsorption on Goethite in Relation to Different Surface Site. *Journal of Colloid and Interface Science* **225** 94-104.

2000 RAICHUR AM and BASU JM (2000) Adsorption of fluoride onto mixed rare earth oxides. *Separation and Purification Technology* **vol 24(1-2)** 121-127.

2001 BERGAYA F and LAGALY G (2001) Surface modification of clay minerals. *Applied Clay Science* **vol 19** 1-3.

2001 LHASSANI A, RUMEAU M, BENJELLOUN D and PONTIE M (2001) Selective demineralization of water by nanofiltration application to the defluoridation of brackish water. *Water Research* **vol 35** 3260-3264.

2001 WANG Y and REARDON EJ (2001) Activation and regeneration of a soil sorbent for defluoridation of drinking water. *Applied Geochemistry* **16** 1-13.

2001 WANG Y and REARDON EJ (2001) Activation and Regeneration of a Soil Sorbent for Defluoridation of Drinking Water. *Applied Geochemistry* **16** 531 – 539.

2001 YAN-HUI L, SHUGUANG W, ANYUAN C, DAN Z, XIANFENG Z, CAILU X, ZHAOKUN L, DIANBO R, JI L, DEHAI W and BINGQING W (2001) Adsorption of fluoride from water by amorphous alumina supported on carbon nanotubes. *Chemical Physics Letters* 1-8.

2002 ALEMAYEHU M, PRADEEP K and ARVIND K (2002) Integrated biological and physiochemical treatment process for nitrate and fluoride removal. *Water Research* **vol 35(13)** 3127-3136.

2002 BUFFLE J and PARTHASARATHY N and W HAERDI (2002) Importance of speciation methods in analytical control of water treatment processes with application to fluoride removal from wastewater. *Water Research* **vol 19(1)** 7-23.

2002 CHERNET T, TRAFI Y and VALLES V (2002) Mechanism of degradation of the quality of natural water in the lakes region of the Ethiopian rift valley. *Water Research* **vol 35(12)** 2819-2832.

2002 LOUNICI H, ADDOUR L, BELHOCINE D, ELMIDAOUI A, BARIOU B and MAMERI N (2002) Novel technique to regenerate activated alumina bed saturated by fluoride ions. *Chemical Engineering Journal* **vol 81(1-3)** 153-160.

2002 LU YC, ESENGUL K and ERSOZ M (2002) Removal of fluoride form aqueous solution by using red mud. *Separation and Purification Technology* **vol 28(1)** 81-86.

2002 MAHRAMANLIOGLU M, KIZILCIKLI I and BICER IO (2002) Adsorption of fluoride from aqueous solution by acid treated spent bleaching earth. *Journal of Fluorine Chemistry* 1-13.

2002 MAHRAMANLIOGLU M, KIZILCIKLI I and BICER IO (2002) Adsorption of Fluoride from Aqueous Solution by Acid Treated Spent Bleaching Earth. *Journal of Fluorine Chemistry* **115** 41-47.

2002 YANG C-L and DLUHY R (2002) Electrochemical generation of aluminum sorbent for fluoride adsorption. *Journal of Hazardous Materials* 1-25.

2003 AGAWAL M, RAI K, SHRIVASTAV R and DASS S (2003) Defluoridation of Water Using Amended Clay. *Journal of Cleaner Production* **11** 439-444.

APPENDIX A
MINERALOGICAL CHARACTERIZATION OF CLAY SAMPLES

Table Of Contents

1. INTRODUCTION

This study aims to provide a method of water defluoridation by means of ion-exchange or adsorption. Clay minerals have the physical property of sorbing certain anions and cations and retaining these in an exchangeable state (Grim, 1962). Furthermore, kaolinites and smectites are also known to readily adsorb F^- anions in exchange of $(OH)^-$-ions on the edge of their crystals (Weiss *et al.*, 1956). Clay is a common and inexpensive natural resource and could be readily and economically available to the rural population of endemic areas of dental fluorosis in South Africa. This part of the study entails the collection and mineralogical characterization of a wide variety of natural clay samples. These samples were then passed on to the Department of Chemistry, RAU, for adsorption studies.

The term clay is confusing in that it can refer either to particle size, mineral or rock type. In this report, the term clay is defined after Le Fond (1989) as 'a natural, earthy substance composed largely of a group of crystalline minerals known as the clay minerals.' In their natural state, clays consist of a) minerals of primary origin, i.e. those present in the igneous rocks and which have undergone no significant alteration in composition and b) minerals of secondary origin (clay minerals) produced by the action of chemical and physical agents on primary minerals resulting in their breakdown and conversion into secondary minerals.

The clay minerals are part of a general group within the phyllosilicates (sheet-silicates). Clay minerals within the phyllosilicates are divided into the *kaolinite group*, the *montmorillonite/smectite group*, the *illite group* and the *chlorite group*. Clays which are composed of a mixture of the above groups and which are intercalated or intergrown on an atomic scale are called the *mixed layer group*. A sixth group of clay minerals, the *palygorskite/sepiolite group*, has sheet-like and ribbon-like structural characteristics and has been classified as 2:1 phyllosilicates,.

2. STRUCTURE AND PROPERTIES OF COMMON CLAY MINERALS

The basic building blocks of the clay minerals are tetrahedral silicate units (Fig.1) and octahedral, most common, aluminum units (Fig.2). In their simplest form, clay minerals consist of an arrangement of tetrahedral and octahedral sheets. In each tetrahedron, a silicon cation is equidistant from four oxygen, or hydroxyl anions. The tetrahedra are arranged so that the tips of all of them point in the same direction, and the bases of all tetrahedrons are in the same plane (fig.1).

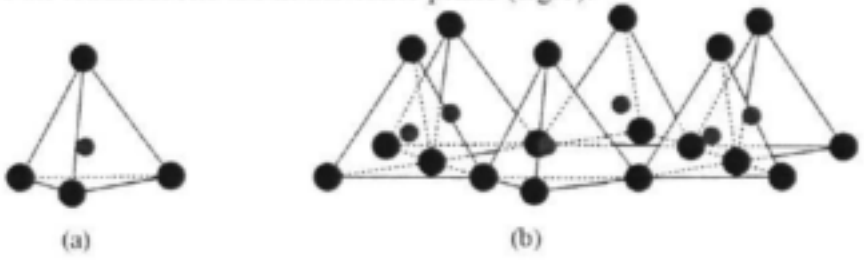

Figure 1: Sketch ilustrating (a) single silica tetrahedron and (b) the sheet structure of silica tetrahedra arranged in a hexagonal network.

The octahedral unit consist of two sheets of closely packed oxygen or hydroxyl anions

in which aluminum, iron, or magnesium atoms are embedded in octahedral coordination, so that they are equidistant from six oxygens or hydroxyls (fig.2).

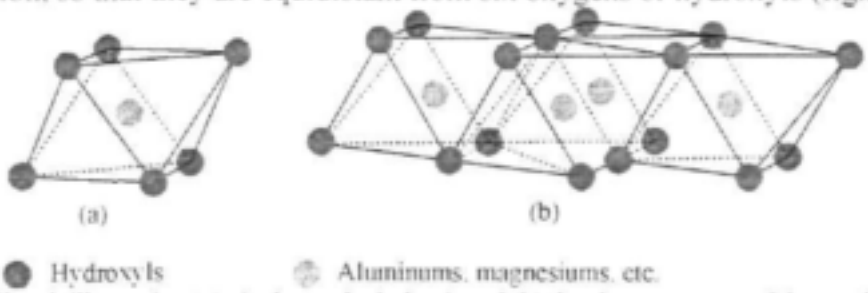

Figure 2: Sketch illustrating (a) single octahedral unit and (b) the sheet structure of the octahedral units (Gibbsite-layer).

In these octahedral units each oxygen will be bonded to two aluminum ions, leaving it with a remaining 1^- charge. The charge can be compensated by attaching a proton (hydrogen ion) to each oxygen. Very similar to the structure of the mineral *gibbsite*. Octahedral layers are referred to as gibbsite-layers, or brucite-layers, if the cations in the octahedral sites are Mg^{2+}.

The chemical formula for gibbsite is $Al(OH)_3$. Gibbsite is one of the minerals that make up the rock *bauxite*. Gibbsite sheets are only held together by weak residual bonds and this results in a very soft, easily cleaved mineral. Although gibbsite usually has a grain-size in the range of other clay minerals (<2μm) it is not classified as a clay mineral, but forms part of the *oxides and hydroxides group*. Iron oxides and hydroxides are also very common in natural clays; the minerals goethite, hematite, lepidocrocite and magnetite are the most common forms of iron oxides found in natural clays.

The octahedral layer has a single negative charge per formula unit, if hydrogen ions are not attached to the oxygen ions. An alternative option to balance the remaining negative charge on the oxygen ions, is to share the apical oxygen of a neighbouring tetrahedral sheet with the octahedral sheet. The resulting three-dimensional unit is called a micelle. Since each micelle is constructed of a tetrahedral layer and an octahedral layer, clay minerals with this structure are called 1:1 clay minerals. These micelles are thus the fundamental structural building blocks of most clay minerals. The micelles are stacked on top of each other and held together by weak hydrogen bonds.

The oxygen ions in the octahedral layer are in a close packed structure, where each oxygen ion shares charges with two aluminum ions. As it turns out, meeting the requirement that one oxygen should share two aluminum ions does not require aluminum occupancy of all possible spaces between the planes of oxygen ions in the octahedral layer. Rather, extra sites are created when the oxygen and aluminum ions come together. Across the entire octahedral layer there is an average of one empty site created for every two aluminum ions in the structure. This situation presents an alternate possibility for building the mineral. Two Al^{3+} ions will produce a total of six positive charges, but so will three Mg^{2+} (or Fe^{2+}) ions. Thus, during mineral formation the octahedral layer might be filled by divalent ions rather than trivalent aluminum ions, the most common of which are Mg^{2+} and Fe^{2+}. If the octahedral layer contains divalent ions in all the possible sites, it is known as a *trioctahedral mineral* and if it

contains trivalent ions in two of every three possible sites, it is known as a *dioctahedral mineral*.

A simple staking of micelles composed of one gibbsite and one silicate unit constitutes the mineral *kaolinite* (Fig.3), while the simple staking of brucite-layers with silicate units results in the mineral talc.

The sum of the many hydrogen bonds between micelles results in the micelles being strongly bonded together. Furthermore, there is no remaining interlayer charge and no space for interlayer cations or molecules. Thus we speak of kaolinite as being a nonexpanding 1:1 phyllosilicate.

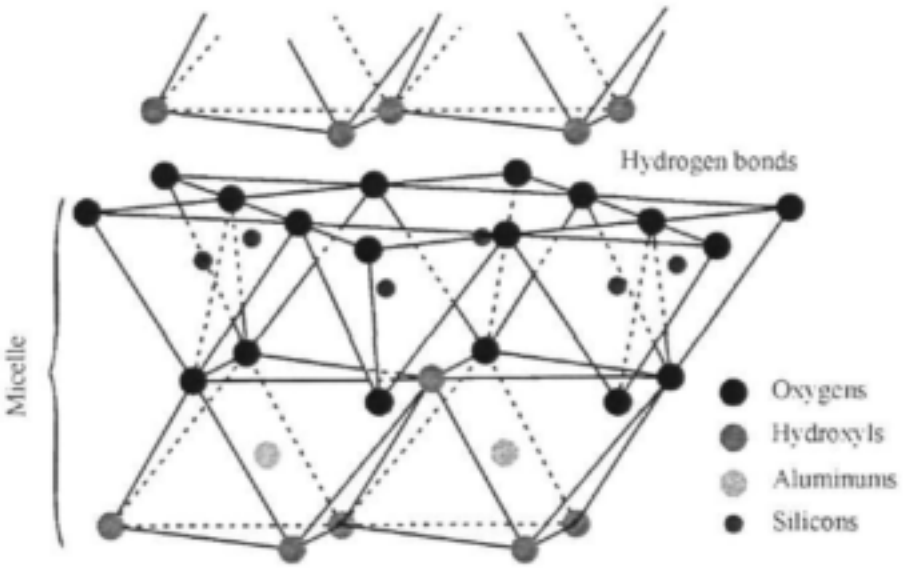

Figure 3: Sketch illustrating the structure of kaolinite, a 1:1 structural type clay, after Grim (1962).

A second silicon tetrahedral layer, creating the basic structure of 2:1 clay minerals, can also replace the layer of hydrogen ions in the octahedral sheet in the 1:1 clay minerals. These minerals consist of two tetrahedral layers sandwiching one octahedral layer (Fig.4). Clay minerals of the montmorillonite/smectite and illite groups are 2:1 clay minerals.

In the more complex mineral groups, such as the smectite and mica groups, large cations such as Na^{+} and Ca^{2+} and small molecules such as H_2O occur in a very loose arrangement between the micelle units. These interlayer molecules/cations and can often readily be exchanged for other cations or molecules (Deer, et al. 1962; Bühmann, 1993; Purbrick, 1993; Bailey, 1980; Murray, 1991). Therefore the smectites are called expandable 2:1 clay minerals. The micas are not expandable but has the potential to exchange ions.

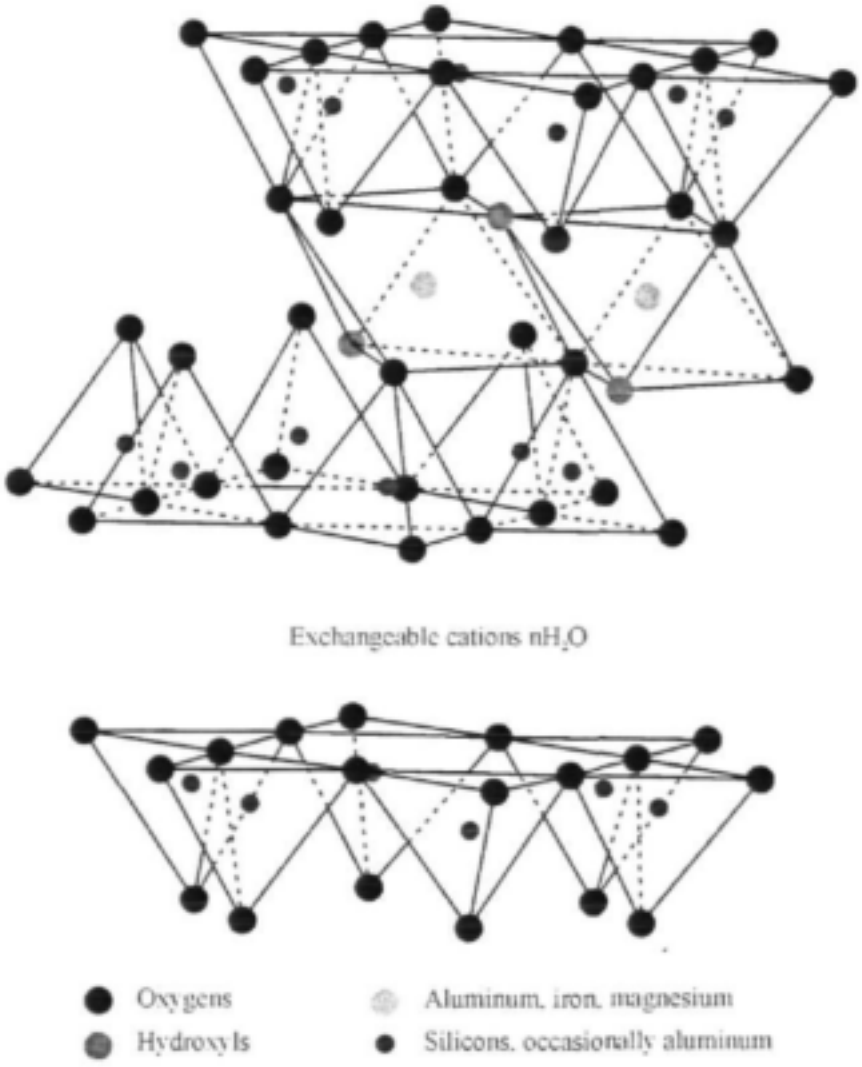

Figure 4: Diagrammatic sketch of the structure of montmorillonite, a 2:1 structural type clay, after Grimm (1962).

In certain situations, a 2:1 clay mineral may have formed in an environment containing an excess of aluminum or magnesium. Under these conditions, an extra aluminum or magnesium octahedral layer (gibbsite/brucite like layer) will form between the micelles. Minerals having this characteristic are known as the chlorite group (Fig.5). The gibbsite/brucite like layer has the effect of binding the micelles tightly so that this group of minerals is also nonexpanding. The chlorites are called nonexpanding 2:1:1 or 2:2 clay minerals.

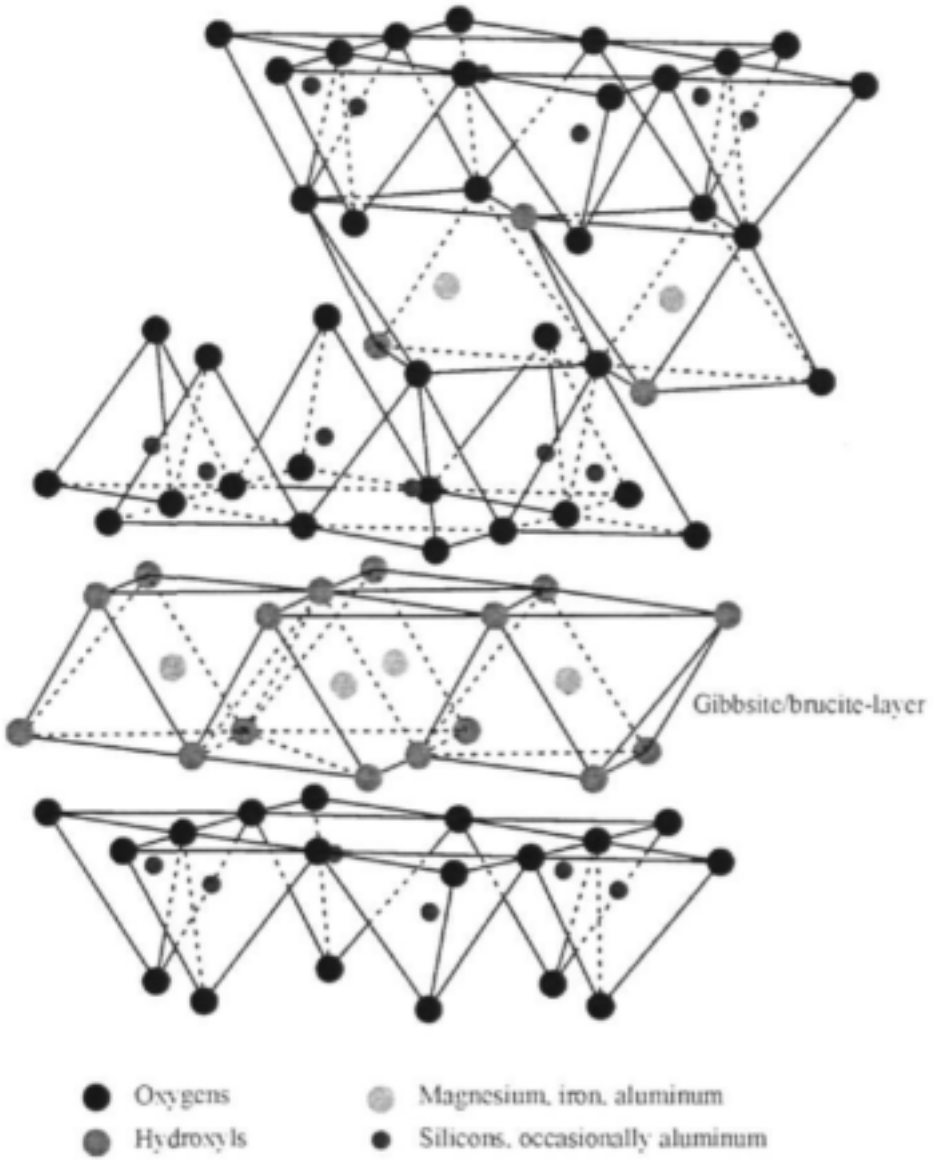

Figure 5: Diagrammatic sketch of the structure of chlorite, after Grim (1962).

Some clay minerals contain charge imbalances within the crystal structure. These minerals are said to contain a *permanent charge*. The tetrahedral and the octahedral units with which the phyllosilicates are build require that the cation:oxygen radius ratio be from 0.255 to 0.414 and from 0.414 to 0.732, respectively, and there are many ions other than Al^{3+} that fit this criteria. It is therefore possible for Al^{3+} to replace some of the Si^{4+} in the tetrahedral polyhedra, resulting in an imbalance of 1^- for each substitution. We also at times find divalent ions in the octahedral layer of dioctahedral minerals and trivalent ions in the octahedral layer of trioctahedral minerals, resulting in the a negative and positive imbalance of charge respectively.

A second possible source of surplus electrical charge in clay minerals occurs along mineral surfaces, where possible chemical bonds remain uncompensated. The structure cannot extend infinitely, so at some point there will be oxygens without all charges satisfied by associating with cations. In these cases a hydrogen ion from solution will normally satisfy the requirement. Whether this can occur will, however, depend on the solution pH. Therefore, these charges are called either pH-dependent

charge of variable charge. Many different kinds of ions or small polar molecules can thus be attached to the mineral surface, this effect becomes more prominent with decreasing grain size and is thus particularly important for clay minerals.

2.1 Kaolinite Group

A generalised formula for the kaolinite group is $Al_2Si_2O_5(OH)_4$. This group has three polytypes, kaolinite, dickite and nacrite. All three have a 1:1 structure in which one tetrahedral sheet combined with one octrahedral gibbsite sheet by sharing the apical oxygen atoms between these sheets (Bühmann, 1993; Bailey, 1980; Murray, 1991). The plasticity, workability, green strengths and refractory nature of kaolinitic clays are some of the physical properties that can be related to its sheet like crystal structure. The grain size of individual kaolinite platelets, which are often less than 1μm in diameter, as well as the degree of preferred orientation of these platelets, correlates, among others, positively with the degree of plasticity of clays. Furthermore, the high-refractory clays often consist of individual clay particles which are randomly orientated, thus limiting the degree of surface contact between individual grains (Bredell, 1987).

Kaolinite is used in ceramics, as filler for paint, rubber and plastics and the largest use is in the paper industry that uses kaolinite to produce a glossy paper such as is used in most magazines.

2.2 Montmorillonite/Smectite Group

This group is composed of 2:1 phyllosilicates including sauconite, saponite, nontronite and montmorillonite. The general formula is (Ca, Na, H)(Al, Mg, Fe, $Zn)_2(Si, Al)_4O_{10}(OH)_2 - xH_2O$, where x represents the variable amount of water that members of this group could contain. Here one octahedral layer is bordered on both sides by two tetrahedral sheets in which the apical oxygens point in opposite directions towards the central octahedral sheet. The 2:1 structure has an excess electrical layer charge, which is balanced by the presence of interlayer ions which could be cations such as K^+, Ca^{2+}, Na^+ or anions such as hydroxyl groups and/or organic molecules (Searle and Grimshaw, 1959; Bühmann, 1993; Purbrick, 1993; Bailey, 1990; Murray, 1991). The fact that these cations can be replaced by other cations in the smectite structure is an important characteristic of the clays of this group because it relates directly to the ease with which the clay can be chemically altered during beneficiation to yield a product used in a wide range of products including absorbents.

Most montmorillionite clays (called bentonitic clays or bentonites) produced in South Africa have Ca^{2+} as the exchangeable cation. The sorptive characteristics of the bentonite are therefore greately enhanced if the Ca^{2+} cations, which naturally occur in the interlayer spaces, are replaced by Na^+. Talk and pyrophyllite also belong to the 2:1 structure, but they don't contain interlayer cations or excess water. Talc's formula, for example, is $Mg_3Si_4O_{10}(OH)_2$.

Usages of these minerals are many and include facial powder (talc), filler for paints and rubbers, electrical insulators, heat and acid resistant porcelain, drilling muds and as a plasticizer in molding sands and other materials.

2.3 Illite Group

Illite is essentially hydrated microscopically fine-grained muscovite mica. The mineral illite is the only common mineral in this group. It is, however, a significant rock forming mineral being a main component of unmetamorphosed shales and other argillaceous rocks. The general formula is $(K, H)Al_2(Si, Al)_4O_{10}(OH)_2 - xH_2O$, where x represents the variable amount of water that the structure of illite can accomadate. The 2:1 structure of this group is similar to that of the montmorillonite group with tetrahedral layers sandwiching a octahedral layer. The variable amounts of water molecules as well as potassium ions would lie between micelles.

Illite is a common constituent in shales and is used as a filler and in some drilling muds.

2.4 Chlorite Group

This group is not always considered a part of the clays and is sometimes left as a separate group within the phyllosilicates. It is a relatively large and complex group of sheet silicates of variable composition. The term chlorite is used to denote any member of this group when differentiation between the different members is not possible. The general formula is $X_{4-6}Y_4O_{10}(OH,O)_8$. The X represents either aluminum, iron, lithium, magnesium, manganese, nickel, zinc or rarely chromium. The Y represents either aluminum or silicon and very rarely boron or iron.

The structure of the chlorite group is composed of tertahedral layers sandwiching an octahedral (brucite-like) layer in between, in a t-o-t stacking sequence similar to the 2:1 phyllosilicate group. However, in the chlorites, there is an extra weakly bonded octahedral (brucite-like) layer in between the t-o-t micelles. This gives the structure an t-o-t-o staking sequence (2:2 or 2:1:1).

2.5 Mixed Layer Group

Interstratified, mixed-layer spiecies of clays are common. These "mixed-layer structures" are the consequence of the fact that the layers of the different clay minerals are similar; all being composed of silica tetrahedral layers and closely packed octahedral layers of oxygens and hydroxyl groups. These include illite-montmorillonite, biotite-vermiculite, montmorillonite-chlorite and vermiculite-chlorite intercalations (Bailey, 1980).

Mixed-layer structures are of two different types. The interstratifications may be regular, that is, the stacking may be a regular repetition of the different layers. In such cases the resulting structure has distinctive characteristics unlike those of the component layers, and the assemblage is described as a distinct mineral species. The other kind of mixed-layer structure is due to random, irregular stratification of layers in which there is no uniform repetition of them. The mixing may be of two or more types of layer units with alternations of random numbers and consequently thicknesses of the different layer units (Grim, 1962). Since random mixed-layers have an inherent variability, they are not given specific mineral names. The study of mixed layers is thus difficult, and identification of components often impossible.

2.6 Palygorskite-Sepiolite Group

Palygorskite (syn. Attapulgite) and sepiolite are classified as three-layer, inverted, hydrated magnesium-aluminium-silicate clay minerals forming the most important members of the palygorskite-sepeolite group of minerals (Germiquet, 1977). It is an odd mineral. Although displaying a 2:1 crystal structure similar to the smectite clay mineral group, palygorskite consists of octahedrally coordinated Al^{3+}, Fe^{2+} and Mg^{2+} bordered on two sides by tetrahedrally coordinated Si^{4+} layers to form chain-like structures. These ribbon-like structures, however, extend in one direction only, thus forming acicular, fibrous or lath-like crystal shapes, in contrast to the sheet-like structures of clay minerals such as smectite which extends in two directions. The ribbon-like texture is the result of a systematic inversion of the two tetrahedral sheets neighbouring the central octahedral sheet, thus pointing the apical oxygens in opposite directions at systematic intervals. Parallel, elongated channels or openings are formed in the lattice yielding the ribbon texture. Exchangeable molecules such as water located in these channels or tubes can be replaced or driven off by thermal treatment contributing to the sorptive qualities of the clay (Searle and Grimshaw, 1959; Bailey, 1980; Murry, 1991). A generalized formula for palygorskite is $(Mg,Al)_2Si_4O_{10}(OH)\ 4H_2O$.

3. SAMPLING

The first phase was to identify target areas for sampling. The endemic areas of dental fluorosis in the western Bushveld area of South Africa (Pilanesberg - Sprinbok Flats) were identified from literature (Grobler *et al.*, 1994; McCaffrey, 1998). Known natural clay deposits situated within 500km from the endemic area were then identified from available literature (Fig.6). The target areas identified were:

1) Warmbad (koalinitc clay and palygorskite),
2) Immerpan (palygorskite),
3) Zebediela (kaolinitic clay),
4) Cyferfontein (smectitic clay),
5) Northam (palygorskite-rich clay soil),
6) Sun City (laterite profile and kaolinitic clays),
7) Koster (kaolinitic clay)

The target areas were inspected and samples were systematically collected of all types and sub-types recognised during visual inspection. At each locality the farm owner and/or farm workers were consulted to find the best place to sample the clay. Samples were extracted using a manual auger, to a maximum depth of 2.5m, but in most cases existing open pits supplied the opportunity to sample at deeper depths.

After preliminary test had shown that most of these samples were not effective fluorine adsorbers, two new target areas from other parts of South Africa were identified. These target areas were:

1) Dwaalboom (palygorskite), and
2) Howick – Mooirivier (bauxite)

Initial tests indicated bauxites as the best fluorine adsorbers, and one bulk bauxite sample (sample MD1, 500kg) was collected from the Mooirivier area for extensive testing of its applicability. A small sample of Australian bauxite (supplied by Prof. Nic Beukes), and one sample of processed aluminium oxide (beneficiated from Australian bauxite) were also tested. Furthermore, G&W Base and Industrial Minerals donated two bulk samples (500kg each), one of bentonite and one of Palygorskite for further test work.

Although chemical investigations indicated that iron-rich samples should be good fluorine adsorbers, the initial laterite samples gave disappointing results. Therefore three new samples were collected from the Ryedale, open pit ferromanganese mine, near Ventersdorp. After further tests, a bulk sample of RYE1 (about 500kg) was collected. A total of 40 samples were collected (Table 1).

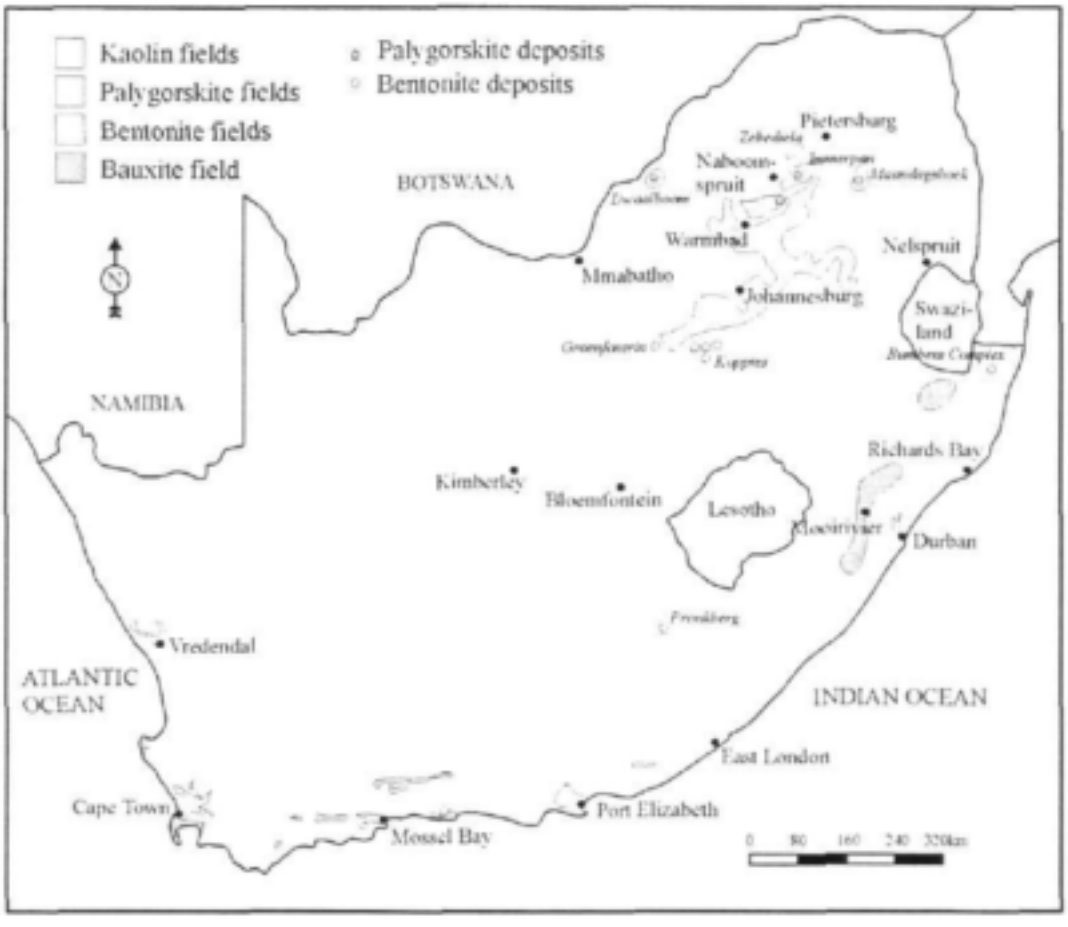

Figure 6: Generalized distribution of known clay deposits in South Africa, modified from Horn and Strydom (1998).

Table 1: Sample names, descriptions and localities of clay samples.

No.	Sample name	Target clay	Description	Location and contact person where possible
1	BBK1	Palygorskite	300mm to 750mm deep, dark-red brown colour clay under 300mm brown topsoil	Farm: Blaawboschkuil, 15km north of Pienaarsrivier on the Warmbad road. Farm owner: Mr. Rall
2	BBK2		50mm to 300mm deep, in shallow depression. Black colour clay	
3	CF1	smectite	Open pit. Below calkreet 1.9m deep. Pink, with white laminae	Farm: Cyferfontein, open pit. Farm owner: Mr. Adriaan Jooste. P.O. Box 1656, Naboomspruit 0560
4	CF2		Open pit. Below pink clay, 2.5m deep. Brown colour	
5	CF3		Open pit. Main white colour bed, approximately 2m thick	
6	CF4		Open pit. Main red colour bed, approximately 2m thick	
7	CF5		Open pit. Weathered shale at base of pit, approximately 15m deep	
8	LW1	palygorskite	800mm – 950mm deep, light brown colour, under 800mm of black topsoil	Farm: Leeuwaarden. Farm owner: Mr. Pieter van Niekerk, P.O. Box 2540, Nylstroom 0510.
9	LW2		950mm – 1.25m deep, light brown colour, becomes sandy at the base	
10	CAL	palygorskite	Open pit. Below calkreet bed, +12m deep. Light brown colour	Farm: Calais, east of Immerpan, past agricultural limestone mine. Pistorius Landboukalk. 800m from the main road, old agricultural limestone pit
11	ZEB1	kaolinite	Open pit. Pure white colour	Zebediela Bricks, open pit. On Lebowakgomo road, east of Potgietersrust. Brickworks: Mr. Peens, P. O. Box 47, Groothoek, 0628
12	ZEB2		Open pit. White colour with greenish tint	
13	ZEB3		Open pit. White colour with red tint	
14	ZEB4		Open pit. White colour with red tint	
15	ZEB5		Open pit. White colour with greenish tint	
16	ZEB6		Open pit. Blood red colour	
17	ZEB7		Open pit. Blood red colour	
18	ZEB8		Open pit. White colour with orange tint	
19	NHM	palygorskite	2.00m - 2.5m deep. Black colour clay	± 8km out of Northam on the Thabazimbi road, diggings next to railway.
20	NHM2		1.5m - 1.75m deep. Black colour clay	
21	NHM3	palygorskite	1.75m – 1.90m deep Black colour clay	
22	NHM4		1.90m – 2.00m deep. Black colour clay	
23	LAT	laterite	Laterite, orange red in colour, below 600mm brown topsoil	At the T-junction on the road from the Pilanesberg Airport to Sun City.
24	RNF	kaolinite	1m to 2.5m deep. Finely laminated orange and white clay in pan.	Renosterfontein, south of Koster.
25	BAUX1	gibbsite	Orange colour and surface texture that resembles a human brain "Brainstone"	West of Howick, Kwazulu-Natal, samples supplied by Prof. Nic Beukes
26	BAUX2	gibbsite	Orange colour, with dolerite core-stone	
27	BAUX3	gibbsite	Orange colour	Australian bauxite sampled by Prof. Nic Beukes in Australia
28	PTA-LAT	laterite	Laterite. Orange-red colour	Sampled by Herman Dorland near Pretoria

No.	Sample name	Target clay	Description	Location and contact person where possible
29	DB1	palygorskite	Open pit approximately 5m deep. Blue white colour clay sampled at base of pit.	Open pit in Artherstone Nature Reserve, north of Dwaalboom. Mr. Micho Ferreira, P.O. Box 21, Dwaalboom 0319. Mined by G&W Base and Industrial Minerals
30	DB2		Open pit. White colour bed, 1.2m thick, below approximately 500mm black topsoil	
31	SCM	kaolinite	White colour, weathering product of granite. Surface sample	40km from Sun City on the Sun City – Rustenburg road.
32	BEN	montmo-rillonite	Bentonite	G&W Base and Industrial Minerals. Technical Support: Mr. Ernest Rood. Tel 082 902 0660
33	KOP	palygorskite	Atapulgite	
35	MD1	gibbsite	Orange colour, weathering profile, below 50cm black soil.	Farm: Middeldraai, east of Mooirivier, Kwazulu-Natal. Farm owner: Mr. Van Niekerk
36	MD2		Orange colour, with dolerite core-stone	
37	MD3		Orange colour, with dolerite core-stone	
38	RYE1	Laterite	Dark red nodular laterite	Ryedale ferromanganese open pit mine, northeast of Ventersdorp.
39	RYE2	Reworked laterite	Dark red silty laterite	
40	RYE3	Manganese wad	Black fine-grained wad	

4. MINERALOGICAL INVESTIGATION

Based on location, colour and texture of samples, 19 samples were selected for preliminary mineralogical investigations. A further 3 samples (MD 1-3) were analysed in further detail after the first round of chemical tests were completed.

4.1 Sample Preparation

Large pieces of plant material and pebbles were picked out by hand. A representative portion of each sample was dried overnight at 30°C, crushed down to a grain size of <180µm and subsequently dispersed in distilled water using an ultrasonic bath. The <2µm fraction was separated by using a standard laboratory centrifuge. In order to identify the different clay minerals in the clay fraction of each sample, sedimented (textured) slides were prepared. To prepare sedimented slides, the suspension of <2µm clay particles and water was concentrated by centrifugation and resuspended in a smaller volume of water. This concentrated suspension was then poured on to a glass slide and allowed to dry slowly to produce an orientated deposit.

Disorientated preparations were also necessary to determine the other minerals present within the samples. Side loading of the <180µm fraction into aluminium sample holders prepared these samples for analyses. Care was taken to avoid pressure orientation of the powder in the sample holders.

4.2 X-ray diffraction (XRD)

Measurements were conducted at the Centralized Analytical Facility at RAU using a Phillips PW 1710 diffractometer. Measurements were carried out with the following diffractometer settings:

Tube anode material	Cobalt
Generator tension	40kV
Wavelength $K\alpha_1$	1.78896A
Wavelength $K\alpha_2$	1.79258A
Intensity ratio $I_{k\alpha1}/I_{k\alpha2}$	2
Divergence diaphragm	1°
Detector diaphragm	0.1mm

Step scans of 4 seconds per step of 0.05°2θ from 2.50°2θ to 16.00°2θ for each orientated sample, prepared from the <2μm fraction, were measured on air-dried, glycolated (swelled) and heat-treated (30 minutes at 550°C) samples. Swelling of clay minerals was carried out with ethylene glycole in an evacuated descicator at 40°C for 24 hours.

Furthermore, routine X-ray powder diffraction analyses were conducted on each sample (<180μm) using side loaded aluminium sample holders to determine the overall mineralogical composition. These measurements were conducted in a step scan mode of 2 seconds per 0.04°2θ step, from 3.00°2θ to 80.00°2θ.

4.3 Identification of clay minerals from X-ray diffraction patterns

Peak position, peak shape and peak intensity were inspected on diffractograms. The swelling or expandability of the clays were tested by examining a diffractogram of an orientated sample in the air-dried state and then another diffractogram in the glycolated state. This is done in the 6-30Å region.

Comparison of the glycolated and air-dried diffractograms, shows weather or not the diffraction maxima have changed position, demonstrating the swelling capacity of the clay. Since we know that the glycole layer increases the interlayer site by 7Å and that the normal hydrated state of swelling clays is either with 2.5 or 5Å beyond the normal 2:1 structural interlayer spacing, it is possible to tell if a clay sample has a full swelling capacity or only a partial swelling capacity. Partial swelling may be due to either an incomplete smectite interlayer structure or the presence of a mixed layer phase.

In those clays that do not change peak position with glycolation, the constant peak position readily identifies the clay family. 14Å chlorites have a constant spacing of 14-14.8Å. Mica-like minerals (illite, glauconite, celadonite) have a constant spacing near 10Å. Kaolinites or 7Å chlorites have a constant peak near 7Å. Looking at the peak position near 3.5Å where the chlorites have spacings less than 3.55Å and kaolinites greater than 3.55Å can make the distinction between the two. Alternatively, the sample may be heat treated in which case the 7Å peak of kaolinite disappears because the structure dehydroxylates. Heat treatment will also lead to an increase in the peak intensity of the 14Å peak of chlorite.

Sepiolite-palygorskites have constant spacing peaks at 12, 7.5, 6.7Å and 10.5, 6.3Å respectively. Talk and pyrophyllite have peaks at 9.6Å. Pyrophyllite, however, is a

comparatively rare mineral found in metamorphic rocks, and therefore a 9.6Å peak in natural clay indicates the presence of talk.

The interpretation of diffraction patterns produced by mixed-layer clays is very difficult (Velde 1992) and falls outside the scope of this study. The XRD method of diagnosis is summarized in Fig.7.

XRD identification of oxides and hydroxides of Fe, Mn or Al in natural clays is difficult, because they are usually found in low abundances and poorly crystallized or in exceptionally small (not diffracting) grain-sizes. The most intense characteristic reflections of iron oxides and hydroxides and aluminous hydrates are given in table 2.

Table 2: Identification of common iron oxides and hydroxides and aluminous hydrates by XRD (Velde, 1992)

Iron oxides and hydroxides:			*Aluminous hydrates:*	
Goethite	*Lepidocrocite*	*Hematite*	*Gibbsite*	*Boehmite*
4.18	6.25	3.70	4.85	6.11
2.69	3.29	2.69	4.37	3.16
2.45	2.47	2.20	4.32	2.34
	1.97	1.83	3.31	1.98
		1.69	2.45	1.86
			2.45	
			2.39	
			2.29	
			2.24	

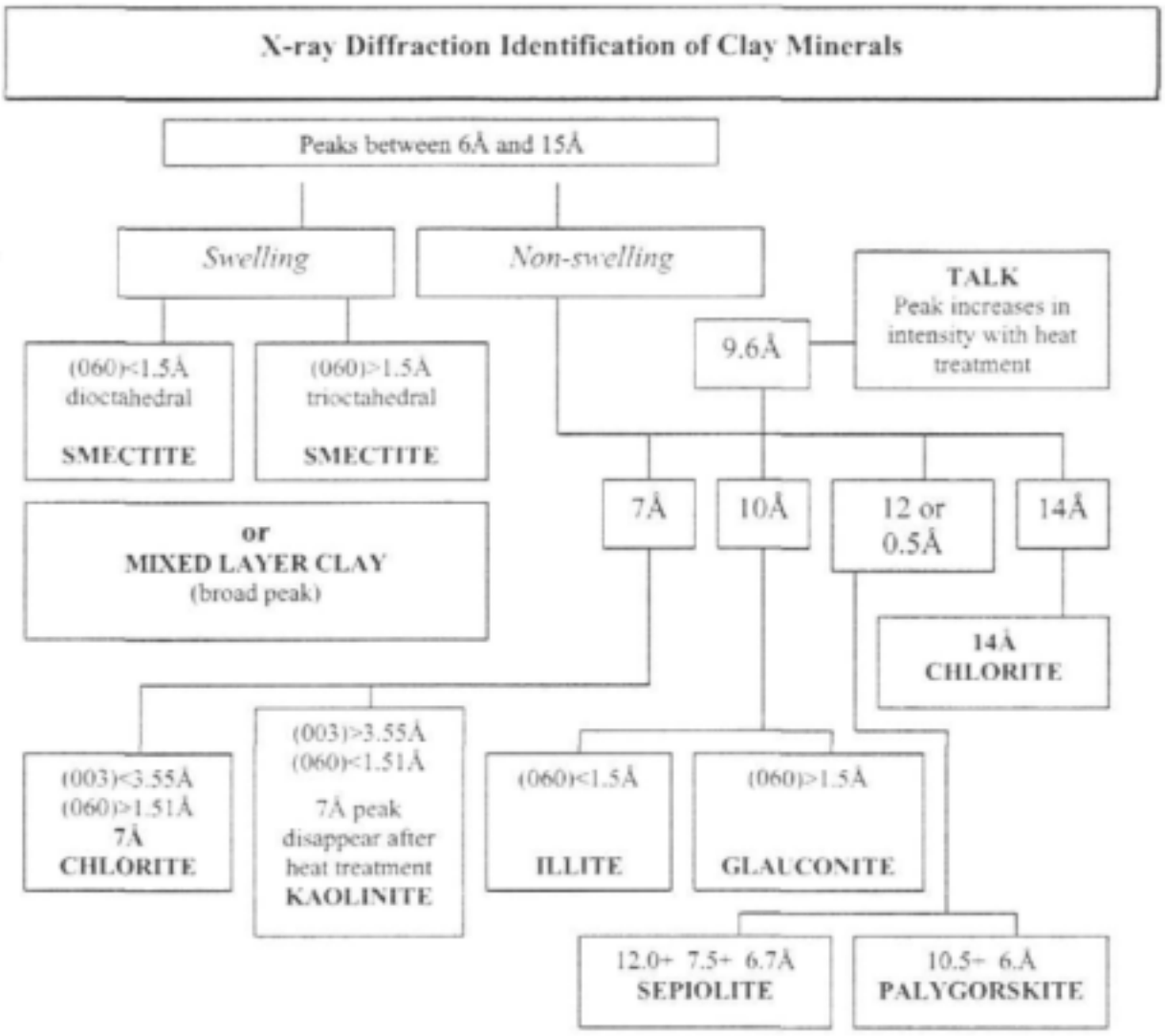

Figure 7: Key for the identification of clay minerals by XRD (supplemented from Velde, 1992).

5. RESULTS

A summary of XRD results for all samples examined is provided in table 2. XRD patterns of individual samples are discussed under the headings, bauxitic clays, kaolinitic clays, bentonitic clays, palygorskite-sepiolite clays and laterites. The XRD patterns are included in the appendix.

Table 2: Semi-quantitative mineralogical composition of natural clay samples.

	sample	quartz	feldspar	dolomite	kaolinite	palygorskite - sepiolite	Mixed-layer clay	smectite	illite	talk	gibbsite	goethite
1	BAUX1	xx									xxxx	xx
2	BAUX2	xx									xxxx	xx
3	BAUX3	xxx									xxxx	x
4	BBK2	xxx						xxx				
5	BEN	xx						xxxx				
6	CAL	x		xxx		xxx		xxx				
7	CF3	xxx						xxxx				
8	CF4	xx			x		xxx	xxx				
9	DB1	xxx		xx		xxxx						
10	DB2	xx		xxxx		xxx						
11	KOP	xx				xxxx	xxx					
12	LAT	xxx	xxx		xx		xxx		xx			
13	LW1	xxxx				xxx	xx	xx				
14	MD1	xxx			xxx		x		xx		xx	xx
15	MD2	xxx					x				xxxx	xx
16	MD3	xxx					x				xxxx	xx
17	NHM	xx			xx			xxxx				
18	PTA/LAT	xxx			xxx							xxx
19	RNF	xxx			xxx			xxx	x	xx		x
20	ZEB1	xx			xxxx				x			
21	ZEB2	xx			xxxx					xx		
22	ZEB6	xx			xxxx		xx	xx	x			
23	RYE1	xxx			xx			x				xxx(hem)
24	RYE2	xxx			xx			x				xxx(hem)
25	RYE3	x	Well defined hematite peaks, major component non-crystalline manganese									

xxxx: dominant (>50%); xxx: major component (20-50%); xx: minor component (5-20%); x: trace

5.1 Bauxitic Clays

XRD patterns of bauxite samples BAUX 1 to 3 have no major peaks in the 2.5 – 16° 2θ range, and XRD scans were thus only obtained for these samples in the full 3 – 80° 2θ range. These samples contain gibbsite, goethite and quartz (Appendix, Fig.1). Sample BAUX3 contains relatively less goethite and more gibbsite than sample BAUX1 and BAUX2 both of the latter have very similar XRD patterns.

Detailed scans in the 2.5 – 16° 2θ range were conducted on samples MD1 to MD3 and it was found that sample MD1 contains less gibbsite than the other samples and contains kaolinite and illite (Appendix, Fig. 2,3 and 4). Furthermore all the bauxite samples have a broad peak in the 4°-2θ area, probably indicating the presence of mixed layer clay.

5.2 Kaolinitic Clays

XRD analyses revealed that sample RNF is composed of smectite, kaolinite, talc, small amounts of illite and quartz (Appendix, Fig. 5). The orange colour of the sample is probably due to small amounts of goethite.

Sample ZEB1 is white in colour and is composed of kaolinite, small amounts of illite and quartz (Appendix, Fig. 6). Sample ZEB2 is composed of smectite, talc, kaolinite and quartz. The smectite is identified as nontronite, the iron-rich smectite (Appendix, Fig.7). Sample ZEB2 has a green colour due to the high smectite content. Sample ZEB6 is composed of kaolinite, small amounts of illite, smectite and a mixed-layer clay (Appendix, Fig.8). Sample ZEB6 has a red colour probably due to small amounts of goethite present.

5.3 Bentonitic Clays

Sample BBK2 is composed of quartz and smectite. The smectite is identified as montmorillonite (Appendix, Fig.9). A peak at d = 3.18 was not identified. [Several attempts were made to prepare orientated samples, but the sample invariably curled up and disintegrated during air-drying].

XRD analyses of sample BEN revealed that the sample is only composed of montmorillonite and a small amount of quartz (Appendix, Fig.10). The 13.6Å montmorillonite peak is exceptionally well defined and shifts about 3Å on glycolation (Appendix, Fig.10). On heat treatment the orientated sample curled up and disintegrated.

Sample CF3 is composed of smectite and quartz (Appendix, Fig.11). The smectite has a sharp peak and is nontronite the iron-rich smectite. On heat treatment, the nontronite peak disappeared. Sample CF4 is composed of a mixed-layer clay with a major smectite component and a small amount of kaolinite and quartz (Appendix, Fig. 12). The smectite is nontronite (Appendix, Fig.12). Sample CF4 contains relatively less quartz than sample CF3. Sample NHM was sampled north of Northam. The sample is black in colour and it contains a smectite, quartz and a small amount of kaolinite (Appendix, Fig. 13). The smectite is montmorillonite (Appendix, Fig. 13). Sample LW1 is composed of a smectite and quartz. The smectite is identified as montmorillonite (Appendix, Fig. 14). Several attempts were made at preparing an orientated sample, however, as soon as the sample is air dried it curls up and disintegrates.

Sample LW1 probably forms part of the overburden of a palygorskite deposit, however due to limitations on sampling depth, the main clay body was not sampled.

5.4 Palygorscite-Sepiolite Clays

Sample CAL, from the Immerpan palygorskite-sepiolite deposit has a light brown colour and is composed of sepiolite, smectite, dolomite and small amounts of quartz (Appendix, Fig. 15). On heat treatment the orientated sample curled up and disintegrated.

The deposits in the Immerpan-Springbok Flats palygorskite field are developed on a flat, poorly drained plain that is underlain by basalts of the Letaba Formation of the Karoo Supergroup (Horn and Strydom, 1998).
Samples DB1 and DB2 are from the Dwaalboom palygorskite deposit. Sample DB1 has a blue-white colour and is composed of palygorskite, quartz and small amounts of dolomite (Appendix, Fig. 16). Sample DB2 has a sharp palygorskite peak (Appendix,

Fig. 17), but has a much higher dolomite content and lower quartz content relative to sample DB1. On heat treatment the palygorskite peak disappeared.

The sample named KOP is a palygorskite sample donated by G&W Base and Industrial minerals, also from the Dwaalboom palygorskite field. The sample is composed of palygorskite, mixed-layer clay with a major smectite component and quartz (Appendix, Fig. 18). The palygorskite is derived from the replacement of precursor minerals such as smectite, a process that requires the presence of Mg in the environment (Horn and Strydom, 1998). An inadequate supply of Mg would result in a mixture of montmorillonitic and palygorskitic clays as observed in the sample. On heat treatment the orientated sample became unusable for X-ray analyses (curled up).

5.5 Laterites

Sample LAT is a laterite sample from the Pilanesberg area. It is composed of quartz, feldspar and a clay component. The clay component is composed of illite, kaolinite and mixed-layer clay (Appendix, Fig. 19). The presence of feldspar is explained by the fact that the laterite is developed on granite. It is odd to find that goethite is not present in sample LAT.

The laterite sample from the Pretoria area (PTA/LAT) is composed of goethite, kaolinite and quartz (Appendix, Fig. 20). Several attempts were made at preparing an orientated sample, however, as soon as the sample is air dried it curls up and disintegrates.

The two laterite samples from the Ryedale mine are composed of quartz, kaolinite and goethite and a little hematite (Appendix, Fig. 21 and 22). The manganese wad sample only display hematite peaks (Appendix, Fig. 23), but it is known that the major component of this material is non-crystalline manganese oxides (Van Niekerk, 1997).

6. CONCLUSION

The natural material characterised during this study can be grouped as follows:

1) Bauxitic clays, found as a weathering product of dolerite in areas of high rainfall. (For a detailed description of these deposits, see Horn, 1986). The main mineral in these clays is gibbsite, other minerals present are quartz, goethite, kaolinite and illite.
2) Kaolinitic clays, with the main minerals being kaolinite and quartz.
3) Bentonitic or smectitic clays, with the main clay mineral being montmorillonite, other minerals present are quartz, nontronite and mixed-clay minerals.
4) Palygorskite-sepiolite clays, and
5) Laterites, which contain the oxide goethite of hematite as well as quartz, kaolinite and remnant primary minerals like feldspar.

7. REFERENCES

Bailey, S.W. (1980). *Structures of layer silicates in Crystal Structures of Clay Minerals and their X-ray identification*. Brindley, G.W. and Brown G. (eds.): Mineralogical Society, Monograph 5, London, 124pp.

Bredell, J.H. (1987). Refractory clays in the Transvaal. *Memoir, Geological Survey of South Africa*, **73**, 176pp.

Bühmann, D. (1993). *The phyllosilicates of clays and their X-ray identification*. Cling Workshop '93, 1 to 3 February 1993: Mineralogical Association of South Africa, p. 2-21 (unpubl.).

Deer, W.A., Howie, R.A. and Zussmann, J. (1962). *Rock Forming Minrals, Volume 3: Sheet Silicates*, Longmans Green & Co. Ltd. London, 266pp.

Germiquet, J.D. (1977). A mineralogical investigation of some palygorskite deposits in South Africa with reference to beneficiation and industrial use. M.Sc. thesis (unpubl.), Rand Afrikaans University, Johannesburg. 144pp.

Grim, R.E. (1962). *Applied Clay Mineralogy*. McGraw-Hill. London. 422pp.

Horn, G.F.J. (1986). *Die Genese van Bauxiet in Natal*. M.Sc. thesis (unpubl.), Rand Afrikaans University, Johannesburg. 274pp.

Horn, G.F.J. and Strydom, J.H. (1998). *Clay*. In Wilson, M.G.C. and Anhaeusser, C.R. (eds.), Mineral resources of South Africa, Handbook 16, Council for Geocience, p. 106-135.

Le Fond, S.J. (ed.) (1989). *Industrial minerals and rocks (Nonmetallics other than Fuels)*, 5th edition: Society of Mining Engineers of the American Institute of Mining, Metallurgical and Petroleum Engineering, p. 585-651.

McCaffrey, L.P. (1998). *Distribution and causes of high fluoride groundwater in the western Bushveld area of South Africa*. Ph.D thesis (unpubl.). University of Cape Town, Cape Town.

Murray, H.H. (1991). Clay mineral applications: Applied Clay Science, 5, p. 379-395.

Purbrick, D.J. (1993). Bentonite in Southern Africa: Cling Workshop '93, 1 – 3 February 1993: Mineralogical Association of South Africa (unpubl.).

Searle, A.B. and Grimshaw, R.W. (1959). *The Chemistry and Physics of Clays and Other Ceramic Materials*. Ernest Benn Ltd. London, p. 143-151.

Van Niekerk, H.S. (1997). Post-Gondwana ferromanganese wad and nodule deposits, Krugersdorp-Lichtenburg area, South Africa. Unpubl. M.Sc. thesis. Rand Afrikaans University, Johannesburg.

Weiss, A., Mehler, A., Koch, G. and Hofmann, U. (1956). Über das Anionen-austauchvermögen der Tonminerale. Zeitschrift fuer anorganische allgemeine Chemie. 284, p. 247-253.

8. XRD PATTERNS FOR INDIVIDUAL SAMPLES

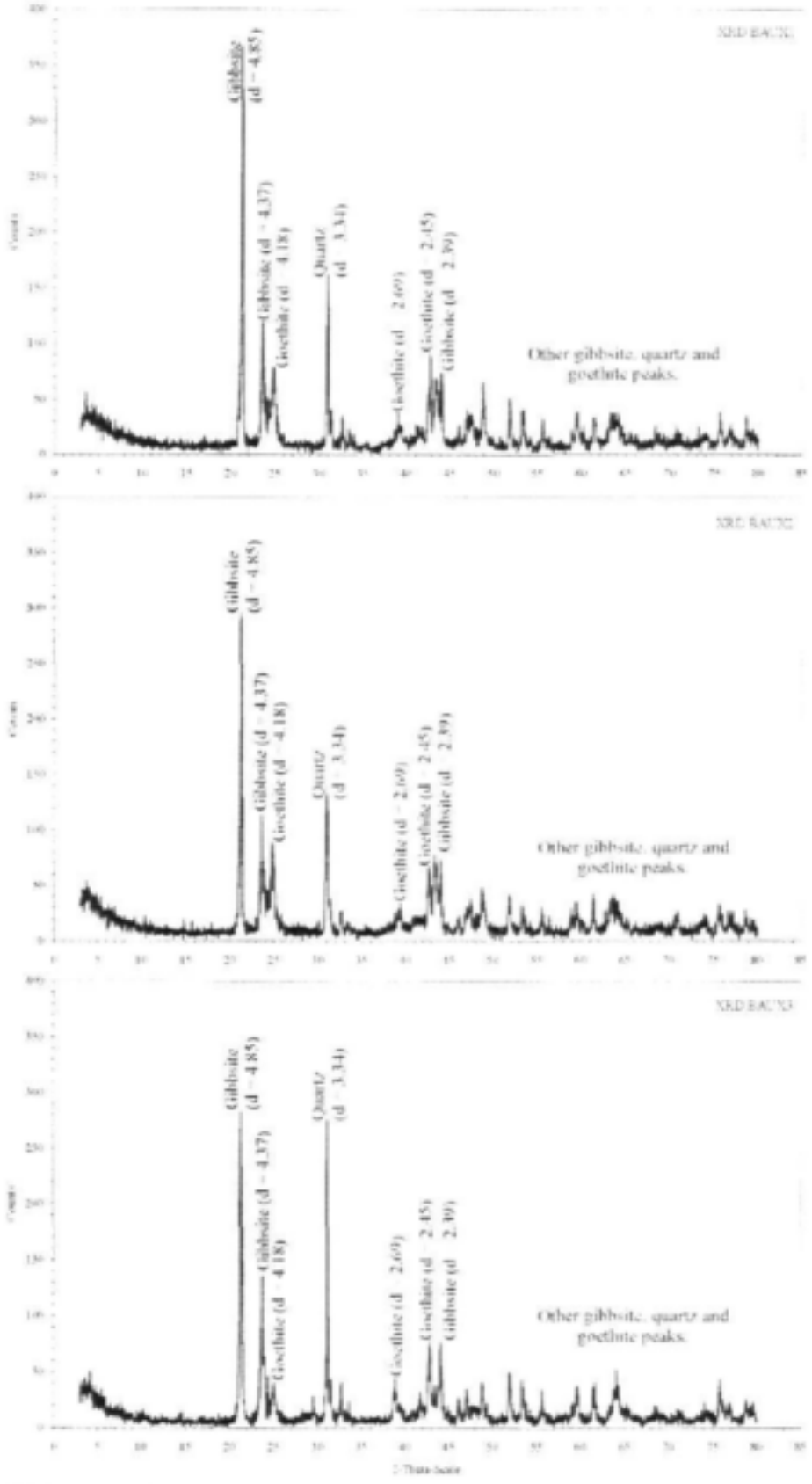

Figure 1: XRD patterns of bauxite samples BAUX 1 to 3.

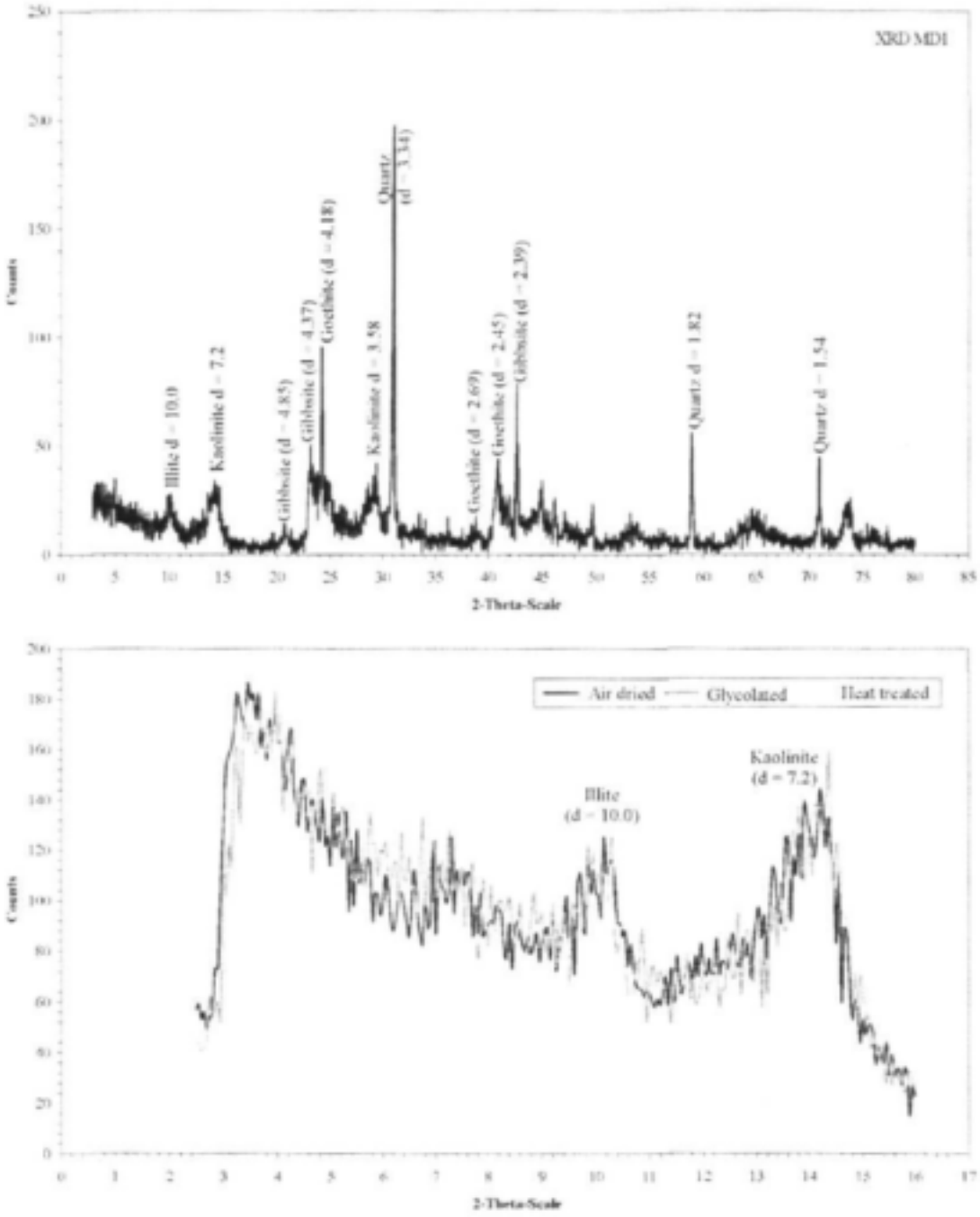

Figure 2: XRD pattern of sample MD1. Lower panel illustrates the XRD patterns of the orientated sample in the 2.5-16°2θ range.

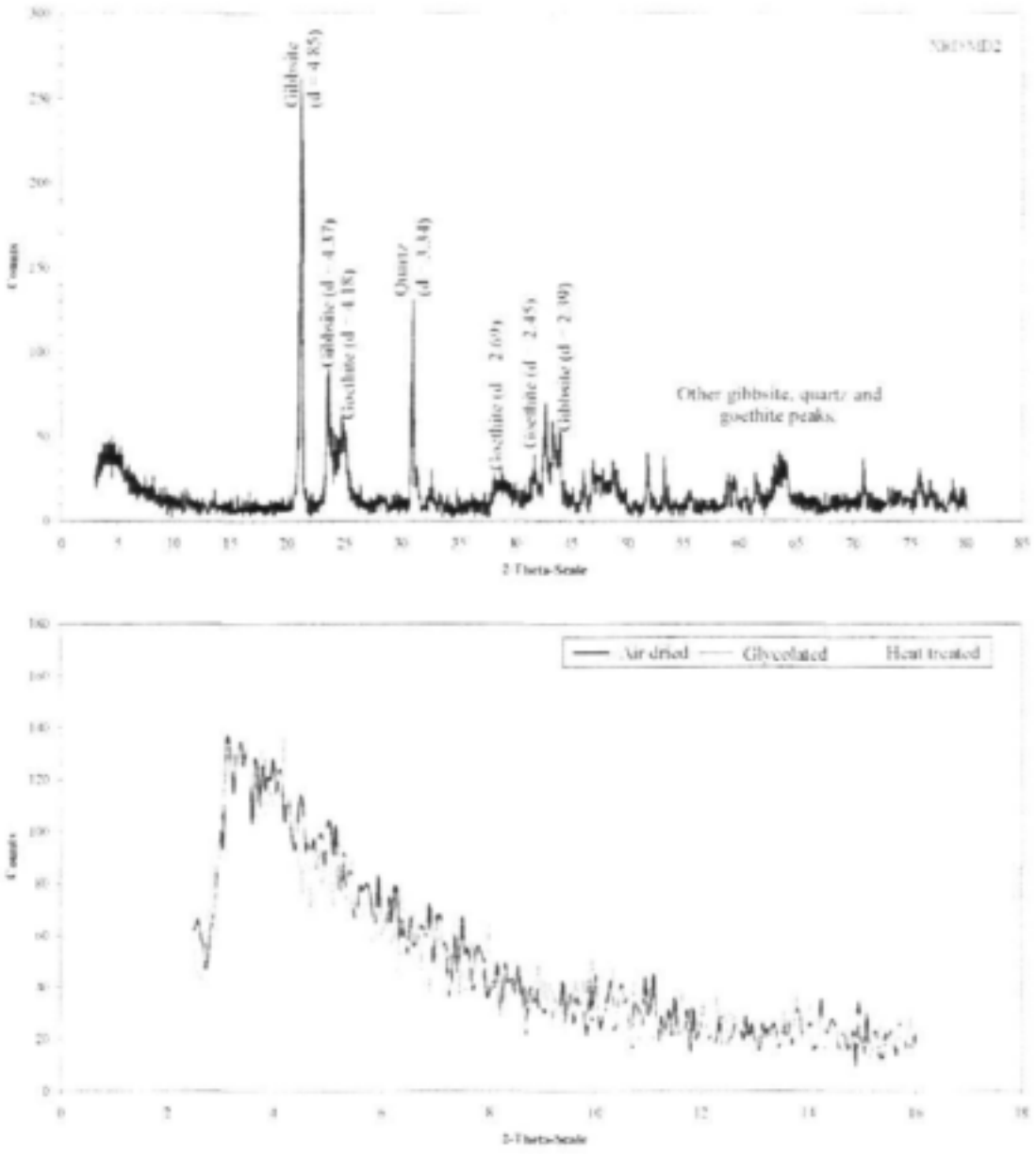

Figure 3: XRD pattern of sample MD2. Lower panel illustrates the XRD patterns of the orientated sample in the 2.5-16°2θ range.

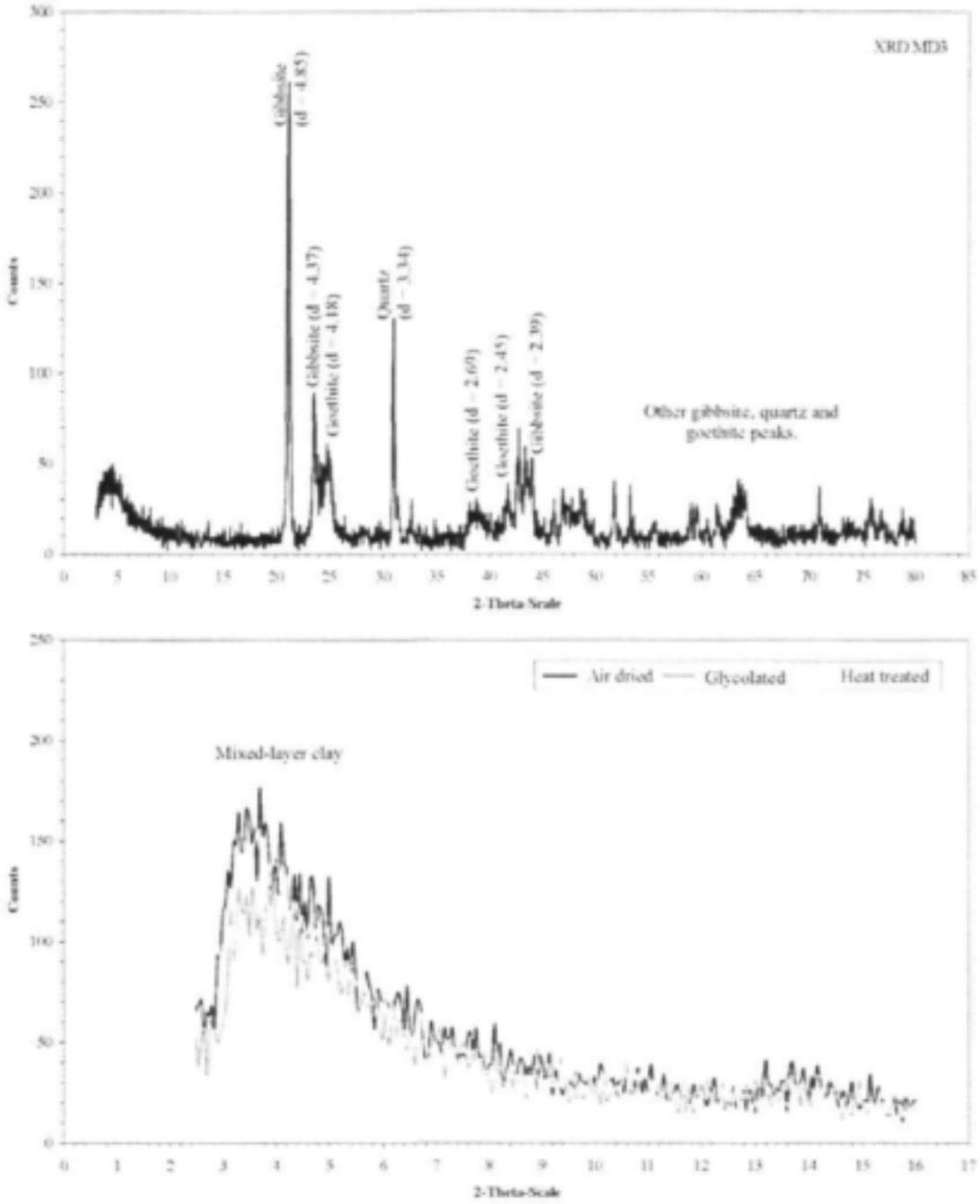

Figure 4: XRD pattern of sample MD3. Lower panel illustrates the XRD patterns of the orientated sample in the 2.5-16°2θ range.

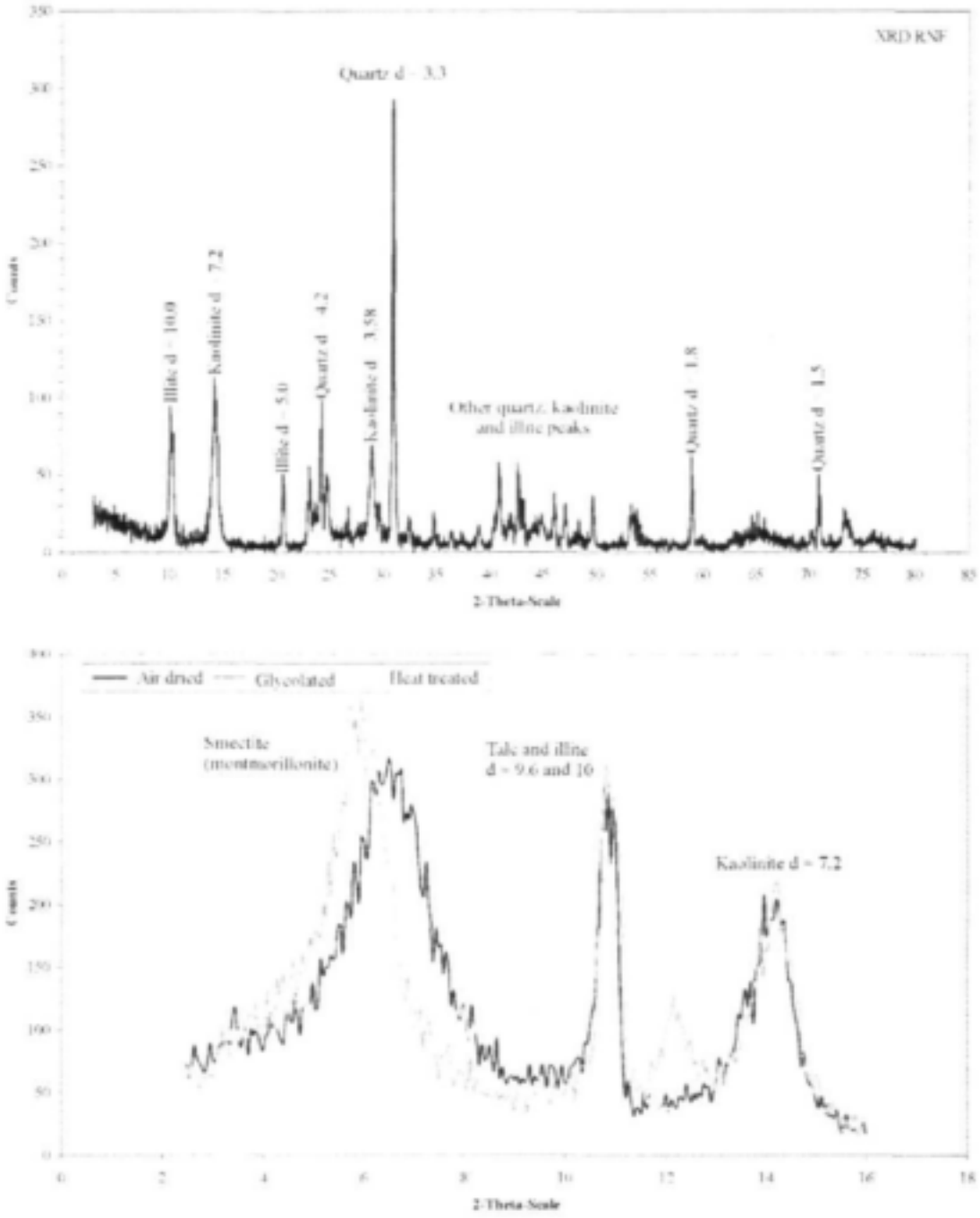

Figure 5: XRD pattern of sample RNF. Lower panel illustrates the XRD patterns of the orientated sample in the 2.5-16°2θ range.

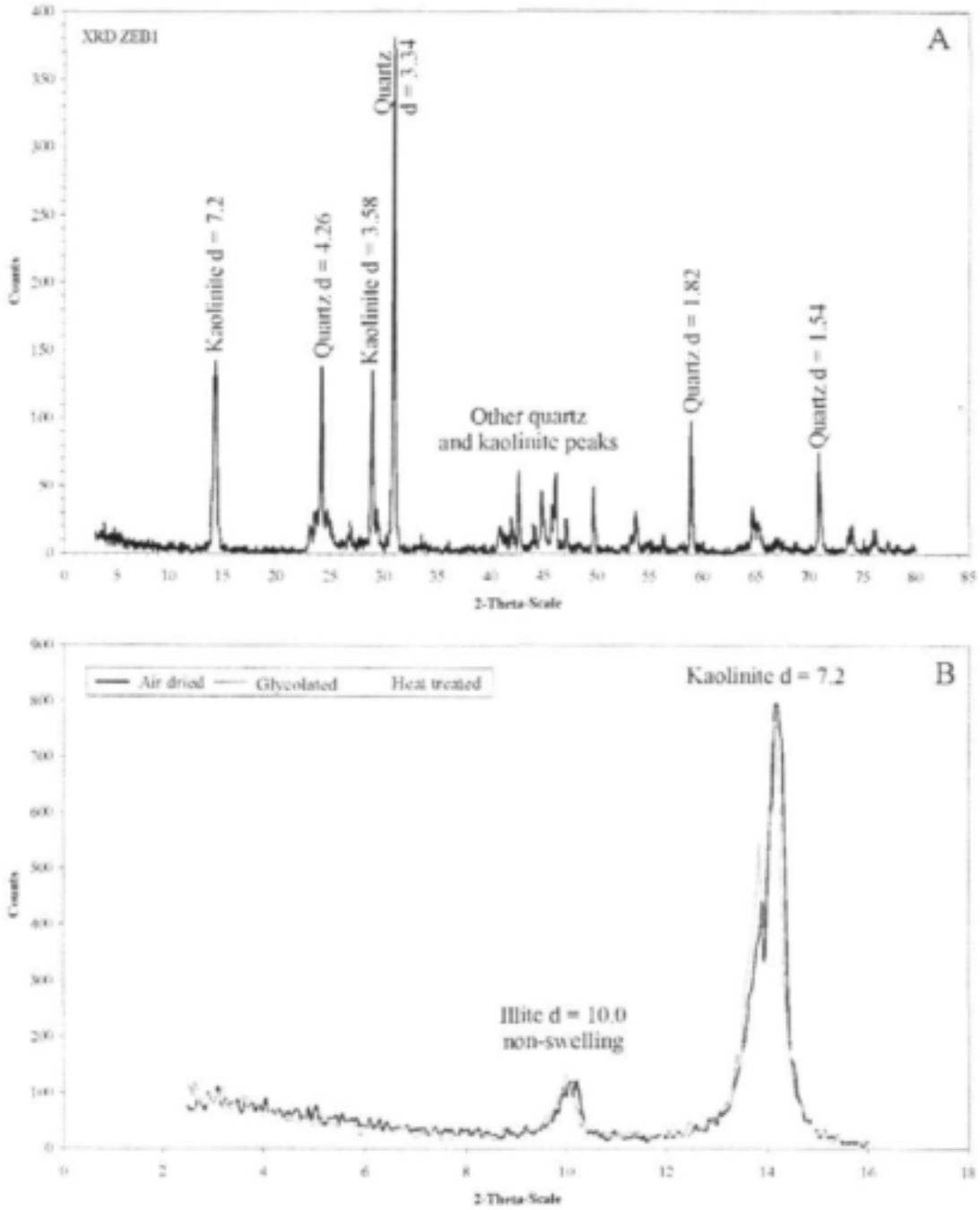

Figure 6: XRD pattern of sample ZEB1. Lower panel illustrates the XRD patterns of the orientated sample in the 2.5-16°2θ range.

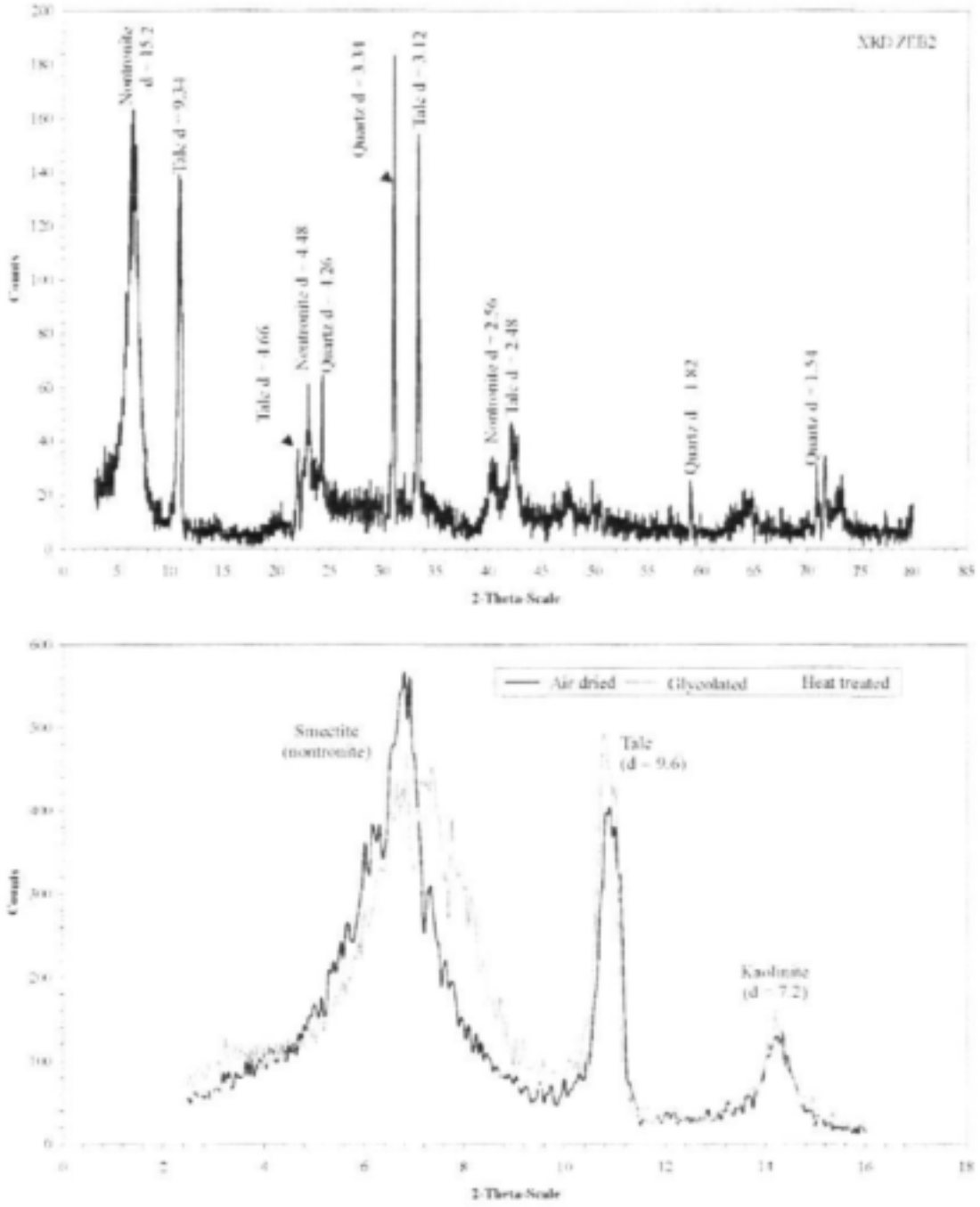

Figure 7: XRD pattern of sample ZEB2. Lower panel illustrates the XRD patterns of the orientated sample in the 2.5-16°2θ range.

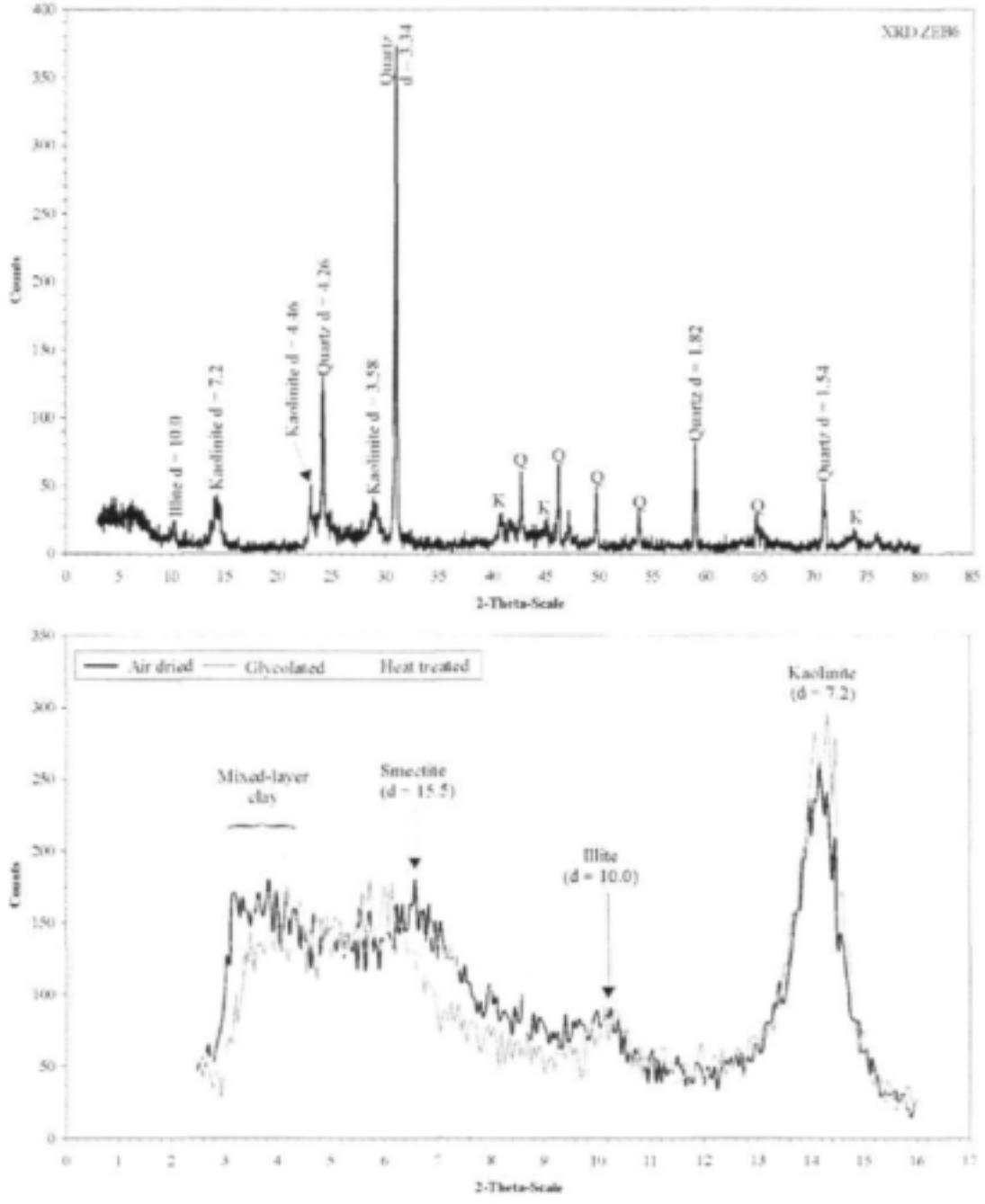

Figure 8: XRD pattern of sample ZEB6. Lower panel illustrates the XRD patterns of the orientated sample in the 2.5-16°2θ range.

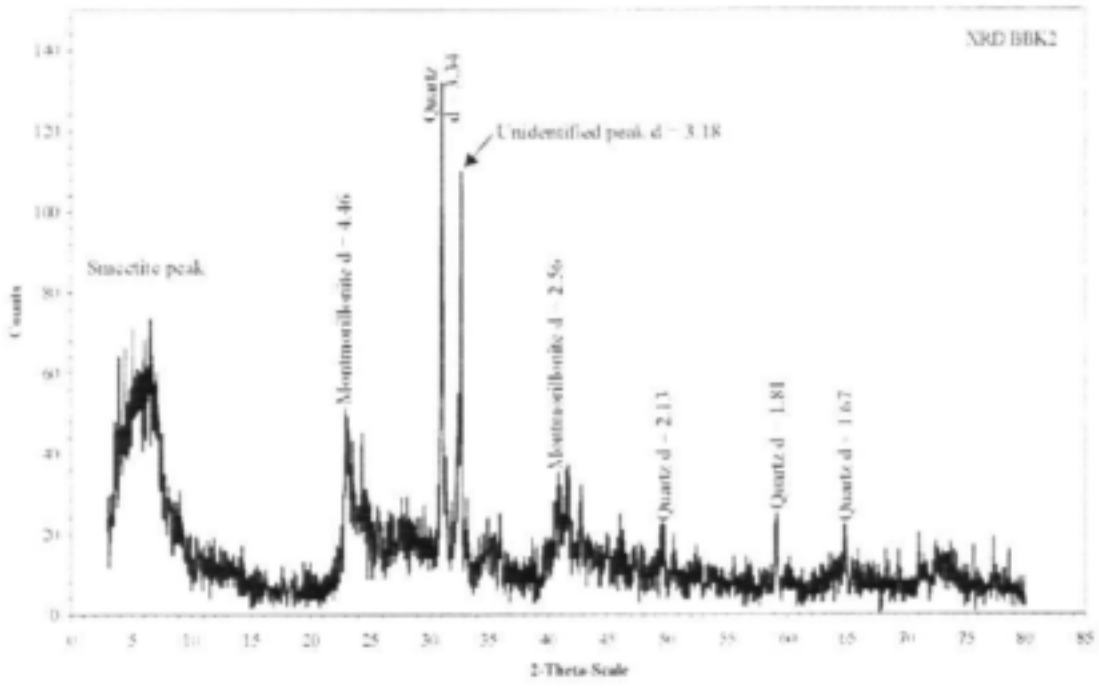

Figure 9: XRD pattern of sample BBK2.

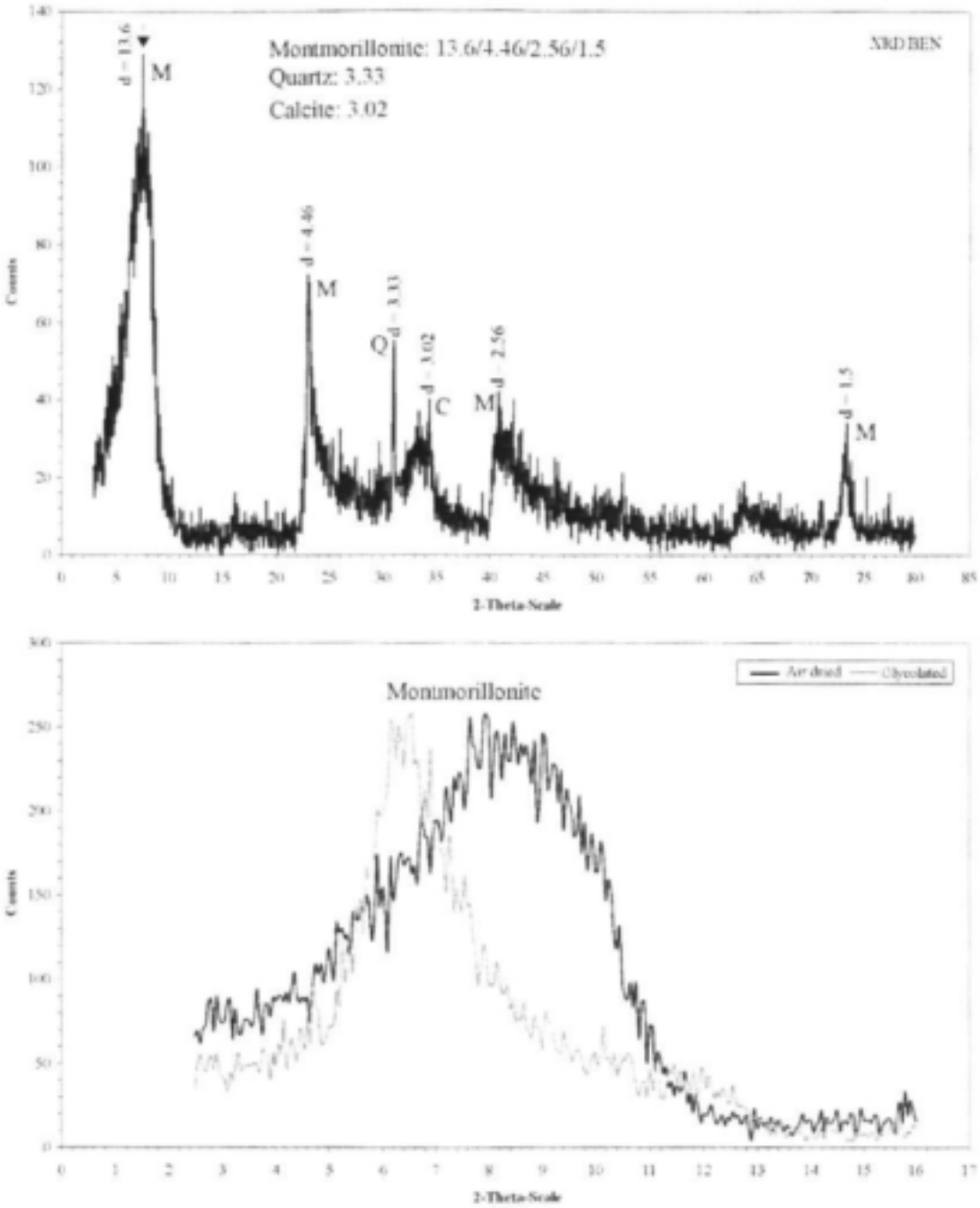

Figure 10: XRD patterns of sample BEN. Lower panel illustrates the XRD patterns of the orientated sample in the 2.5-16°2θ range.

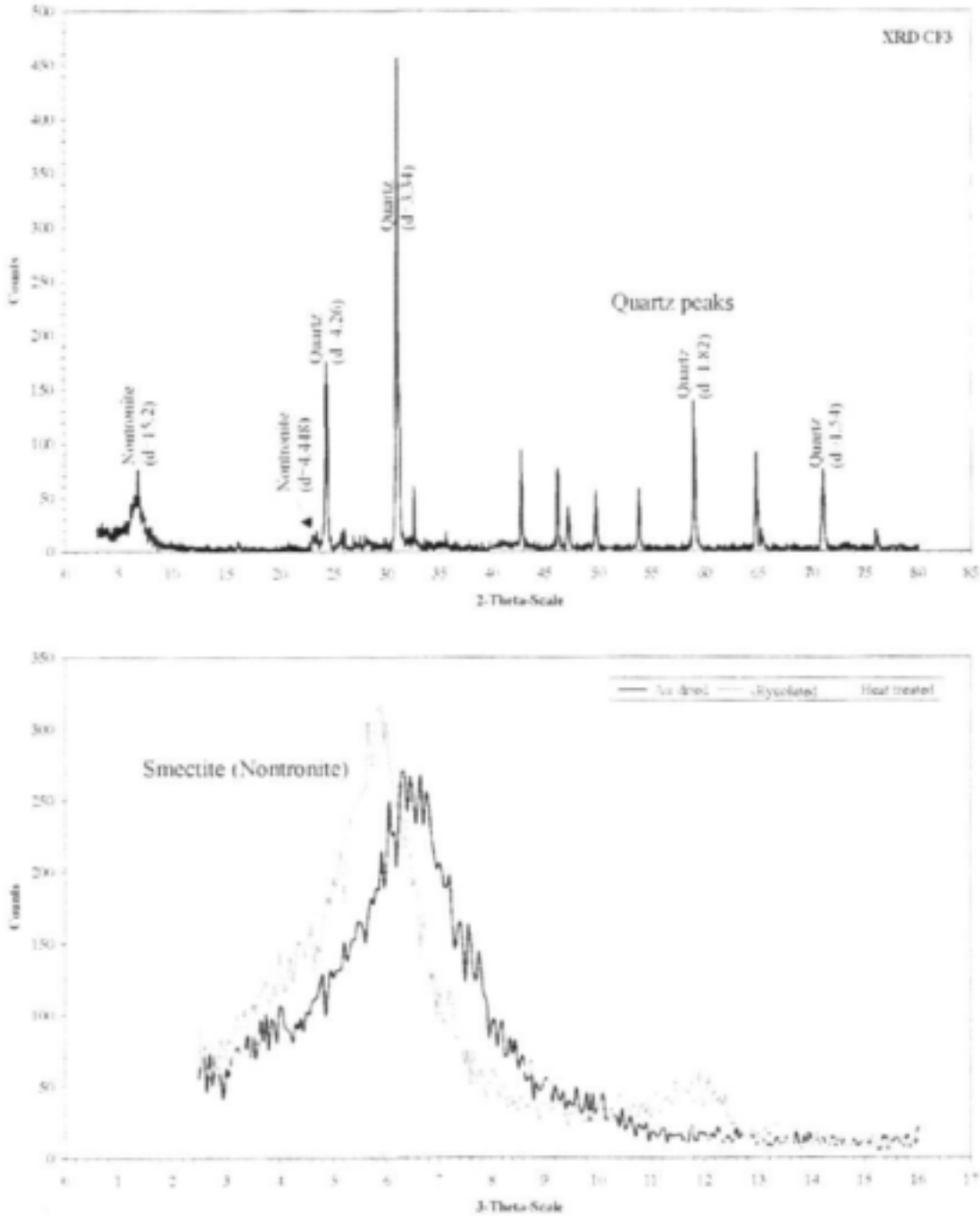

Figure 11: XRD pattern of sample CF3. Lower panel illustrates the XRD patterns of the orientated sample in the 2.5-16°2θ range.

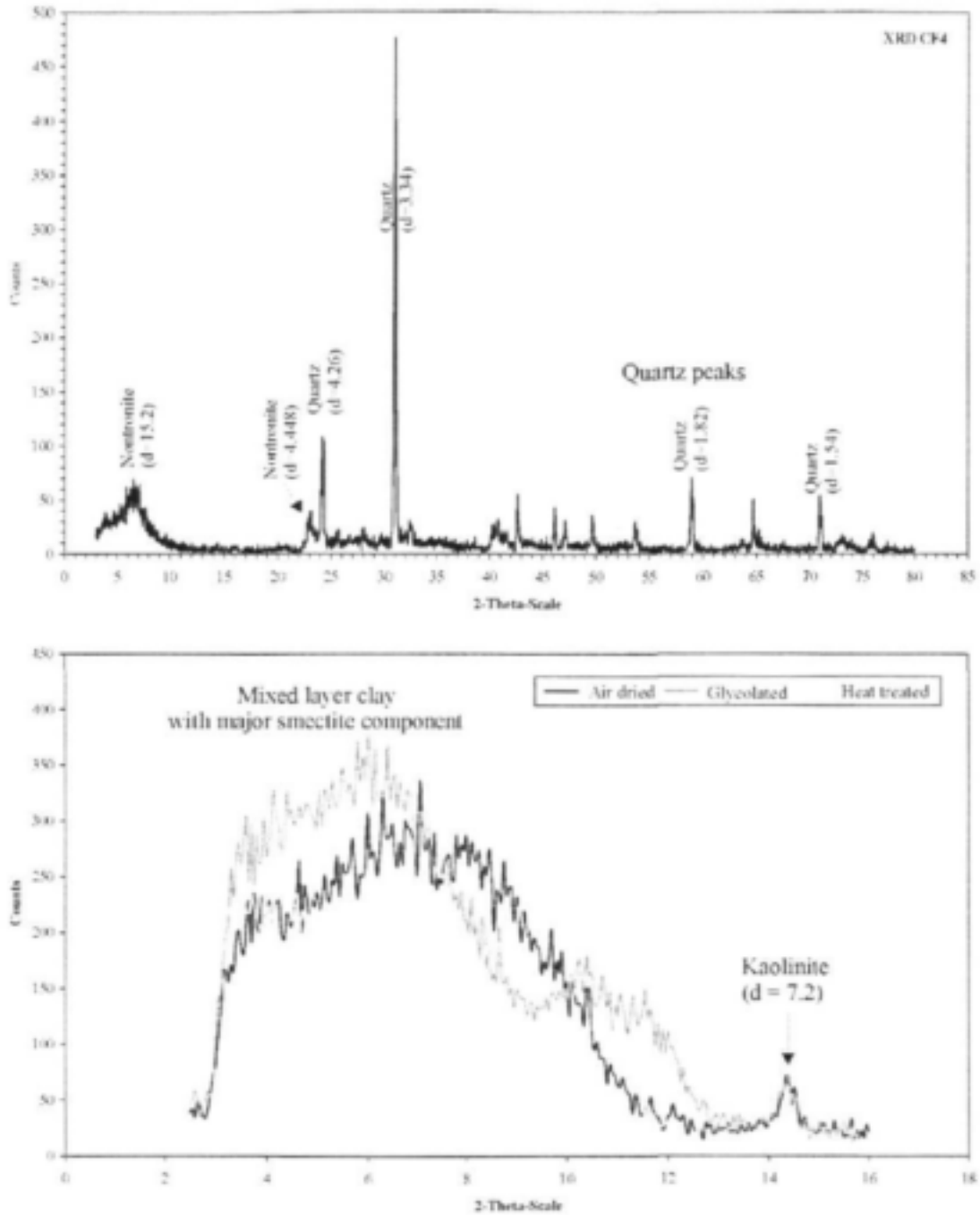

Figure 12: XRD pattern of sample CF4. Lower panel illustrates the XRD patterns of the orientated sample in the 2.5-16°2θ range.

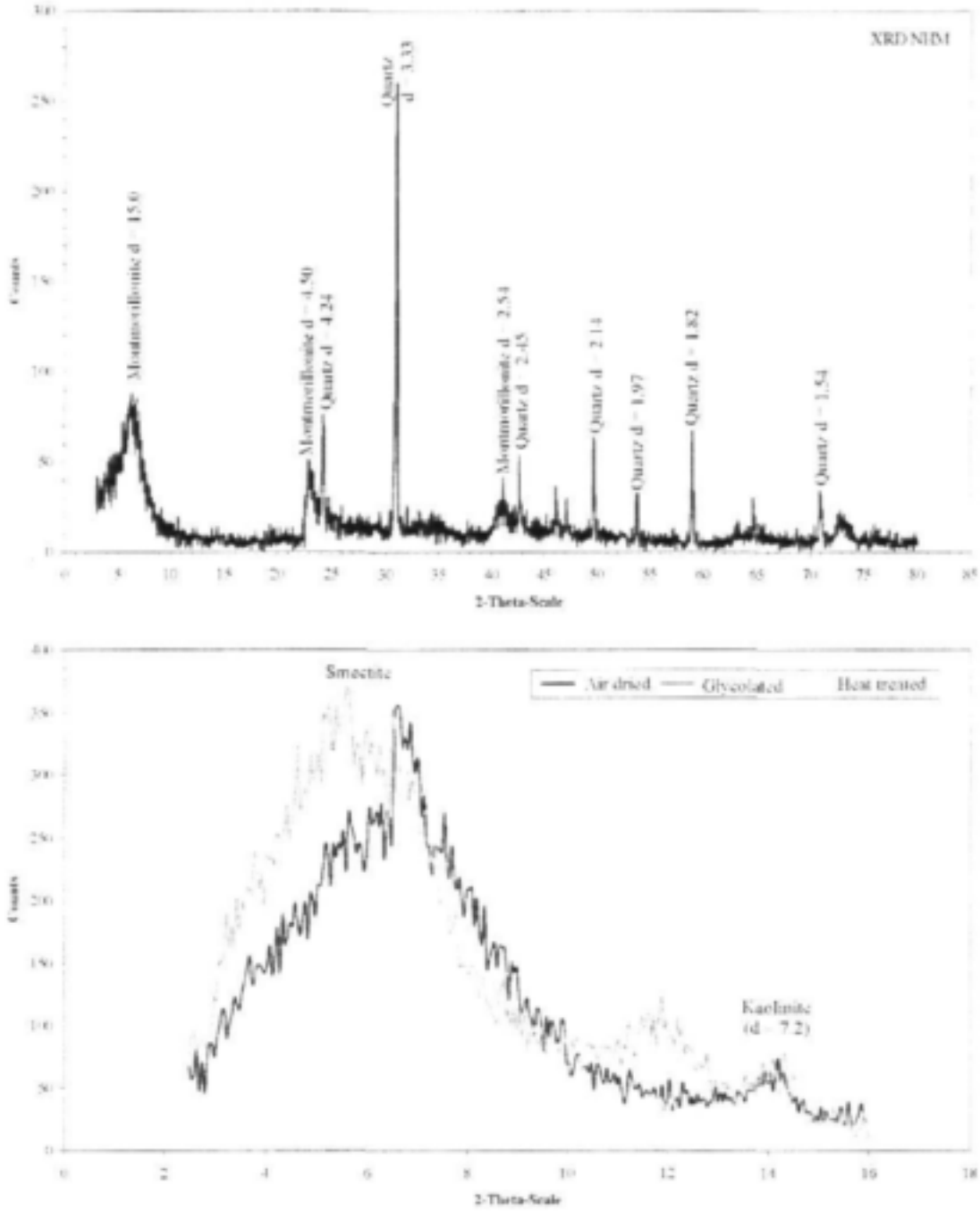

Figure 13: XRD pattern of sample NHM. Lower panel illustrates the XRD patterns of the orientated sample in the 2.5-16°2θ range.

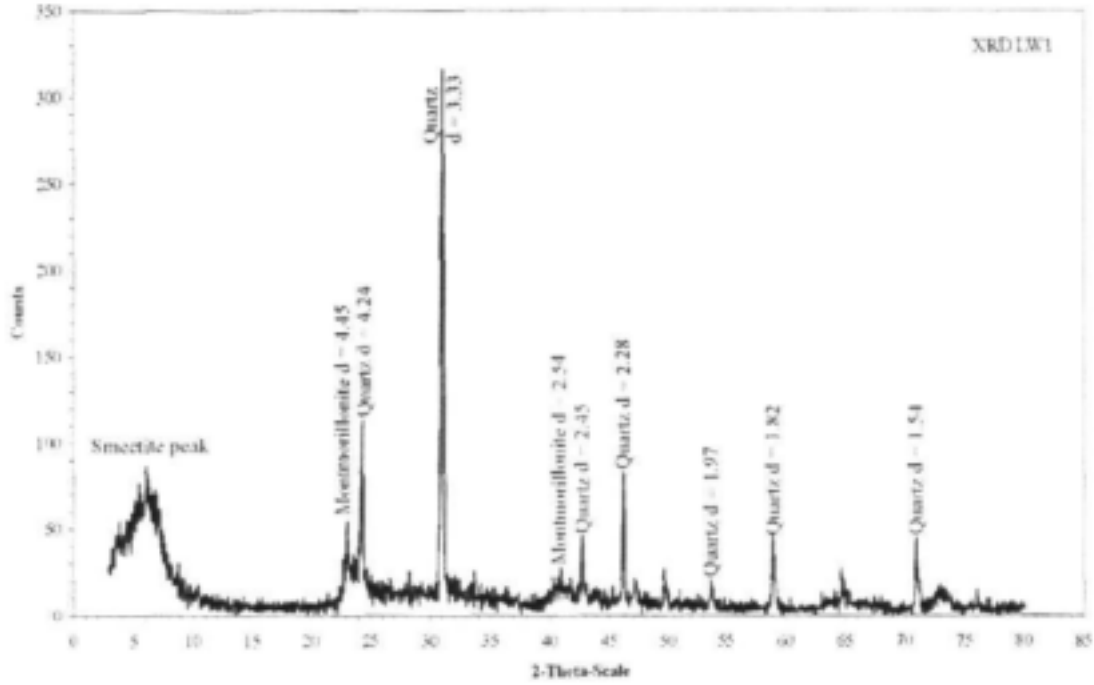

Figure 14: XRD pattern of sample LW1.

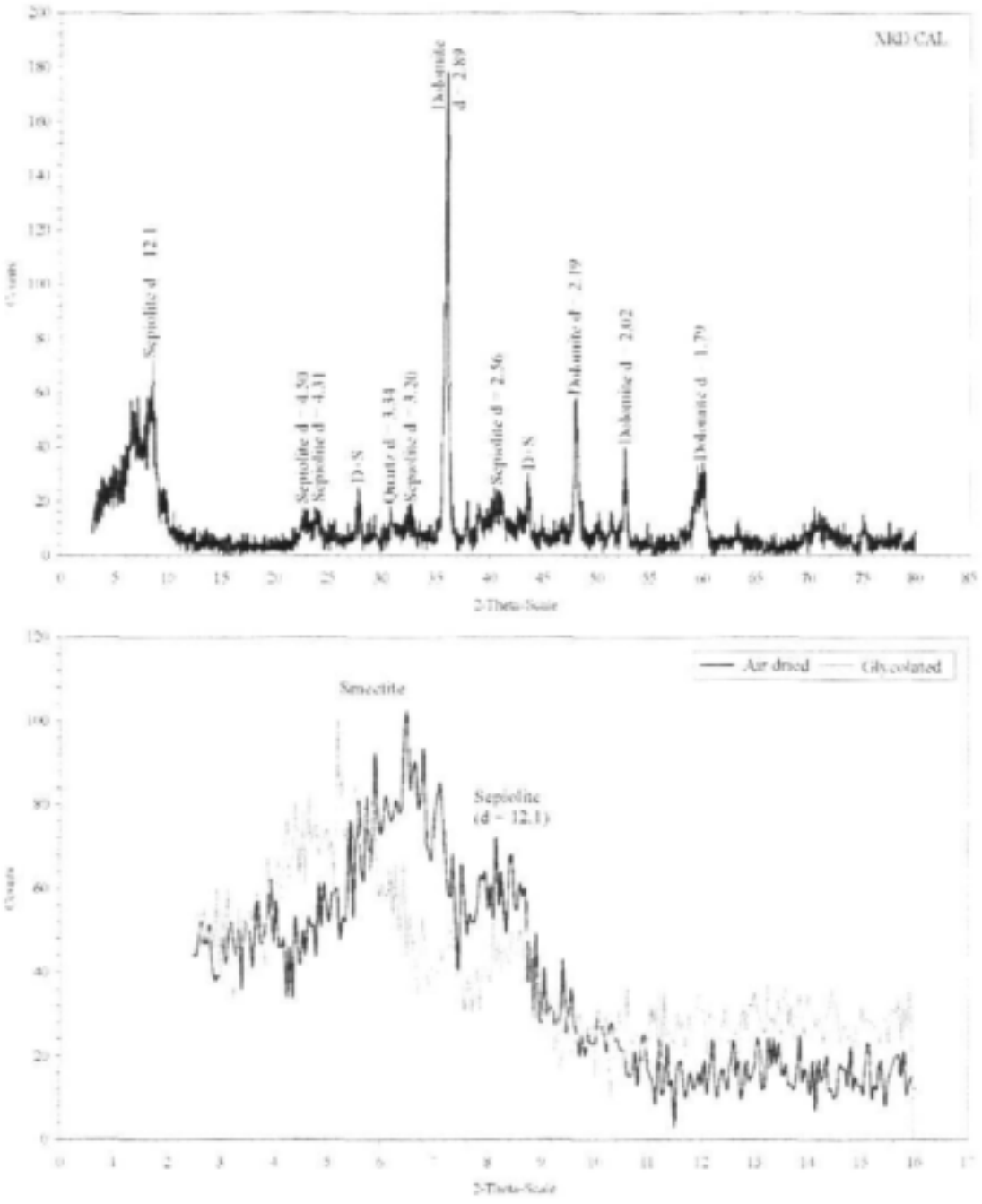

Figure 15: XRD pattern of sample CAL. Lower panel illustrates the XRD patterns of the orientated sample in the 2.5-16°2θ range.

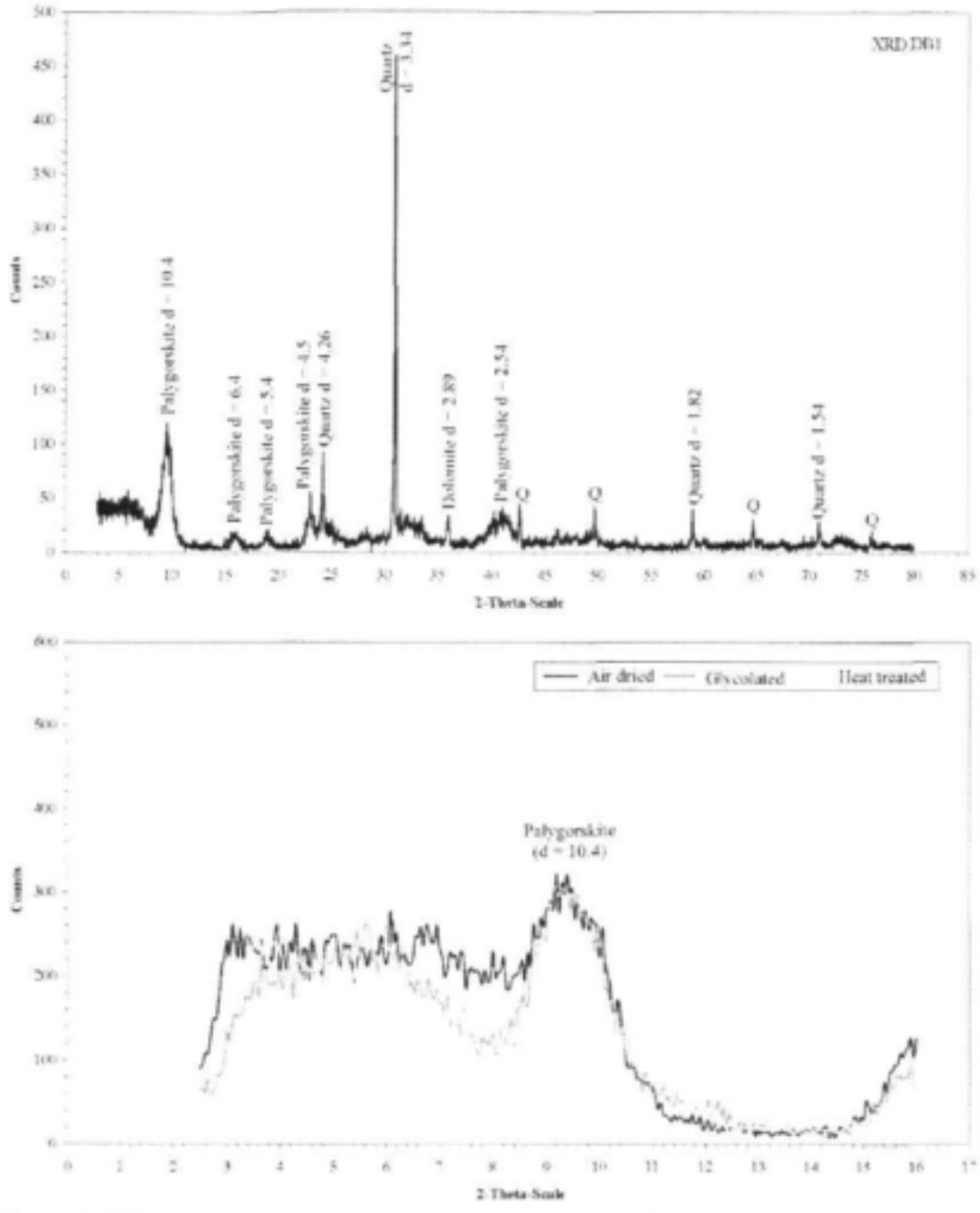

Figure 16: XRD pattern of sample DB1. Lower panel illustrates the XRD patterns of the orientated sample in the 2.5-16°2θ range.

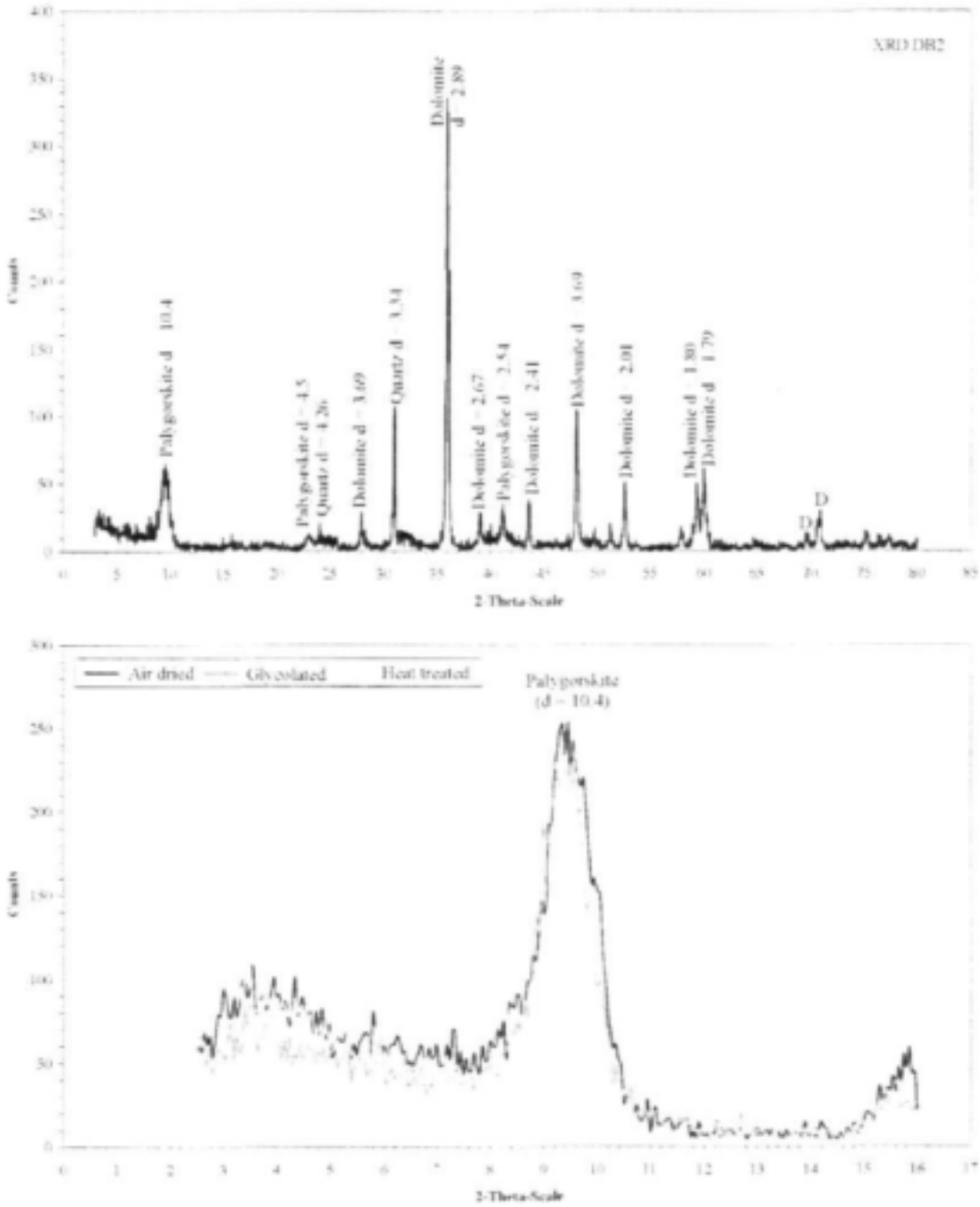

Figure 17: XRD pattern of sample DB2. Lower panel illustrates the XRD patterns of the orientated sample in the 2.5-16°2θ range.

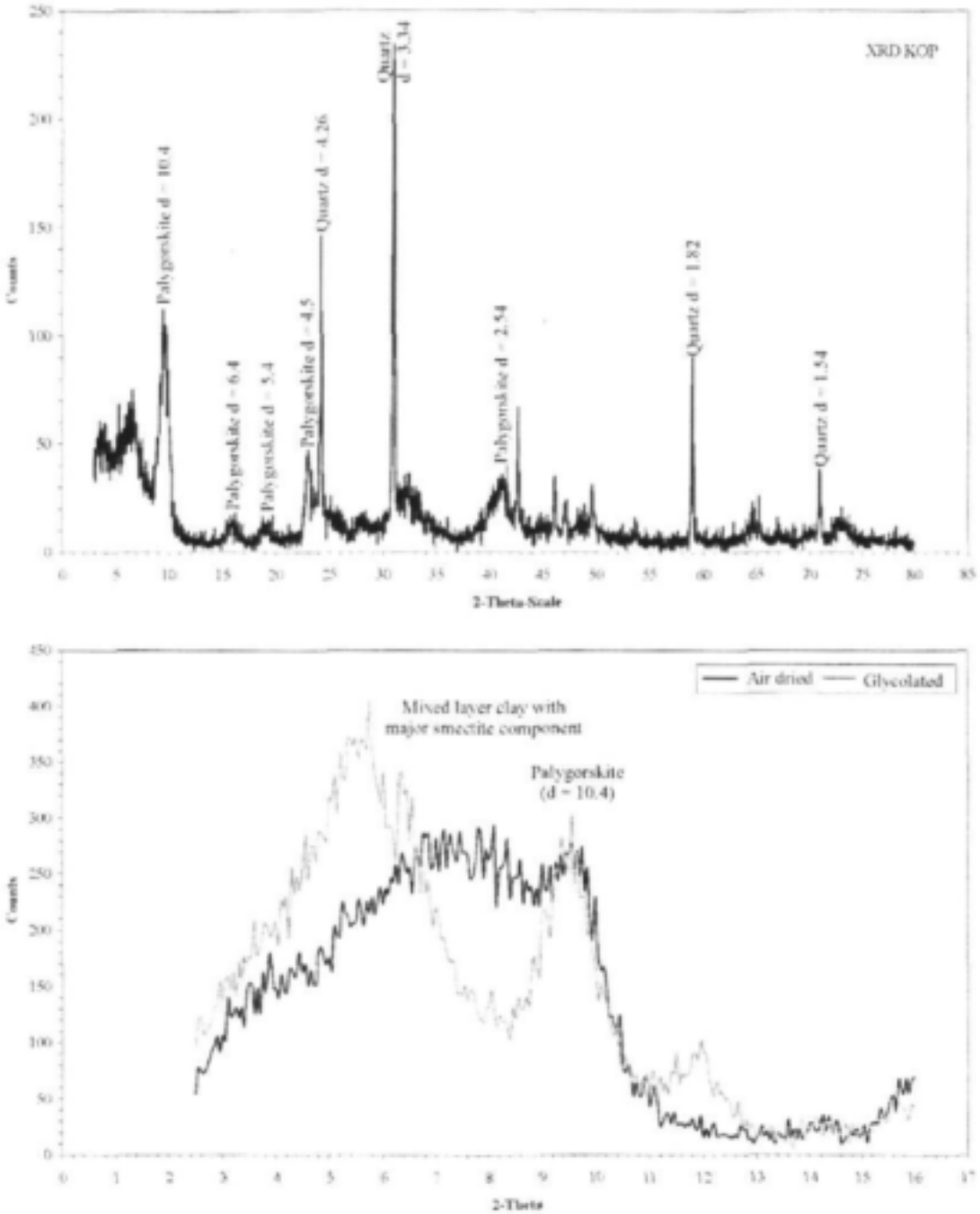

Figure 18: XRD pattern of sample KOP. Lower panel illustrates the XRD patterns of the orientated sample in the 2.5-16°2θ range.

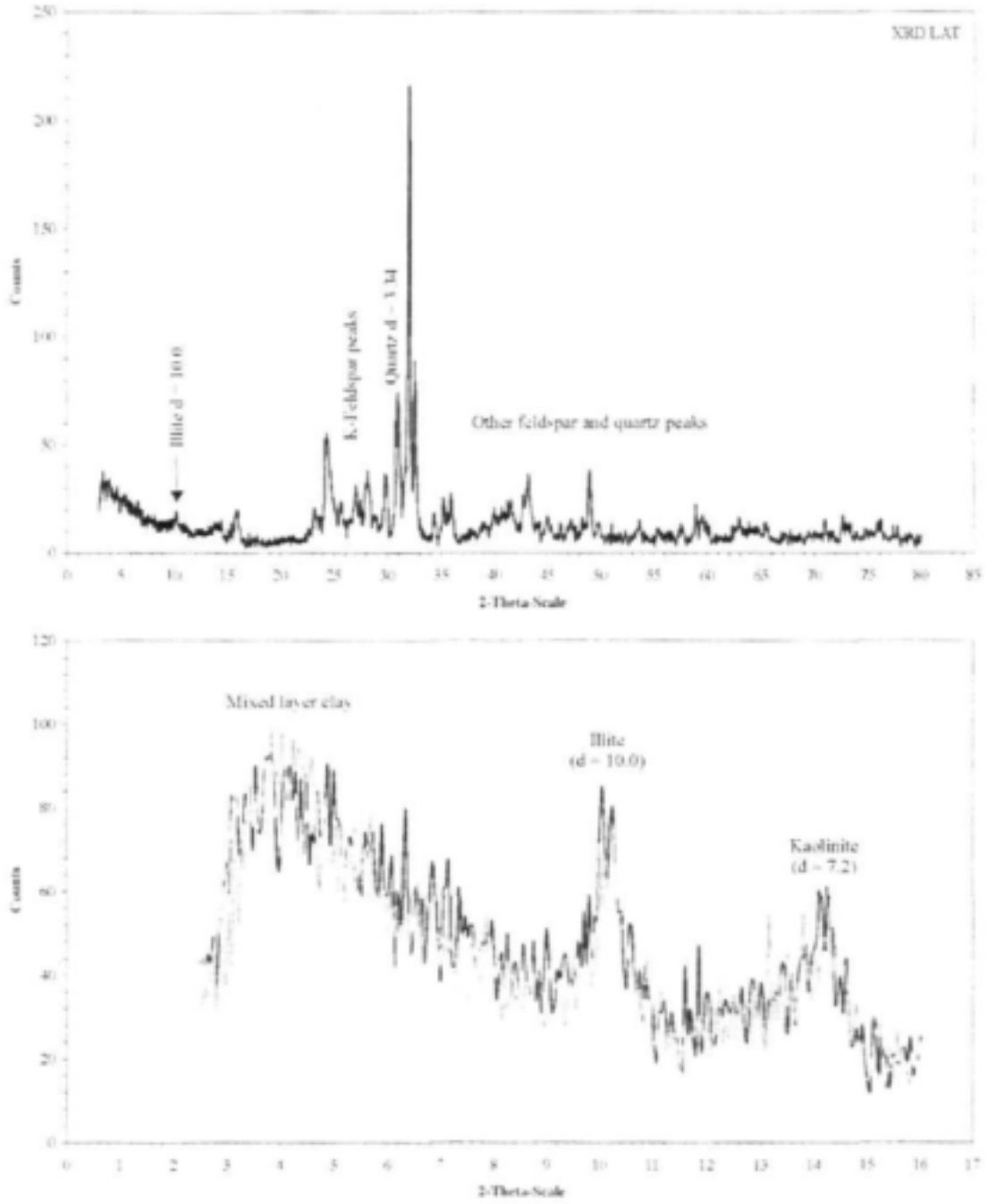

Figure 19: XRD pattern of sample LAT. Lower panel illustrates the XRD patterns of the orientated sample in the 2.5-16°2θ range.

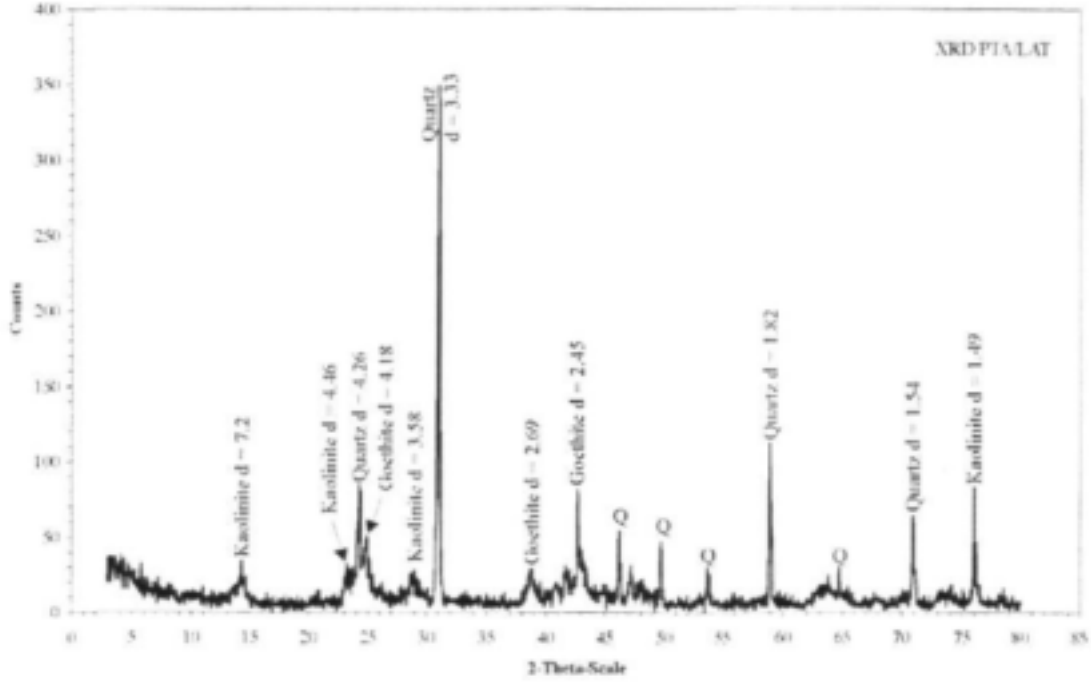

Figure 20: XRD pattern of sample PTA/LAT.

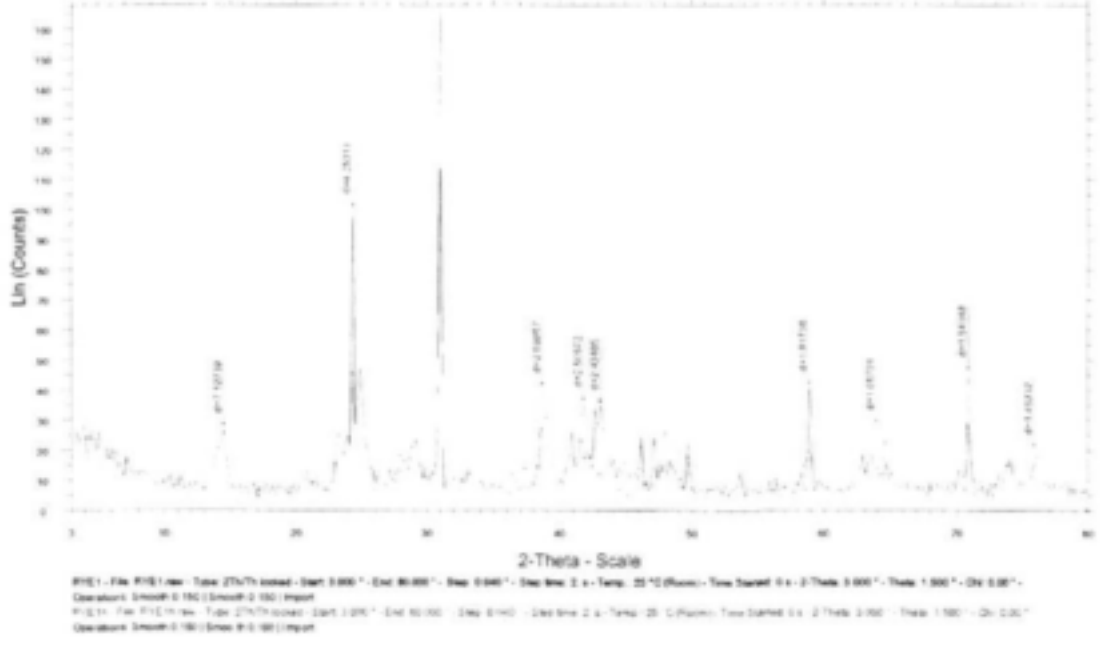

Figure 21: XRD pattern of sample RYE1. Heat-treated sample indicated by red line.

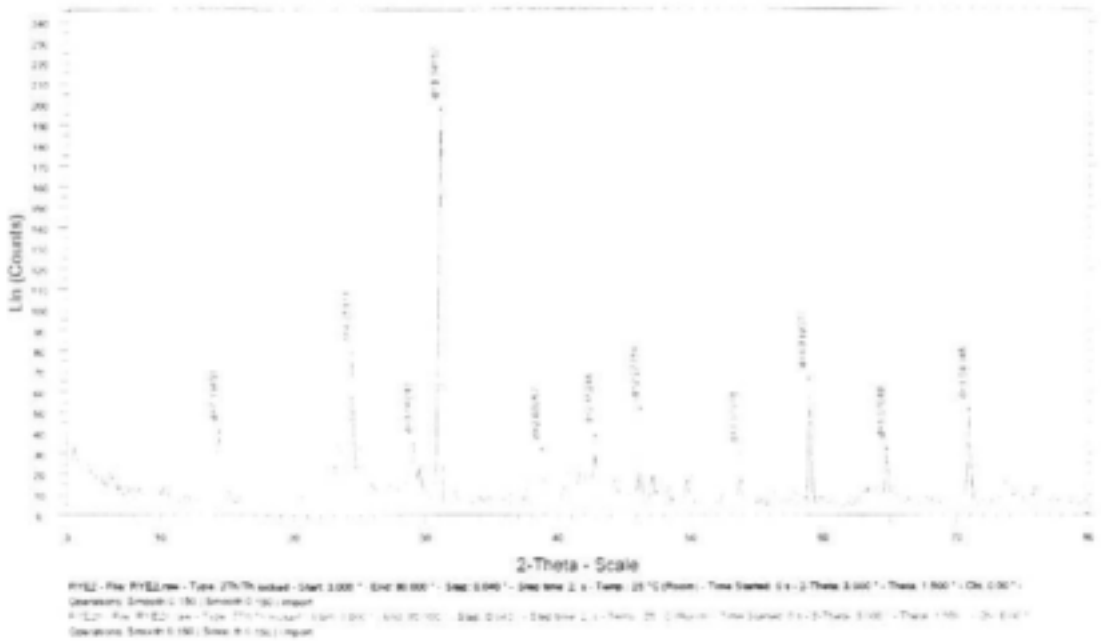

Figure 22: XRD pattern of sample RYE2. Heat-treated sample indicated by red line.

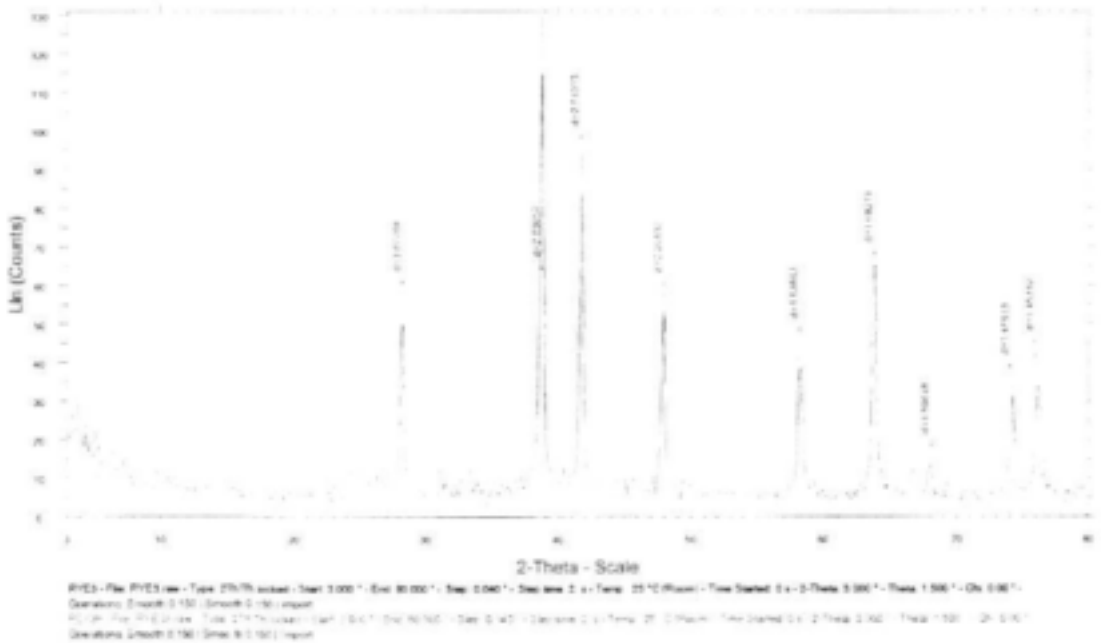

Figure 23: XRD pattern of sample RYE1. Heat-treated sample indicated by red line. Note that these are all hematite peaks.

APPENDIX B
EXPERIMENTAL PROCEDURES

Table Of Contents

1. MINERALOGICAL CHARACTERISATION OF THE CLAYS

(a) *Sample preparation*

A representative portion of each sample was dried overnight at 30°C, after visible pieces of plant material and pebbles were taken out by hand. Each sample was lightly crushed in a swing-disk mill to an arbitrary chosen grain size of <180 µm. Each sample was then dispersed in distilled water using an ultrasonic bath. The clay fraction was separated by using standard centrifugal techniques (USGS, open file report 01-041). Decantation was not an acceptable alternative to centrifugation in this study because normal gravitational methods of particle sedimentation take an inordinate amount of time, and for particles finer than < 0.5 µm Brownian motion interferes with settling (Folk, 1974 and Syvitski, 1991). For each sample, three sedimented samples were prepared on glass slides and allowed to dry slowly to produce orientated deposits. One was heat-treated for 30 min at 550°C, one was left in a desiccator with ethelene glycol at 40°C for 24 h, and one was kept in a desiccator for X-ray diffraction.

(b) *Identification of clay minerals from X-ray diffraction*

Step scans of 4 s per step of 0.05°2 θ from 2.50°2 θ to 16.00°2 θ were done on air-dried, glycolated and heat-treated samples using a Phillips PW 1710 X-ray diffractometer with the following settings:

Tube anode material	Cobalt
Generator potential	40 kV
Wavelength $K\alpha_1$	1.78896 Å
Wavelength $K\alpha_2$	1.79258 Å
Intensity ratio $I_{K\alpha1}/I_{K\alpha2}$	2
Divergence diaphragm	1°
Detector diaphragm	0.1 mm

The changes in peak position on swelling and heating were used to confirm mineral identification (Velde, 1995). X-ray powder diffraction analyses were conducted on each sample using side loaded aluminium sample holders to determine the overall mineralogical composition. These measurements were conducted in a step scan mode of 2 s per 0.04°2 θ step, from 3.00°2 θ to 80.00°2 θ.

A detailed discussion of the mineralogical characterisation of the selected clays is presented in Appendix A.

2. ANALYTICAL METHODS FOR THE DETERMINATION OF F^-

Two analytical methods, high performance ion chromatography (HPIC) and F^- ion selective electrodes (FISE) were used for F^- determinations.

(a) *HPIC*

A Dionex DX-120 ion chromatographic system equipped with a Dionex anion exchange column AS14A was used for the determination of F^- concentrations < 0.1 $mg.L^{-1}$ and other anions leached from the clay sorbents during adsorption tests. The standard HCO_3^-/CO_3^{2-} (1.0 mM HCO_3^- + 3.5 mM CO_3^{2-}) eluent recommended for anion determinations with this column was used in all determinations.

(b) *FISE*

Orion F- ion selective electrodes were used for routine determination of F^- for concentrations > 0.1 mg.L^{-1}

A Total Ionic Strength Adjustment Buffer (TISAB III or TISAB IV) was added to standards and samples. This buffer ensures:

- that a constant ionic strength is maintained in test solutions and standards. This is important because the F^- electrode actually measures activity and not concentration. The measured result is therefore strongly dependent on the ionic strength of the medium because the activity a, given by the equation below,

$$a = \gamma_F[F^-]$$

  will depend on the activity coefficient of the F^- ion, γ_F at the particular ionic strength of the solution.
- that the pH is kept constant at 5.5. This is achieved by an acetic acid buffer in the TISAB III solution and a tartrate buffer in the case of TISAB IV. It is important to maintain the pH of samples and standards above 4 because increasing protonation of F^- at pH < 4 could lead to a negative error. The F^- sensitive membrane does not respond to F^- when it is in its protonated form, HF.
- that F^- is released from its metal ion complexes if present. Of particular importance are AlF^{2+} and AlF_2^+. TISAB III contains CDTA (cyclohexane diamine tetra acetic acid) that forms a very strong complex with metal ions such as Al^{3+} replacing the F^- in the process. For very high levels of Al^{3+} and other metals forming complexes with F^-, TISAB IV was used. TISAB IV contains hydroxymethyl aminomethane as complexing agent. In the case of low concentration F^- determinations a special low level TISAB solution is recommended because TISAB III and IV do not produce accurate results when applied under these conditions. The low level TISAB, however, does not contain a complexing agent such as CDTA and can therefore not compensate for interferences caused by complexation of F^- with metals such as Al^{3+}.

FISE offers linear calibration graphs for concentrations larger than 0.1 mg.L^{-1}. Below 0.1 mg.L^{-1}, curvature in the calibration curve increases and it becomes more difficult to compensate for electrode drift and special procedures need to be followed to produce accurate results. These procedures include a 20 min equilibration of the membrane in 0.1 M F^- solution prior to calibration and the analysis. Even then the electrode requires more than 10 min to stabilise after each transfer to a new sample or standard. Groundwaters in the study area in most cases have pH values > 7. In alkaline waters the presence of metal cations such as Al^{3+} that can form complexes with F^- is unlikely and the inclusion of CDTA in the TISAB solution is not mandatory. In this study F^- determinations were also required in acidic solutions where Al^{3+} leached from the clay substrates could interfere with the measurement. This would lead to an underestimation in the F^- concentration. In this study TISAB III and IV was therefore used as ionic strength adjustment buffer.

(c) *Comparison of the methods*

Consistent differences in the determination of F^- in natural waters using FISE and HPIC have been reported (McCaffrey, 1994) using the older generation of anion exchange columns and F^- membrane electrodes. One of the problems with these columns using the standard

HCO_3^-/CO_3^{2-} eluent was that the F^- peak appeared immediately after the water dip which made the accurate determination of the baseline difficult. The Dionex AS14A columns used in this study produced a F^- peak well separated from the water dip. To ensure accurate analytical results it was nevertheless decided to perform a limited study to compare the two techniques for F^- determination in the test solutions encountered in this study. Orion 94-09SC fluoride ISE's were used in this study.

The procedure used in this comparative study included the following steps. The two techniques were calibrated using exactly the same set of standards. In case of FISE, however, TISAB III or TISAB IV was added to both samples and standards. Test solutions obtained from spiking deinonised water, tap water and aqueous extracts from selected clay sorbents were then analysed in triplicate by both methods. The results obtained by the two methods are summarised in Table B1. Tap water contained 0.09 $mg.L^{-1}$ F^- and the measured samples were therefore corrected by subtracting this amount. In Figure B1 ISE results for spiked tap water samples using TISAB III and TISAB IV buffers are plotted vs F^- concentrations obtained by IC. The results show a good correlation at F^- concentrations between 0.1 and 10 $mg.L^{-1}$. Both techniques are therefore capable of analysing correctly in relatively undemanding matrices such as tap water. Accurate determination of F^-, however, becomes rather challenging in more complex matrices such as the extracts obtained from adsorption experiments on clay samples. Table B2 compares the results obtained by analysing a spiked extract obtained from RBM. RBM is an aluminium oxide which releases small amount of Al during extraction. Extracts were prepared by extracting 10g of clay with 300 mL deionised water for 1h. The extract contained 2.58 $mg.L^{-1}$ F^- and the measured samples were therefore corrected by subtracting this amount. The accurate determination of F^- in this matrix proved to be problematic when using IC. Lower concentrations from 0.1 to 2 $mg.L^{-1}$ were over estimated and higher concentrations underestimated. The results obtained using ISE with TISAB IV buffer produced the most accurate results and were used as standard analytical procedure in this study.

Table B1 F^- determined in spiked samples by IC and ISE using TISAB III and TISAB IV, Concentrations in $mg.L^{-1}$

	ISE							
	TISAB III							
Matrix	Deionised water				Tap water			
Spiked F	[F]	SD	%recovery	% error	[F]	SD	%recovery	% error
0.1	0.10	0.001	100.0	0.0	0.09	0.002	90.0	-10.0
0.2	0.20	0.003	100.0	0.0	0.18	0.001	90.0	-10.0
0.5	0.49	0.001	98.0	-2.0	0.49	0.002	98.0	-2.0
1	1.01	0.003	101.0	1.0	0.96	0.003	96.0	-4.0
2	2.01	0.017	100.5	0.5	1.95	0.029	97.5	-2.5
3	2.93	0.016	97.7	-2.3	2.89	0.008	96.3	-3.7
5	5.00	0.014	100.0	0.0	4.92	0.014	98.4	-1.6
7	6.94	0.019	99.1	-0.9	6.81	0.098	97.3	-2.7
10	10.07	0.112	100.7	0.7	9.77	0.028	97.7	-2.3
	ISE							
	TISAB IV							
Matrix	Deionised water				Tap water			
Spiked F	[F	SD	%recovery	% error	[F]	SD	%recovery	% error
0.1	0.1	0.001	100	0.0	0.1	0.002	100.0	0.0
0.2	0.2	0.002	100	0.0	0.2	0.002	100.0	0.0
0.5	0.5	0.002	100	0.0	0.5	0.004	100.0	0.0

1	1.01	0.001	101	1.0	0.98	0.001	98.0	-2.0
2	1.98	0.003	99	-1.0	1.99	0.015	99.5	-0.5
3	3.01	0.01	102	0.3	2.96	0.011	98.7	-1.3
5	4.96	0.02	99.2	-0.8	4.95	0.02	99.0	-1.0
7	6.99	0.01	99.9	-0.1	6.96	0.032	99.4	-0.6
10	9.98	0.03	99.9	-0.2	9.98	0.025	99.8	-0.2
	ION CHROMATOGRAPHY							
Matrix	Deionised water				Tap water			
Spiked F)	[F]	SD	%recovery	% error	[F]	SD	%recovery	% error
0.1	0.1	0.002	100.0	0.0	0.09	0.002	90.0	-10.0
0.2	0.21	0.001	105.0	5.0	0.18	0.004	90.0	-10.0
0.5	0.49	0.001	98.0	-2.0	0.53	0.001	106.0	6.0
1	0.99	0.003	99.0	-1.0	0.99	0.002	99.0	-1.0
2	2.03	0.005	101.5	1.5	1.97	0.003	98.5	-1.5
3	3.01	0.002	100.3	0.3	2.96	0.002	98.7	-1.3
5	4.95	0.01	99.0	-1.0	4.97	0.011	99.4	-0.6
7	7	0.009	100.0	0.0	7.01	0.02	100.1	0.1
10	10.02	0.021	100.2	0.2	9.95	0.024	99.5	-0.5

Table B2 [F^-] determined in spiked RBM extract samples by IC and ISE using TISAB III and TISAB IV. Concentrations in $mg.L^{-1}$

RBM	TISAB III			TISAB IV			IC		
Spiked [F]	[F]	%recovery	% error	[F]	%recovery	% error	[F]	%recovery	% error
0.1	0.12	120.0	20.0	0.12	120.0	20.0	0	0	
0.2	0.3	150.0	50.0	0.22	110.0	10.0	0.74	370	270
0.5	0.49	98.0	-2.0	0.54	108.0	8.0	1.13	226	126
1	0.97	97.0	-3.0	1.1	110.0	10.0	1.47	147	47
2	1.9	95.0	-5.0	2.13	106.5	6.5	2.45	122.5	22.5
3	3	100.0	0.0	3.26	108.7	8.7	2.96	98.7	-1.3
5	5.23	104.6	4.6	5.33	106.6	6.6	4.84	96.8	-3.2
7	7.69	109.9	9.9	7.55	107.9	7.9	6.6	94.3	-5.7
10	11.03	110.3	10.3	10.25	102.5	2.5	8.61	86.1	-13.9

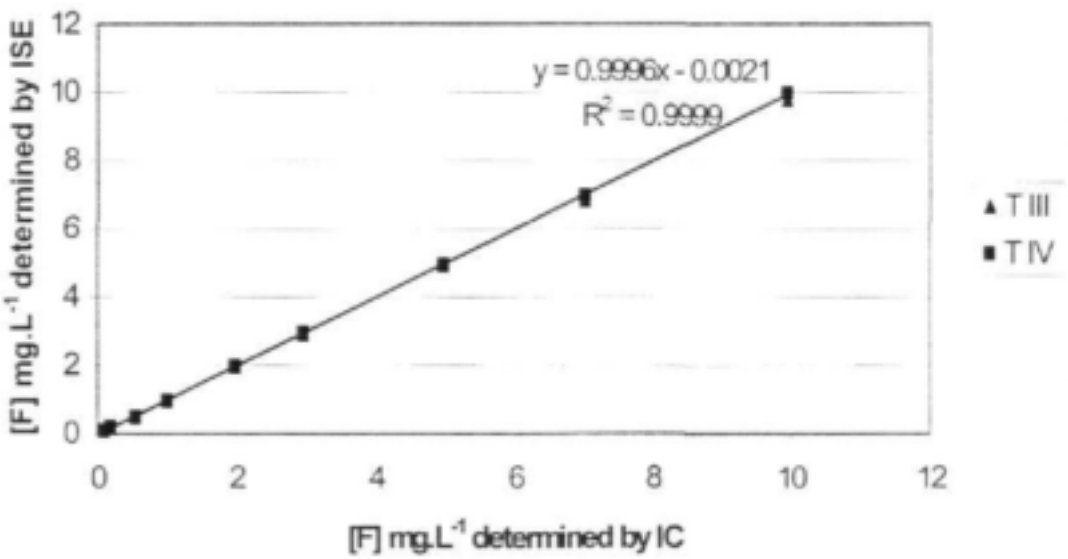

Figure B1 F^- concentrations in spiked tap water samples determined by ISE using TISAB III and IV vs determinations by IC

3. DETERMINATION OF ELEMENTAL COMPOSITION

(a) *Solid samples*

The major element composition of selected clay samples was determined by XRF by Set Point Technologies.

(b) *Solutions*

Inductively coupled plasma optical emission spectrometry (ICP-OES) was used to determine the elemental composition in solution samples. A method was developed for the determination of the elements: Al, Fe, Mn, Cu, Ca, Mg, Cr, Mn, Ni, Zn, and As using the Varian Liberty 100 ICP-OES spectrometer. A 1000 $mg.L^{-1}$ Multi IV (Merck SA) multi-element ICP-OES standard was used to prepare calibration standards by appropriate dilution with 2% HNO_3.

The analytical wavelengths and experimental conditions used in the ICP OES measurements are summarised in Table B3 and Table B4, respectively.

Table B3 Analytical wavelengths for the determination of metals in solution by ICP-OES

Elements	Analytical Wavelength (nm)	Instrumental detection limit
Al	396.153	0.10
Fe	259.940	0.05
Cu	324.754	0.02
Ca	393.366	0.05
Mg	279.553	0.05
Cr	267.716	0.05
Mn	257.610	0.02
Ni	231.604	0.05
Zn	213.856	0.05
As	188.979	0.05

Table B4 ICP-OES operational conditions

Parameter	Setting
Generator power	1.3 Kw
Plasma gas flow	15.0 $L.min^{-1}$
Nebuliser pressure	150 kPa
Sample uptake rate	1 $mL.min^{-1}$
Integration time	3 s
Viewing height	2-8 mm
PMT voltage	450-650 V
Order	2

4. PRETREATMENT PROCEDURES

(a) *Wash procedure to remove water extractables*

All clay samples were extracted by shaking with deionised water in a 1:10 mass(g) to volume(mL) ratio for 10 m, centrifuged at 3900 rpm for 5 m and decanted. Extraction was repeated until clays were free from water extractable ions indicated by the absence of Cl^- in ion chromatograms of the extracts. The washed clay was dried overnight at 105 °C, pulverised in an agate mortar and stored in a desiccator.

(b) *Heat treatment*

Clay samples, placed in porcelain crucibles, were heat-treated at the desired temperature in a preheated muffle furnace for 2 h. To study the effect of heating clays at different temperatures, the same procedure was followed through the temperature range 200 to 900°C in steps of 100°C. A temperature of 600 °C was selected for heat treatment. After heat treatment clays were cooled, pulverised and stored in a desiccator.

(c) *Chemical pretreatment*

Clay samples containing F^- were chemically treated to remove F^- through an ion exchange process with hydroxide. Chemical treatment was also used to activate clay surfaces before F^- adsorption. In the chemical pretreatment procedure clays were stirred with 0.1 M $NaCO_3$ for 30 min in a mass(g) to volume (mL) ratio of 1 to 5, centrifuged for 5 min and decanted. The residue was washed with deionised water to remove excess sodium carbonate and again centrifuged and decanted. The residue was then treated with 1% HCl for 30 m in a mass(g) to volume(mL) ratio of 1 to 5 and rinsed until Cl^--free. The rinsed solution was tested with $AgNO_3$ solution initially and finally with HPIC. The residue was dried overnight at 105 °C, pulverised in an agate mortar and stored in a desiccator.

(d) *Chemical treatment for alkaline clays*

Alkaline clays such as clays containing substantial amounts of dolomite or Ca and Mg carbonates, required modification of the chemical pretreatment procedure. The acid treatment

was excluded from the procedure described in Section 4c of Appendix B, because adding acid to dolomitic clays would cause dissolution of the Ca and Mg carbonates according to the reaction:

$$CaCO_3 + HCl \rightleftharpoons Ca^{2+} + 2Cl^- + H_2O + CO_2$$

(e) *Sequential pretreatment procedure*

In the sequential treatment, samples were first heated for 1 h at 600°C and then treated chemically with Na_2CO_3 and HCl as above.

Table B5 summarises the different pretreatment procedures and the notation used in this study.

Table B5 Notation of pretreatment procedures

Procedure	**Notation**
Removal of water extractables	CR
Heat treatment	C
Chemical treatment	CT
Heat followed by chemical treatment	CTC

(f) *Substrate regeneration procedure*

Regeneration of clay substrates was done using the same solutions, 0.1 M Na_2CO_3 and 1% HCl as for chemical pretreatment.

5. AMMONIUM OXALATE EXTRACTION

The ammonium oxalate extraction (Parfitt RL, (1989) removes materials without a well-developed crystalline structure and is specificly designed to dissolve Al, Fe and Mn from amorphous soil phases. A sample is shaken for 4 h in the dark with ammonium oxalate at pH 3.

0.5 g of clay sample was weighed into a 100 mL poly ethylene flask which was wrapped in aluminium foil to protect it from light induced reactions. 50 mL 0.2 M ammonium oxalate at pH 3 was added. The flask was then placed in a shaker for 4 h. After filtration and appropriate dilution the Al, Fe and Mn concentrations were determined in the filtrate by ICP-OES.

6. BATCH ADSORPTION PROCEDURES:

(a) *Adsorption at pH 6*

Adsorption capacities were determined at pH 6 by shaking 1 g of washed and dried (2 h at 105°C) clay with 50 mL of 10 mgF.L^{-1} NaF solution (C_0) for 2 h in polyethylene bottles at

22 °C. The initial pH was adjusted to approximately 6 using NaOH or HCl depending on the acid or base properties of the sample. After equilibration the solutions were centrifuged, the pH measured to ensure that the pH was within ±0.2 pH unit from the target pH, and the residual F^- concentration (C_e) determined using ion chromatography or a F^- ion selective electrode. The % adsorption was calculated from the residual F^- concentration using the equation:

$$\%Adsorption = 100 \times \frac{(C_o - C_e)}{C_o}$$

To ensure that F^- does not adsorb on the inner walls of the adsorption vessels, blank runs were performed. In this procedure a 10 $mgF.L^{-1}$ solution was added to a polyethylene vessel and the F^- concentration measured after 2 h and again after 12 h. No reduction in F^- concentration was found.

(b) *Adsorption curves (% adsorption vs pH)*

The same method as described in Section 6(a) was followed for equilibrium solution pH values of about 2, 3, 4, 5, 6, 7, 8, and 9.

(c) *Competitive adsorption*

The effect of other anions on the adsorption of F^- was studied by determining the residual F^- concentration in the presence of Cl^- and SO_4^{2-}. The same procedure was used as in Section 6(a).

(d) *Determination of adsorption kinetics*

Adsorption kinetics were determined using the batch adsorption procedure described in Section 6(a). Residual F^- concentrations were, however, measured at the time intervals 10, 20, 30, 45, 60, 120, and 300 m.

7. DETERMINATION OF ADSORPTION ISOTHERMS

Adsorption isotherms were determined using chemically pretreated clays. 1 g of clay was equilibrated in 45 mL 0.1 M $NaClO_4$ at pH 6 for 14 h. Appropriate amounts of a 1000 $mg.L^{-1}$ F^- stock solution were and 0.1 M $NaClO_4$ were then added to the equilibrated samples to prepare 50 mL test solutions with initial concentrations: 2, 5, 10, 20, 50, 100, and 200 $mgF.L^{-1}$. These solutions were equilibrated for 2 h to complete the adsorption process and the residual fluoride concentration and final pH determined.

8. DETERMINATION OF ΔPH CURVES

Clay samples of 1 g each were equilibrated for 14 h in 50 mL 0.1 M $NaClO_4$ solution at pH 3 to 9. After equilibration 0.5 mL of a 1000 $mg.L^{-1}$ F^- stock solution was added so that the initial F^- concentration was 10 $mg.L^{-1}$.

The pH was adjusted with 1M $HClO_4$ or NaOH. The pH was measured at 1h after pH adjustment (pH_{1h}), again after 14h equilibration (pH_i), and then at different times after addition of 10 $mg.L^{-1}$ fluoride (For example pH_{15} denotes 15 m after addition of F^-).

9. LEACHING PROCEDURES

Heavy metals leached from clays during the F^- adsorption procedure were determined by ICP-OES. 1g clay sample was extracted with 50 mL of F^- solution (1 and 10 $mg.L^{-1}$) at pH 6 for 2 h. The suspension was centrifuged and the extracted metals determined in the solution after decanting by ICP-OES.

10. EXPERIMENTS WITH MINI COLUMNS

(a) *Preparation of clays for column experiments*

Clay samples were washed with deionised water until F^- free, dried at 105 °C, compacted in a Perkin Elmer pellet press at 5 t and pellet diameter 35 mm, heat-treated at 600 °C for 2 h, cooled in a desiccator, and crushed in a Siebtechnik mill to particle size < 2 μ. This procedure was followed to stabilise the clay samples to prevent loss of small particles during column operation.

(b) *Description of columns*

Mini columns consisted of 180 x 14 mm glass tubes fitted with no 1 porosity frits on both ends. The columns were connected to a Gilson Minipuls 3 peristaltic pump using Tygon tubing. Columns were typically packed with 4 g sorbent. The flow direction was from bottom to top. The pH of F^- feed solutions were adjusted to pH 6 to ensure proper conditions for adsorption to occur.

(c) *Determination of breakthrough curves and adsorption capacities*

Columns were packed with 4 g dry sorbent (or other mass as indicated). The columns were then equilibrated by pumping deionised water at pH 6 through the column using a Gilson Minipuls 3 peristaltic pump. The flow rate was 4 $mL.min^{-1}$. F^- feed solutions were adjusted to pH 6 before being pumped through the columns. Samples were taken at regular intervals and the F^- concentration determined by FISE. Residual F^- concentration was plotted against time; Breakthrough times were determined graphically and used to calculate breakthrough volumes and adsorption capacities of the columns.

11. REFERENCES

FOLK RL (1974). The petrology of sedimentary rocks. *Hemphill Pub., Austin*, 182 pp.

McCAFFREY LP (1994). Fluoride electrode vs ionchromatographic analysis of groundwater. *Abstract Volume, Analytika 94, Stellenbosch*, 8-13 December 1994, p87

SYVITSKI JPM (Ed.) (1991). Principles, Methods, and Applications of Particle Size Analysis. *Cambridge Univ. Press, New York*, 368 pp.

VELDE B (1995). Composition and mineralogy of clay minerals. In: Velde B (ed.) *Origin and mineralogy of clays*. Springer-Verlag, New York, 8-42.

PARFITT RL (1989). Optimum conditions for extraction of Al, Fe and Si from soils with acid oxalate. *Commun. Soil Sci. Plant Anal.* **20**, 801-816.

K5/1289/0/1

CAPACITY BUILDING REPORT

This project made it possible to support four persons:

Cecil Chibi is enrolled for a Ph.D (Civil Engineering) at RAU. The bulk of his experimental work was completed as part of this project and reflected in the final report.

Raymond Puka is enrolled for a M.Sc (Chemistry) at RAU and on the process of submitting his final thesis. All the work done forms part of the WRC project.

Simon Mubenga is a technical assistant in the Department of Chemistry at RAU and was involved throughout the project. His financial support was partly provided by the project funds.

Lucky Khoza was recruited as a labourer (unemployed since matriculating) to manufacture the clay pellets. Since completion of the pellet manufacture, he was retained by the Water Research Group. He is now trained in-house as a laboratory assistant with considerable computer skills and does all scanning and image processing for the Water Research Group. This project thus added significantly to his skills base.

The first three candidates had the opportunity to present their work at the Biennial Conference of the Water Institute of Southern Africa in Durban in May 2002.

Other related WRC reports available:

Investigation of inorganic materials derived from water purification processes for ceramic applications

Boucher PS; Van Eeden JJ

Sludges and silts produced by waterworks often create disposal problems and can spoil land or foul waterways. The main objective was to study the technical and economic feasibility of using waterworks sludges for the production of bricks, blocks, tiles or other ceramics.
Production of bricks with small perforations counteracted their tendency to crack in the unfired state. Calcination and an optimised firing cycle were used to avoid cracking and warping of tiles. The sludge obtained from Wiggins Waterworks was found to be suitable for the production of rustic tiles and stock or face bricks, particularly for use in low-cost housing.

Report Number: 538/1/95 **ISBN: 1 86845 161 5**

TO ORDER: Contact **Publications** - Telephone No: 012 330 0340
Fax Number: 012 331 2565
E-mail: publications@wrc.org.za

Water Research Commission
Private Bag X03, Gezina, 0031, South Africa
Tel: +27 12 330 0340, Fax: +27 12 331 2565
Web: http://www.wrc.org.za